DEFINING THE MECHANISM BY WHICH SYNTHETIC POLYMER SURFACES SUPPORT HUMAN PLURIPOTENT STEM CELL SELF-RENEWAL

by

Xu Qian

A dissertation submitted in partial fulfillment
of the requirements for the degree of
Doctor of Philosophy
(Oral Health Sciences)
in The University of Michigan
2015

Doctoral Committee:
Professor Paul H. Krebsbach, Chair
Professor Yvonne L. Kapila
Professor Joerg Lahann
Professor Russell S. Taichman

DEDICATION

To my beloved family

ACKNOWLEDGEMENTS

I would like to express my sincere gratitude to the individuals who have contributed and supported me to accomplish my doctoral studies. Firstly, I would like to thank my mentor and dissertation committee chair, Dr. Paul Krebsbach for providing me with outstanding scientific resources and incredible support. He is an excellent mentor who truly listens to the students and creates a wonderful environment for us to work and grow. What I have learned from him, both in and beyond science, are invaluable for my future career and life.

I would like to express my appreciation to other members of my committee: Dr. Joerg Lahann, for his contribution as a thesis committee member and for his great support in design of the experimental models, preparing and characterizing the polymer coatings. Dr. Yvonne Kapila, for her continuous support and mentoring since my first lab rotation in 2009. Dr. Russell Taichman, for being a wonderful teacher in stem cell biology and inspiring me to conduct the induced pluripotent stem cell studies. They all make a significant contribution in shaping this thesis and improving my scientific reasoning and problem solving skills.

I would also like to thank both the past and current members of Krebsbach lab: Dr. Luis G. Villa-Diaz and Dr. Jin Koo Kim for providing me excellent teaching and tremendous support from the first day I joined the lab. Wilbur Tong for his technical support and laboratory management. Dr. Hongli Sun, Dr. Feng Zhu, Dr. Erica Scheller, Dr. Yaseen Elkasabi, Dr. William king, Dr.

Yoshihiro Komatsu, Joe Nguyen, Tugba Aydin, Dr. Daniela Mendonca, Dr. Gustavo Mendonca and Dr. Elisa Sartor, for their great support and creating a pleasant working environment.

My sincere appreciation also goes to members of Lahann lab: Ramya Kumar, Dr. Aftin Ross, and Gowthamy Venkidasubramonian for their collaborations in preparing and characterizing the polymer coatings.

Special thanks go to Dr. Charlotte Mistretta and Dr. Jan Hu, the former and current directors of the Oral Health Sciences PhD program, for their exceptional support throughout the past six years. I gratefully acknowledged all the Oral Health Sciences and dental school faculty members, especially Dr. William Giannobile, Dr. Laurie McCauley and Dr. J. Christopher Fenno for their guidance in research and laboratory training. Dr. Yuji Mishina, Dr. Renny Franceschi, Dr. Vesa Kaartinen, Dr. David Kohn, Dr. Nisha D'Silva and Dr. Jacques Nör for their help in improving my scientific thinking and presentation skills. Dr. Peter Polverini, Dr. Sunil Kapila, Dr. Fei Liu and Dr. Zhengyan Wang for their suggestions and support in my career development. I would like to thank the staff of the Oral Health Sciences Research Office, Patricia Schultz, Landon Manette, Charlene Erickson, Kimberly Smith, Misty Gravelin and Sarah Ellerholz, for their extraordinary administrative assistance all through my PhD training.

I am very grateful to all the past and current Oral Health Sciences PhD students for their inspiring support and friendship. I also want to thank all my friends at Michigan Biointerfaces. Without their help and encouragement, I would not have been able to complete this thesis work.

I sincerely appreciate the financial support that enabled me to complete my studies. The funding resources include the Dean’s Scholarship from the School of Dentistry, Block Grant Awards and

Student Research Grant from Rackham School of Graduate Studies, and support from the Department of Biological and Materials Sciences.

Full acknowledgement of the journals, *Journal of Dental Research*, *Biomaterials* and *Stem Cells* for their permission of the use of our published or under revision manuscripts in Chapters 2, 3, and 4.

I sincerely acknowledge the faculty of Sichuan University West China School of Dentistry, for their outstanding dental education and for inspiring me to pursue a career in academic dentistry, especially Dr. Xiaobing Li, Dr. Song Chen, Dr. Zhihe Zhao and Dr. Bing Shi, for their continuous encouragement and support all through the past years before and after my graduation.

Finally, I am extremely grateful for the love and support from my family and friends. I especially thank my parents, Weiping and Jin, my parents-in-law, Mingsu and Yien, my grand parents, my son Taotao and my husband Peng. Thank you all.

TABLE OF CONTENTS

DEDICATION ..... **ii**

ACKNOWLEDGEMENTS ..... **iii**

LIST OF FIGURES ..... **viii**

LIST OF TABLES ..... **x**

ABSTRACT ..... **xi**

CHAPTER 1. INTRODUCTION **1**

1.1 Problem Statement 1
1.2 General Hypothesis 3
1.3 Specific Aims 3
1.4 Summary of Thesis Contents 4
1.5 References 6

CHAPTER 2. REVIEW OF LITERATURE **9**

2.1 Progress in Human Pluripotent Stem Cell Culture: from Dependence on Feeder Cells to Culture on Synthetic Matrices 9
2.2 Culture Medium, Supplements and Cell Signaling 13
2.3 Cell Lineage Differentiation of Human Pluripotent Stem Cells 15
2.4 Derivation of Human Induced Pluripotent Stem Cell 17
2.5 New Trends in Inducing Specific Cell Lineages 19
2.6 The Transcriptional Regulatory Network of Pluripotency 21
2.7 Figures 23
2.8 References 25

CHAPTER 3. ENHANCEMENT OF THE PROPAGATION OF HUMAN EMBRYONIC STEM CELLS BY MODIFICATIONS IN THE GEL ARCHITECTURE OF PMEDSAH POLYMER COATINGS **32**

3.1 Abstract 32
3.2 Introduction 33
3.3 Materials and Methods 34
3.4 Results 42
3.5 Discussion 46

3.6 Figures 53
3.7 Tables 63
3.8 References 65

CHAPTER 4. DPPA5 PROMOTES PLURIPOTENCY AND REPROGRAMMING BY REGULATING NANOG TURNOVER 68

4.1 Abstract 68
4.2 Introduction 69
4.3 Materials and Methods 71
4.4 Results 78
4.5 Discussion 83
4.6 Figures 88
4.7 Tables 98
4.8 References 101

CHAPTER 5. CONCLUSION AND PROSPECTUS 106

5.1 Summary 106
5.2 Prospectus 109
5.3 Figures 114
5.4 References 115

LIST OF FIGURES

CHAPTER 2

Figure 2-1: Controlled cell lineage induction by manipulation of signaling pathways and gene expression *in vitro* 23

CHAPTER 3

Figure 3-1: Differences in properties of PMEDSAH coatings. 53

Figure 3-2: Gel architecture influences the undifferentiated colony formation and expansion of hESCs (CHB 10 cells). 55

Figure 3-3: Gel architecture influences the undifferentiated colony formation of hESCs (H9 cells) 57

Figure 3-4: Expression of SSEA-4 in hESCs cultured on different substrates after multiple passages 58

Figure 3-5: Modified PMEDSAH supports hESC stemness and keeps the genomic stability 60

Figure 3-6: Modified PMEDSAH supports hESC pluripotency 62

CHAPTER 4

Figure 4-1: Gene expression differences between hESCs cultured on PMEDSAH versus on MEFs 88

Figure 4-2: Differences in *DPPA5* gene expression and protein levels in hPSCs cultured on irradiated MEFs and feeder-free substrates 89

Figure 4-3: Soluble factors and ECM secreted by irradiated MEFs inhibited *DPPA5* expression in hPSCs compared to feeder-free conditions 90

Figure 4-4: Differences in *DPPA5* expression between hPSCs and differentiated cells .. 91

Figure 4-5: Induced specific lineage differentiation from hESCs with expression of genes representing different germ layers..... 93

Figure 4-6: The regulation of NANOG protein levels by DPPA5 in hPSCs 94

Figure 4-7: Protein interaction and stabilization between DPPA5 and NANOG in hPSCs 95

Figure 4-8: Regulation of the expression of NANOG target genes by DPPA5 in hPSCs 96

Figure 4-9: DPPA5 increased hiPSC-reprogramming efficiency 97

CHAPTER 5

Figure 5-1: Future modifications of PMEDSAH structure. 114

LIST OF TABLES

CHAPTER 3

Table 3-1: Calculated total cell number of hESCs cultured on different substrates. 63

Table 3-2: Embryoid body (EB) formation with expression of genes representing different germ layers. 64

CHAPTER 4

Table 4-1: Embryoid body (EB) formation from hESCs with expression of genes representing different germ layers..... 98

Table 4-2: Embryoid body (EB) formation from Con-hiPSCs with expression of genes representing different germ layers..... 99

Table 4-3: Embryoid body (EB) formation from d6+D-hiPSCs with expression of genes representing different germ layers..... 100

ABSTRACT

DEFINING THE MECHANISM BY WHICH SYNTHETIC POLYMER SURFACES SUPPORT HUMAN PLURIPOTENT STEM CELL SELF-RENEWAL

by

Xu Qian

Chair: Paul H. Krebsbach

Human pluripotent stem cells (hPSCs), which include embryonic stem cells (hESCs) and induced pluripotent stem cells (hiPSCs), have become a promising resource for regenerative medicine and research into early development because these cells are able to indefinitely self-renew and are capable of differentiation into specialized cell types of all three germ layers and trophoectoderm. However, a major limitation for successful therapeutic application of hPSCs and their derivatives is the potential xenogeneic contamination and instability of current culture conditions. Synthetic polymers, such as poly[2-(methacryloyloxy) ethyl dimethyl-(3-sulfopropyl) ammonium hydroxide] (PMEDSAH), offer multiple advantages over mouse embryonic fibroblasts (MEFs) and Matrigel for hPSC culture. The main purpose of this dissertation is to define the mechanisms by which hPSCs are propagated on synthetic polymers.

By physical modifications of PMEDSAH, we found that modifying substrate thickness changed the physical properties, and thus altered pluripotent stem cell behavior. Our data suggest that the

105 nm thick atom transfer radical polymerization (ATRP) PMEDSAH possesses the optimal gel architecture for hPSC expansion with its intermediate thickness, hydrophilicity, surface charge, and a moderate degree of inter-chain association. Our findings demonstrate the importance of polymer physical properties in hPSC expansion. The 105 nm thick ATRP PMEDSAH and similar modifications may be used to obtain scalable populations of clinical-grade hPSCs for regenerative medicine.

Although a specific group of transcription factors, such as OCT4, SOX2 and NANOG, are known to play critical roles in hPSC pluripotency and reprogramming, other factors and the key signaling pathways regulating these important properties are not completely understood. In this dissertation, we also investigated the role of the PSC marker Developmental Pluripotency Associated 5 (DPPA5) in hPSCs. Our data demonstrate higher expression of DPPA5 in hPSCs under PMEDSAH and other feeder-free conditions, compared to MEFs. DPPA5 stabilizes protein levels and enhances the function of NANOG. Finally, DPPA5 increases the hiPSC-reprogramming efficiency. These results provide new molecular insight into the function of the DPPA5 in hPSCs. Our findings extend our understanding of the mechanism by which PMEDSAH and other feeder-free conditions support hPSC self-renewal, and offers improvements to current protocols in hPSC maintenance and reprogramming.

CHAPTER 1

INTRODUCTION

1.1 Problem Statement

Human pluripotent stem cells (hPSCs) include embryonic stem cells (hESCs) derived from the inner cell mass of blastocyst-stage embryos and induced pluripotent stem cells (hiPSCs) generated by reprogramming somatic cells by the overexpression of key transcription factors [1-3]. The capacity for indefinite self-renewal and differentiation into specialized cell types of all three germ layers and trophoectoderm makes hPSCs a promising resource for regenerative medicine, tissue engineering, disease modeling, drug screening and understanding early events in human development. However, a key prerequisite for successful therapeutic application of hPSCs and their derivatives is the ability to develop strategies for large-scale production of clinical-grade cells [4-6] .

Currently, the large-scale production of clinical-grade hPSCs is limited by potential xenogeneic contamination and instability of current culture conditions [1, 7, 8]. To overcome these limitations, synthetic polymers [9-17] have been developed for propagation of hESCs because of the following features: completely defined chemical composition, stability during storage, reproducibly synthesized and cost-effectiveness [18]. Among the synthetic substrates,

poly[2-(methacryloyloxy) ethyl dimethyl-(3-sulfopropyl) ammonium hydroxide] (PMEDSAH), a fully defined synthetic polymer coating has demonstrated effective capacity to support hPSC self-renewal and expansion in long-term culture [12, 19, 20]. Currently, PMEDSAH is the only truly synthetic substrate that contains no biologic components such as proteins, peptides or sugars. A complete understanding of the mechanism by which PMEDSAH supports hPSC self-renewal is a key to unlock its great potential for large-scale propagation of hPSCs.

Recent studies demonstrated that physical properties such as hydrophilicity [12], surface roughness [21] and stiffness [22, 23] impact the capability of synthetic substrates to support hESC growth [18]. However, the mechanisms by which PMEDSAH and other synthetic substrates maintain self-renewal of hPSCs are not yet clearly understood. Moreover, although a specific group of transcription factors, such as OCT4, SOX2 and NANOG, are known to play important roles in hPSC pluripotency and reprogramming [24-27], other factors and the key signaling pathways regulating these properties are not clearly understood. Appropriate culture conditions are critical to maintain the pluripotency of hPSCs *in vitro*. From a molecular biological perspective, these culture methods should be able to support the transcriptional and signaling networks maintaining pluripotency. Compared to the most widely used hPSC culture condition, mouse embryonic fibroblasts (MEFs), PMEDSAH and other feeder-free conditions may have different transcriptional and signaling networks that support hPSC self-renewal. Currently, very few publications focus on the mechanism and impact of *in vitro* conditions on pluripotency regulatory networks. In this thesis, we investigated the mechanism by which PMEDSAH support hPSC self-renewal from two different perspectives: 1) physical mechanism - the physical properties and the extent to which these physical properties of PMEDSAH impact its capacity to support hPSC self-renewal; 2) molecular mechanism - the molecules and signaling

pathways that play critical roles in supporting hPSC self-renewal on PMEDSAH and other feeder-free substrates.

1.2 General Hypothesis

The physical properties of coating surfaces and specific pluripotency-related factors play important roles in hPSC self-renewal on synthetic polymers.

1.3 Specific Aims

Two specific aims are proposed to test the hypothesis.

Specific Aim 1. To determine the effects of physical properties on the ability of synthetic polymer coatings to support hPSC self-renewal

By increasing the reaction time of atom transfer radical polymerization (ATRP), we expect to modify the gel architecture of PMEDSAH without changing its chemical structure. Polymer characterization will be performed to determine what physical properties are modified. We aim to identify cell adhesion, proliferation and self-renewal by determining the number and area of undifferentiated colonies, total cell number, stem cell marker expression and pluripotency of the hPSCs cultured on grafted or ATRP PMEDSAH. By accomplishing this specific aim, we expect to identify which physical properties of synthetic polymer coatings and the extent to which these physical properties influence hPSC maintenance and expansion.

Specific Aim 2 To determine which molecules and signaling pathways are essential in supporting hPSC self-renewal on synthetic polymers

Using microarray analysis, we expected to identify the genes that have significantly different expression levels between hPSCs cultured on PMEDSAH and MEFs. Quantitative RT-PCR will

be used to validate the results by microarray. The genes related to pluripotency, cell attachment or/and proliferation, and that consistently expressed differently between different hPSC lines on PMEDSAH and MEFs will serve as our targets for further investigation. These studies include their expression on other feeder-free substrates and their impact on hPSC self-renewal and reprogramming. By accomplishing this specific aim, we expect to find novel signaling networks regulating hPSC pluripotency on synthetic polymers, and likely discover new factors that support hPSC self-renewal.

1.4 Summary of Thesis Contents

Chapter 2 is a review of literature based on our published manuscript in *Journal of Dental Research (Critical Reviews in Oral Biology and Medicine)* [28]. This chapter summarizes recent advances in hPSC maintenance and methods to induce hiPSCs and controlled lineage differentiation by regulating cell-signaling pathways, altering gene expression and manipulating the extracellular environment that stem cells experience.

Chapter 3 is written based on our published manuscript in *Biomaterials* [29]. This chapter details the experiments we conducted to address Specific Aim 1: to determine the effects of physical properties on the ability of synthetic polymer coatings to support hPSC self-renewal. hPSCs were cultured on grafted and ATRP PMEDSAH. Cell expansion and self-renewal were assayed by determining the number of undifferentiated colonies and total cells, cell stemness and pluripotency. We found that the105 nm thick ATRP PMEDSAH possesses the optimal gel architecture for hPSC expansion with its intermediate thickness, hydrophilicity, surface charge, and a moderate degree of inter-chain association. Our findings suggest that physical properties influence the ability of PMEDSAH to support hPSC self-renewal. Modifying the physical

properties through increasing the film thickness of PMEDSAH may advance our current techniques for hPSC maintenance and expansion.

Chapter 4 is written based on our manuscript that is under revision for *Stem Cells* [30]. This chapter describes our work to address Specific Aim 2: to determine which molecules and signaling pathways are essential for supporting hPSC self-renewal on synthetic polymers. Microarray and quantitative RT-PCR demonstrated that compared to MEFs, hPSCs cultured on PMEDSAH and other feeder-free substrates had higher gene expression of Developmental Pluripotency Associated 5 (DPPA5), a PSC marker with unknown function in hPSCs, while the expression of other pluripotency-related factors such as OCT4, SOX2 and KLF4 had no significant differences. We then focused on the function of DPPA5 in hPSCs and found that the extracellular matrix deposited by irradiated MEFs, as well as secreted soluble factors, inhibited the expression of DPPA5, while its expression and function were permissive under feeder-free conditions. DPPA5 plays an important role in supporting hPSC self-renewal and reprogramming by stabilizing protein levels and enhancing the function of NANOG, a key transcription factor for hPSC pluripotency. Our findings that *in vitro* conditions impact DPPA5 expression and the pluripotency regulatory networks advance our understanding of the mechanism by which synthetic polymers and other feeder-free substrates support hPSC self-renewal. We also provide new molecular insight into the function of the pluripotent stem cell marker DPPA5 in hPSCs.

Chapter 5 is a summary of the thesis results and a prospectus for future directions of the work.

1.5 References

[1] Thomson JA, Itskovitz-Eldor J, Shapiro SS et al. Embryonic stem cell lines derived from human blastocysts. Science 1998;282:1145-7.

[2] Yu J, Vodyanik MA, Smuga-Otto K et al. Induced pluripotent stem cell lines derived from human somatic cells. Science 2007;318:1917-20.

[3] Takahashi K, Tanabe K, Ohnuki M et al. Induction of pluripotent stem cells from adult human fibroblasts by defined factors. Cell 2007;131:861-72.

[4] McCall MD, Toso C, Baetge EE et al. Are stem cells a cure for diabetes? Clin Sci (Lond) 2010;118:87-97.

[5] Dominguez-Bendala J, Inverardi L, Ricordi C. Stem cell-derived islet cells for transplantation. Curr Opin Organ Transplant 2011;16:76-82.

[6] Laflamme MA, Chen KY, Naumova AV et al. Cardiomyocytes derived from human embryonic stem cells in pro-survival factors enhance function of infarcted rat hearts. Nat Biotechnol 2007;25:1015-24.

[7] Richards M, Tan S, Fong CY et al. Comparative evaluation of various human feeders for prolonged undifferentiated growth of human embryonic stem cells. Stem Cells 2003;21:546-56.

[8] Xu C, Inokuma MS, Denham J et al. Feeder-free growth of undifferentiated human embryonic stem cells. Nat Biotechnol 2001;19:971-4.

[9] Derda R, Li L, Orner BP et al. Defined substrates for human embryonic stem cell growth identified from surface arrays. ACS Chem Biol 2007;2:347-55.

[10] Klim JR, Li L, Wrighton PJ et al. A defined glycosaminoglycan-binding substratum for human pluripotent stem cells. Nat Methods 2010;7:989-94.

[11] Kolhar P, Kotamraju VR, Hikita ST et al. Synthetic surfaces for human embryonic stem cell culture. J Biotechnol 2010;146:143-6.

[12] Villa-Diaz LG, Nandivada H, Ding J et al. Synthetic polymer coatings for long-term growth of human embryonic stem cells. Nat Biotechnol 2010;28:581-3.

[13] Mei Y, Saha K, Bogatyrev SR et al. Combinatorial development of biomaterials for clonal growth of human pluripotent stem cells. Nat Mater 2010;9:768-78.

[14] Irwin EF, Gupta R, Dashti DC et al. Engineered polymer-media interfaces for the long-term self-renewal of human embryonic stem cells. Biomaterials 2011;32:6912-9.

[15] Li YJ, Chung EH, Rodriguez RT et al. Hydrogels as artificial matrices for human embryonic stem cell self-renewal. J Biomed Mater Res A 2006;79A:1-5.

[16] Brafman DA, Chang CW, Fernandez A et al. Long-term human pluripotent stem cell self-renewal on synthetic polymer surfaces. Biomaterials 2010;31:9135-44.

[17] Melkoumian Z, Weber JL, Weber DM et al. Synthetic peptide-acrylate surfaces for long-term self-renewal and cardiomyocyte differentiation of human embryonic stem cells. Nat Biotechnol 2010;28:606-10.

[18] Villa-Diaz LG, Ross AM, Lahann J et al. Concise review: The evolution of human pluripotent stem cell culture: from feeder cells to synthetic coatings. Stem Cells 2013;31:1-7.

[19] Nandivada H, Villa-Diaz LG, O'Shea KS et al. Fabrication of synthetic polymer coatings and their use in feeder-free culture of human embryonic stem cells. Nat Protoc 2011;6:1037-43.

[20] Villa-Diaz LG, Kim JK, Lahann J et al. Derivation and long-term culture of transgene-free human induced pluripotent stem cells on synthetic substrates. Stem Cells Transl Med 2014;3:1410-7.

[21] Chen W, Villa-Diaz LG, Sun Y et al. Nanotopography influences adhesion, spreading, and self-renewal of human embryonic stem cells. ACS Nano 2012;6:4094-103.

[22] Sun YB, Villa-Diaz LG, Lam RHW et al. Mechanics Regulates Fate Decisions of Human Embryonic Stem Cells. PLoS One 2012;7.

[23] Jiang XW, Chen HY, Galvan G et al. Vapor-based initiator coatings for atom transfer radical polymerization. Adv Funct Mater 2008;18:27-35.

[24] Hay DC, Sutherland L, Clark J et al. Oct-4 knockdown induces similar patterns of endoderm and trophoblast differentiation markers in human and mouse embryonic stem cells. Stem Cells 2004;22:225-35.

[25] Boyer LA, Lee TI, Cole MF et al. Core transcriptional regulatory circuitry in human embryonic stem cells. Cell 2005;122:947-56.

[26] Hyslop L, Stojkovic M, Armstrong L et al. Downregulation of NANOG induces differentiation of human embryonic stem cells to extraembryonic lineages. Stem Cells 2005;23:1035-43.

[27] Fong H, Hohenstein KA, Donovan PJ. Regulation of self-renewal and pluripotency by Sox2 in human embryonic stem cells. Stem Cells 2008;26:1931-8.

[28] Qian X, Villa-Diaz LG, Krebsbach PH. Advances in culture and manipulation of human pluripotent stem cells. J Dent Res 2013;92:956-62.

[29] Qian X, Villa-Diaz LG, Kumar R et al. Enhancement of the propagation of human embryonic stem cells by modifications in the gel architecture of PMEDSAH polymer coatings. Biomaterials 2014;35:9581-90.

[30] Qian X, Kim JK, Tong W et al. DPPA5 promotes pluripotency and reprogramming by regulating NANOG turnover. Stem Cells. (manuscript under revision)

CHAPTER 2

REVIEW OF LITERATURE

2.1 Progress in Human Pluripotent Stem Cell Culture: from Dependence on Feeder Cells to Culture on Synthetic Matrices

Human pluripotent stem cells (hPSCs) include embryonic stem cells (hESCs) derived from the inner cell mass of blastocysts and induced pluripotent stem cells (hiPSCs) generated by the overexpression of key transcription factors in somatic cells [1-3]. The derivation and culture of human embryonic stem cell (hESC) lines was originally described using the same procedure described for mouse ESCs (mESCs). These methods included gamma irradiated mouse embryonic fibroblasts (MEFs) as feeder cells and culture medium supplemented with fetal bovine serum (FBS) [1]. However, since the nature of mouse and human ESCs is not identical [4], the culture conditions to support their growth have proved to be different as well. Due to its undefined conditions and variability, the above-mentioned medium was replaced with knockout serum replacer and fibroblast growth factor 2 (FGF2) for hPSC culture. As feeder cells, MEFs provide attachment sites for hPSCs and secrete multiple, but largely uncharacterized factors that induce signaling networks to regulate hPSC fate. However, the interactions among hPSCs and murine feeder cells highlight xenogeneic contamination as a major concern and thus limit the use of MEFs in therapeutic applications for humans.

Micro-organisms and non-human bioactive molecules are two general sources of xenogeneic contamination of hPSCs when co-cultured on MEFs. Viruses may be transferred from feeder cells to contaminate the cell derivatives of hPSCs. Compared to other micro-organisms, viral contamination is difficult to detect and address during cell culture. Viruses such as lymphocytic choriomeningitis virus (LCMV), first isolated from mouse colonies, have been reported to infect cell lines [5]. Certainly, the possible presence of viruses in MEFs and serum would increase the risk for culturing clinical-grade hPSCs. Furthermore, non-human bioactive molecules such as Neu5Gc have been identified on the surface of hESCs when co-cultured with MEFs [6]. These bioactive molecules may induce an immune response in recipients of transplanted hPSC-derivatives. In addition, gamma-irradiation, which is used to inhibit MEF proliferation, induces apoptosis in feeder cells and leads to instability of the culture microenvironment [7], impacting both mechanistically driven research and clinical application of hPSCs.

To avoid the risks of animal contamination from MEFs, human feeder cells have been used for hPSC culture [8]. Multiple types of human cells—including fibroblasts derived from fetal muscle, fetal skin, adult fallopian tubal epithelium, placenta, uterine endometrium, foreskin and mesenchymal cells—have been validated for their capability to support hPSCs self-renewal. Among human feeder cells, fibroblast-like cells derived from hPSCs offer a potential autogenic system to support self-renewal of hPSCs. In addition to the diversity of human feeder cell lines, other innovations have been introduced, such as the use of FGF2 secreting human fibroblasts as feeder cells. This strategy reduced the need for exogenous supplementation of FGF2 to the culture medium [9]. Another innovation in hPSC culture is the use of an indirect co-culture system that is based on a microporous polymer membrane that allows real-time conditioning of the culture medium by human fibroblasts, while maintaining complete separation between hPSCs

and feeder cells [10]. Nevertheless, the risk of contamination by human pathogens remains a concern when using human feeder cells. Therefore, comprehensive screening and tests are required before feeder cells can be used in the culture of hPSCs intended for clinical applications.

To reduce the instability and potential contamination brought on by feeder cells, feeder-free culture systems for hPSCs have been developed. Matrigel™, the trade name for an extracellular matrix (ECM) extracted from Engelbreth-Holm-Swarm (EHS) mouse sarcomas, was the first example of a feeder-free substrate for hPSC culture [11]. To determine which components of Matrigel™, as well as other ECM molecules, may support hPSCs, a variety of specific ECM proteins have been examined. It has been reported that human recombinant (hr) laminin isoforms -111, -332 and 511, and hr vitronectin support the growth of undifferentiated hPSCs [12, 13]. Human recombinant E-cadherin, another cell-cell interaction mediator, has also been reported to support hPSC self-renewal [14]. These purified proteins are examples of defined and xenogeneic-free substrates being used for hPSC culture. Because these proteins are generated as recombinant factors, they may not be subjected to lot-to-lot variations observed in Matrigel™ extracts and other potential contaminations. However, human recombinant proteins are labor intensive and costly to produce, which complicates their large-scale use. Therefore, the development of fully synthetic substrates for hPSC culture represents a new milestone in hPSC culture by overcoming many of the obstacles presented by biological substrates. Synthetic substrates have the following superiorities: they are defined, reproducible and stable, show minimal lot-to-lot variability, demonstrate better scalability, are cost-effective and easily prepared [15]. All these advantages make synthetic substrates promising for large-scale expansion of clinical-grade hPSCs and their derivatives for therapeutic use.

Peptide-based systems with surface arrays of self-assembled monolayers have been used to identify peptide surfaces that support hPSC self-renewal. Arrays of laminin-derived peptides, heparin-binding peptides and high-affinity cyclic RGD peptides have all been shown to support hPSC culture [16-18]. The composition of surface array elements, specifically density and sequence of peptides, has been reported to impact the ability of substrates to support hPSC growth [16].

Numerous polymer-based substrates have been developed by different methodologies. For example, poly[2-(methacryloyloxy) ethyl dimethyl-(3-sulfopropyl) ammonium hydroxide] (PMEDSAH) is a fully defined synthetic polymer substrate developed through a surface-initiated graft polymerization technique [19]. Hit 9 and the aminopropylmethacrylamide, APMAAm, are both fabricated by photopolymerization [20, 21]. Both the semi-interpenetrating polymer hydrogel poly(N-isopropylacrylamide-co-acrylic acid) and the poly(methyl vinyl ether-alt-maleic anhydride) (PMVE-alt-MA), an anhydride containing polymer substrate, are generated by radical polymerization [22, 23]. In addition, combinatorial approaches for polymer substrates have been implemented by using polymers as base substrates that are modified with biomolecules such as vitronectin and amino-containing peptides [20, 24]. All these substrates have demonstrated effective capacity to support hPSC growth.

Synthetic substrates for sustained hPSC culture are generally more stable and reproducible when compared to the first generation culture systems. Clearly, understanding the molecular mechanisms that maintain self-renewal of hPSC will be critical for the modification and improvement of the currently available technologies. Although not yet completely understood, the following physico-chemical properties may impact the capability of substrates to support hPSC growth: hydrophilicity, surface roughness, stiffness [15] as well as the application of cell

adhesion elements such as heparin-binding peptides [17] and laminin-derived peptides [16]. Additionally, the compatibility of synthetic substrates with common sterilization techniques such as ultraviolet (UV) light radiation is another characteristic that may impact the effectiveness of substrate preparations. For example, substrates with biological components such as proteins and peptides are usually incompatible with common sterilization methods because biological components may undergo denaturation or degradation during the sterilization process. From this point of view, the pure polymer-based synthetic substrates may be superior to other substrates for hPSC culture.

2.2 Culture Medium, Supplements and Cell Signaling

In addition to feeder cells and feeder-free substrates, another key component of an effective hPSC culture system is the culture medium. Accompanied by the evolution of other components of the culture system, the development of new culture medium has undergone the following evolution: from medium containing serum to serum-free medium, and from feeder cell-conditioned medium to chemically-defined and xenogeneic-free medium. As mentioned above, the culture of hPSCs was originally performed with fetal bovine serum (FBS) to supplement the culture medium [1] and later was replaced by knockout serum replacer and fibroblast growth factor 2 (FGF2) [25]. Human serum has also been used to replace animal-derived serum for the purpose of pursuing xenogeneic-free conditions. However, it has been reported that human serum may only support hPSC for up to 10 passages [8]. At the early stages of feeder-free culture system development, MEF conditioned medium (CM) was commonly used [11]. However, to avoid drawbacks such as multiple unknown and variable factors that CM contains, chemically defined media have been developed to work with xenogeneic-free substrates. This advancement not only paves the way for future large-scale production of clinical-grade hPSCs, but also

provides an ideal system for studying the molecular mechanisms of hPSC self-renewal [15]. For example, mTesR medium was the first xenogeneic-free and serum-free commercial medium developed [26], and further research has improved it into a chemically defined medium that contains only human proteins and 8 defined components [27].

A variety of biological and chemical supplements for culture medium have been reported to facilitate hPSC self-renewal. Many of these discoveries and applications are the result of a greater understanding of hPSC pluripotency, which has been translated to the development of better additives and conditions. Some of these factors include FGF2, insulin, TGFβ, BMP, Wnt and IGF-II. In feeder cell culture systems, FGF2 has been shown to support hPSC self-renewal by promoting the expression of IGF-II, Activin A (a member of TGFβ superfamily) and Gremlin (a BMP antagonist) in feeder cells [28, 29]. In feeder-free cell culture systems, FGF2 has been reported to support undifferentiated hPSC growth without conditioned medium at a concentration of 100ng/ml [30]. In other studies, dual activation of Smad3 and Erk by Activin A and FGF2 in serum-free and xenogeneic-free culture conditions was shown to support long-term maintenance of hESCs [28]. Moreover, it has been also reported that hESCs secrete a low-molecular-mass FGF2 (18-kDa) isoform and express its receptor, FGFR1. Blocking this receptor with a pharmaceutical inhibitor (SU5402) results in cell differentiation, suggesting a critical role for autocrine FGF signaling in maintaining hPSC self-renewal [31]. In addition, studies have indicated that Activin A is an effective medium supplement for hPSC self-renewal because it can enhance the expression of transcription factors, such as *OCT4*, (also known as *POU5F1*), *SOX2* and *NANOG* in hESCs [28]. The observation of phosphorylation and localization of SMAD2/3 in the nucleus also indicates the activation of TGFβ/ Activin A / Nodal pathways in undifferentiated hPSCs [32].

Similar to the TGFβ signaling pathway, the activation of the Wnt signaling pathway by a GSK-3-specific inhibitor has been reported to support the self-renewal of hPSCs [33]. BMP has the opposite effects of TGFβ and Wnt signaling pathways on hPSC self-renewal, since its inhibition supports self-renewal of these cells. For example, Noggin (500ng/ml), a BMP antagonist, can support undifferentiated hESCs on Matrigel^{TM} in combination with FGF2 (40ng/ml) [34]. However, the studies of signaling pathways regulating hPSC self-renewal are still limited and it remains unclear whether other signaling molecules or pathways may be involved.

2.3 Cell Lineage Differentiation of Human Pluripotent Stem Cells

Just as culture conditions to expand hPSC in the undifferentiated state have evolved to the point of using defined and xeno-free conditions, the protocols to induce *in vitro* cell lineage differentiation have been improved significantly in the past few years. This advancement is essential for maximizing the potential of hPSC derivatives for therapeutic use and to improve our understanding of the molecular mechanisms of tissue and organ development. Initial protocols to induce differentiation of hPSCs involved the formation of embryoid bodies (EB) in serum-containing medium, followed by adherent culture of EBs on gelatin-coated plates. Subsequent outgrowth of a heterogeneous cell population can then be sorted or selected for the desired cell lineage. This methodology was implemented, for example, to derive mesenchymal stem cells from hESCs [35].

In contrast, by recapitulating lessons from embryonic development, controlled cell lineage conversion toward progenitors and fully differentiated cells has been achieved by treatment of monolayer cultures of hPSCs and derivatives with morphogens and chemical inhibitors in serum-free medium. The following are a few examples of controlled differentiation into cells

representative of the three germ layers and trophoectoderm (Figure 2-1). The capacity of hPSCs to differentiate into trophoblasts has been demonstrated by treatment with several members of the TGFβ superfamily, such as BMP4, BMP2, BMP7 and GDF5, but not with TGFβ1 or Activin A [36]. Conversely, the dual inhibition of BMP and TGFβ by Noggin and SB431542, a specific chemical inhibitor, direct the differentiation of hPSCs towards a neuronal lineage ($PAX6^+$ cells). Once this initial differentiation is directed, neural crest stem cells can be isolated by flow cytometry using p75 and HNK1 antibodies [37]. Further neuronal specification of $PAX6^+$ cells towards motor neurons has been achieved by first promoting the caudalization of induced neurons with retinoic acid, followed by treatment with sonic hedgehog (SHH) to induce neuronal ventralization. Maturation into motor neurons is finally promoted by treatment with BNDF, GNDF and IGF-I [38].

The formation of definitive endoderm (DE) is a prerequisite for further differentiation into mature endoderm derivatives from anterior foregut, midgut and posterior foregut endoderm. Thus, to induce formation of DE, undifferentiated hPSCs are treated with Activin A [39]. To specify their identity towards anterior foregut endoderm (AFE) progenitor cells, Activin A-induced DE cells are treated with dual inhibition of TGFβ and BMP signaling. AFE-induced cells can then be directed towards cells expressing ventral AFE markers such as *NKX2.1, PAX1* and *NKX2.5* if treated with a combination of WNT3a, KGF, FGF10, BMP4 and EGF. In turn, ventral induced-AFE cells can give rise to cells expressing high *SFTPC* mRNA levels, when exposed to a regimen of retinoic acid, Wnt3a, FGF10 and FGF7, suggesting the derivation of lung cells. Treatment of ventral induced-AFE cells with either FGF8 or sonic hedgehog (SHH) induces the up-regulation of the parathyroid-specific marker *GCM2* [40]. Derivatives from the posterior foregut endoderm lineages have also been induced *in vitro* by treatment of DE cells

derived from hPSCs. For example, to generate hepatic cells, Activin A-induced DE cells are stimulated with FGF4 and BMP2 [41], while intestinal cell differentiation requires treatment with FGF4 and WNT3a in three dimensional culture conditions [42]. Pancreatic cells have been derived by sequential treatment of DE cells with FGF10 and KAAD-cyclopamine followed by retinoic acid [43].

The derivation of multipotent mesoderm progenitors has been achieved by treatment of hPSCs with BMP4 and Activin A [44, 45]. Interestingly, the progression towards defined differentiation conditions for mesoderm progenitors includes the use of synthetic substrates functionalized with peptide ligands for α5β1 and α6β1 integrins instead of Matrigel^{TM} [46]. To induce differentiation towards primitive streak-mesendoderm, the precursor of mesoderm, hPSCs are treated with Activin A, Wnt3a, FGF2 and BMP4. Subsequently, to reduce expression of endoderm genes in these populations, Activin A and Wnt3a are substituted with follistatin. In turn, directed-mesoderm cells can be induced to chondrocytes by subsequent treatment with GFD5 instead of BMP4 [47]. Effective cardiomyocyte differentiation of hPSCs has been achieved with temporal modulation of canonical Wnt signaling by treatment with Gsk3 inhibitors followed by inhibitor of Wnt production-4 (IWP4) supplementation. Alternatively, similar results can be obtained when the later chemical inhibitor is replaced by shRNA inhibition of *β-catenin* [48].

2.4 Derivation of Human Induced Pluripotent Stem Cells

The discovery that somatic cells could be reprogrammed into iPSCs has been recognized as a milestone in finding the true potential of cells in disease modeling, drug screening and regenerative medicine. hiPSCs were first derived from adult human dermal fibroblasts by transducing cells with four preprogramming factors, *OCT4*, *SOX2*, *LKF4* and *C-MYC* into the

cells [2]. Other combinations of reprogramming factors such as OCT4, SOX2, NANOG and Lin 28 have also been found able to redirect human somatic cells into hiPSCs by a lentiviral delivery system [3]. However, the low reprogramming efficiency (~0.1%) [2, 3, 49] and the risk of insertional mutations by genomic integration of these reprogramming factors are the major challenges in the field [50].

Alternative approaches have been applied for generating "safer" hiPSCs by avoiding vector sequences that may become integrated into the cell genome. Non-integrating viruses such as adenoviruses and Sendai viruses have been used as expression vectors in hiPSC-reprogramming. Compared to adenoviruses with very low hiPSC-reprogramming efficiency (0.0002%) [51], Sendai viruses are able to reprogram more types of somatic cells into hiPSCs with large amounts of protein production and significantly higher reprogramming efficiency (~1%) [52-54]. Using non-viral methods in hiPSC-reprogramming is another major trend to prevent genomic integration. For example, mRNAs of the reprogramming factors were manufactured using *in vitro* transcription (IVT) reactions and transfected into human fibroblasts to generate hiPSCs, resulting in high reprogramming efficiency (1.4%). However, this method is labor and cost-intensive, and has been validated only in one somatic cell type [55]. In addition, proteins of the reprogramming factors were delivered into human fibroblasts by an *E. Coli* expression system for hiPSC generation. Minicircle DNA vectors containing the promoter and cDNA of the reprogramming factors were also transfected into human adipose stromal cells to derive hiPSC [56]. The major limits for using proteins and Minicircle vectors in hiPSC derivation are their poor reprogramming efficiency (~0.006%) and validation in few cell types.

Besides the significant impact of reprogramming approaches including different combinations of reprogramming factors [3, 57, 58], the efficiency of hiPSC derivation is also related to factors

such as parental cell types, cell plating density and culture medium. Numerous molecules have been demonstrated to increase the hiPSC-reprogramming efficiency through different mechanisms: valproic acid and sodium butyrate inhibit histone deacetylation [59, 60]; Vitamin C and Rho-associated coiled coil forming protein serine/threonine kinase (ROCK) inhibitor promotes cell survival [61, 62]; PD0325901 blocks MEK pathway, while SB43152 inhibits TGFβ pathway [63]; PS48 and Oxygen (5%) promotes glycolysis [64, 65]. In addition, a recent study demonstrated the benefit of sequential introduction of reprogramming factors in which a sequential EMT-MET (epithelial-to-mesenchymal transition followed by mesenchymal-to-epithelial transition) mechanism increased reprogramming efficiency [66]. Taking the above factors into consideration can optimize protocols in hiPSC-reprogramming.

2.5 New Trends in Inducing Specific Cell Lineages

The observation that genetic manipulation can be used to induce specific cell lineage fate is reinforced by the recent development of hiPSCs by overexpressing key transcription factors that are able to redirect the cell-fate of somatic cells [2, 3]. This has opened an exciting new avenue of research on directing the fate of somatic cells into specific cell types without passing through a pluripotent state. One early example of direct reprogramming, even before the derivation of iPSCs, was the generation of induced-skeletal muscle cells by overexpression of *MyoD* in fibroblasts and other somatic cells, suggesting that this transcription factor is a master regulator of myogenesis [67]. Subsequently, the reprogramming of fibroblasts into other specific cell types has been reported. Cardiac myocytes, for example, have been induced from fibroblasts after the overexpression of three developmental transcription factors, *GATA4, MEF2C* and *TBX5* [68].

The direct generation of proliferative neuronal precursor cells and functionally distinct neuronal subtypes from mouse and human fibroblasts has been described by forced expression of selected transcriptions factors. Neuronal precursor cells capable of self-renewal and differentiation into neurons, astrocytes and oligodendrocytes have been induced by reprogramming fibroblasts with combinations of transcription factors that include *SOX2, FOXG1* and *BRN2* [69] or *BRN4/POU3f4*, *SOX2, KLF4, C-MYC* and *E47/TCF3* [70]. Interestingly, *SOX2* seems to function as a master regulator in the neuronal stem cell fate, since its single overexpression is able to induce multipotent neural stem cells [71]. Conversely, overexpression of *MYT1l* and *BRN2* in combination with microRNA-124 induce the generation of functional neurons that exhibit typical neuronal morphology, marker gene expression, generate action potentials and produce functional synapses between each other [72]. Induction of dopaminergic neurons has been reported by force expression of *MASH1* (also known as *ASCL1*), *NURR1* (also known as *NR4A2*) and *LMX1a* [73], while the induction into spinal motor neurons required the use of seven factors: *ASCL1, BRN2, MYT1l, LHX3, HB9, ISL1* and *NGN2* [74]. In contrast, the induction of neural crest stem cells (NCSC) with capacity to differentiate into multiple neural crest-derived mesenchymal and neuronal lineages has been achieved by the single ectopic expression of *Notch1* in melanocytes [75]. NCSCs are precursors of melanocytes, which indicates that the later cells may already have NCSC-related pathways that become activated by a single master regulator. Importantly, direct lineage reprogramming is possible between cell types with different germ layer origins. For example, it has been demonstrated that terminally differentiated hepatocytes (endoderm) can be induced into neurons (ectoderm) using the same neuronal transcription factors (*ASCL1, BRN2, MYT1l*) that will convert fibroblasts—which may have a mesoderm-neural crest origin—into induced-neurons [76].

It has been observed that during the reprogramming of fibroblasts to iPSCs, subpopulations of cellular intermediates emerge that co-express genes associated with differentiated lineages. Those subpopulations fail to establish a pluripotent state, but have the potential to be re-directed into specified cell lineages with appropriated signaling inputs. In this way, fibroblasts with forced expression of *OCT4* and treatment with FLT3 and SCF are directed into multi-lineage blood progenitors that give rise to granulocytic, monocytic, megakaryocytic and erythroid lineages with *in vivo* engraftment capacity [77]. Similarly, transient transduction of *OCT4, SOX2, KLF4* and *C-MYC* into fibroblasts followed by treatment with FGF2, EGF and FGF4 induces transdifferentiation into neuronal progenitor cells [78]. In contrast, when followed by inhibition of the JAK-STAT pathway, cardiomyocyte formation is induced [79].

2.6 The Transcriptional Regulatory Network of Pluripotency

Appropriate culture conditions and approaches are essential to support the pluripotency and self-renewal of hPSCs. From a molecular biological perspective, this pluripotent state is maintained by a network of transcriptional factors and signaling pathways.

The transcription factors OCT4, SOX2 and NANOG are known as gatekeepers of pluripotency in hPSCs because of their specific expression pattern and essential roles in hPSCs and early development [80-84]. Studies demonstrate that down-regulation of these genes in hPSCs induces differentiation, while overexpression of the genes support hPSC self-renewal and pluripotency. OCT4, SOX2 and NANOG compose the core transcriptional regulatory circuitry in hPSCs by co-occupying a substantial portion of their target genes, many of which encode transcription factors strongly associate with pluripotency and development. Interestingly, OCT4, SOX2 and NANOG also co-bind to the promoters of their own genes and form positive auto-regulatory

loops [85]. The finding of this transcriptional regulatory circuitry including auto-regulatory and feed-forward loops not only provides new insight into the molecular mechanism by which OCT4, SOX2 and NANOG support hPSC pluripotency, but also indicates the complexity of the pluripotency regulatory network.

Although core transcription factors such as OCT4, SOX2 and NANOG are found to play critical roles in both mouse and human PSCs, the pluripotency regulatory networks contain substantial differences between the two species. For example, studies suggest that fibroblast growth factor 2 (FGF2) and Activin/Nodal signaling pathways are essential for hPSC maintenance, while which is not required in mPSCs [28, 34, 86-90]. In addition, the protein PRDM14 has been identified as an effective pluripotency regulator in hPSCs but not in mPSCs because PRDM14 enhances *OCT4* expression in hPSCs and induces differentiation when being down-regulated. These results were not found in mPSCs [91-93]. However, compared to mPSCs, less is known about the pluripotency regulatory network in hPSCs. More studies are needed to identify new pluripotency regulatory factors and characterize novel signaling pathways supporting hPSC self-renewal.

2.7 Figures

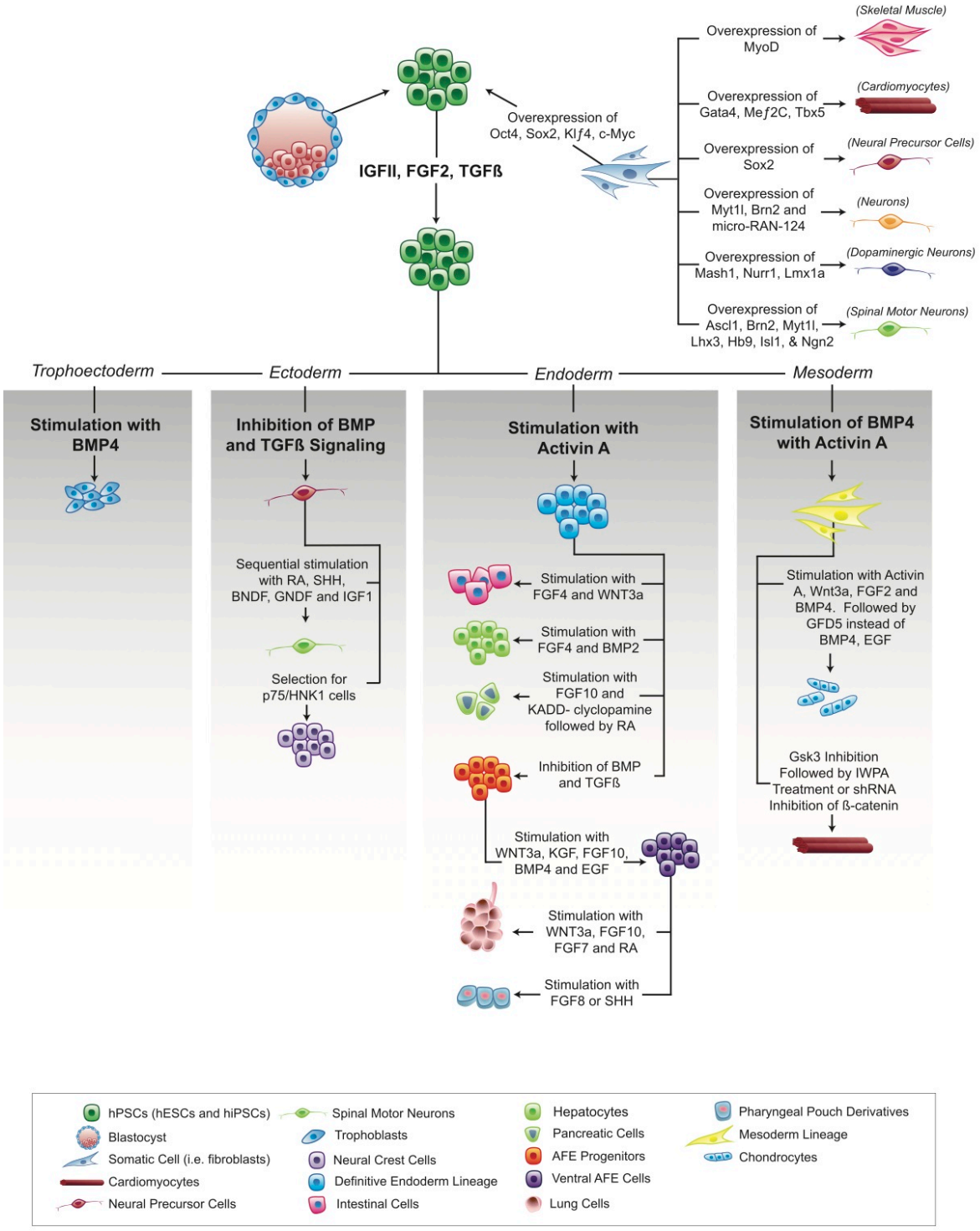
(Skeletal Muscle)
Overexpression of MyoD
(Cardiomyocytes)
Overexpression of Gata4, Mef2C, Tbx5
(Neural Precursor Cells)
Overexpression of Sox2
(Neurons)
Overexpression of Myt1l, Brn2 and micro-RAN-124
(Dopaminergic Neurons)
Overexpression of Mash1, Nurr1, Lmx1a
(Spinal Motor Neurons)
Overexpression of Ascl1, Brn2, Myt1l, Lhx3, Hb9, Isl1, & Ngn2
Overexpression of Oct4, Sox2, Klf4, c-Myc
IGFII, FGF2, TGFß
Trophoectoderm
Ectoderm
Endoderm
Mesoderm
Stimulation with BMP4
Inhibition of BMP and TGFß Signaling
Sequential stimulation with RA, SHH, BNDF, GNDF and IGF1
Selection for p75/HNK1 cells
Stimulation with Activin A
Stimulation with FGF4 and WNT3a
Stimulation with FGF4 and BMP2
Stimulation with FGF10 and KADD- cyclopamine followed by RA
Inhibition of BMP and TGFß
Stimulation with WNT3a, KGF, FGF10, BMP4 and EGF
Stimulation with WNT3a, FGF10, FGF7 and RA
Stimulation with FGF8 or SHH
Stimulation of BMP4 with Activin A
Stimulation with Activin A, Wnt3a, FGF2 and BMP4. Followed by GFD5 instead of BMP4, EGF
Gsk3 Inhibition Followed by IWPA Treatment or shRNA Inhibition of ß-catenin
hPSCs (hESCs and hiPSCs)
Blastocyst
Somatic Cell (i.e. fibroblasts)
Cardiomyocytes
Neural Precursor Cells
Spinal Motor Neurons
Trophoblasts
Neural Crest Cells
Definitive Endoderm Lineage
Intestinal Cells
Hepatocytes
Pancreatic Cells
AFE Progenitors
Ventral AFE Cells
Lung Cells
Pharyngeal Pouch Derivatives
Mesoderm Lineage
Chondrocytes

Figure 2-1. Controlled cell lineage induction by manipulation of signaling pathways and gene expression *in vitro*. This illustration shows how human pluripotent stem cells (hPSC) - human embryonic stem cells (hESC) and human induced pluripotent stem cells (hiPSC) - can be maintained in the pluripotent state or directed into specific cell lineages by manipulating key signaling pathways and gene expression. hESCs are derived from the inner cell mass of the blastocyst, while hiPSCs are induced by overexpression of pluripotent genes in somatic cells (top center). Similarly, overexpression of other specific genes in somatic cells can induce their reprogramming into different cell identities (top right). Both hPSCs can be directed into derivatives of the three germ layers (ectoderm, endoderm and mesoderm) and trophoectoderm by sequential stimulation and inhibition of signaling pathways with morphogens and chemical inhibitors (bottom). IGF: insulin-like growth factor, FGF: fibroblast growth factor, TGFβ: transforming growth factor β; BMP: bone morphogenetic protein, RA: retinoic acid, SHH: sonic hedge-hoc, BNDF: brain-derived neurotrophic factor, GNDF: glial-derived neurotrophic factor, EGF: epidermal growth factor GDF: growth differentiation factor. *Credit: Xu Qian, et al. J Dent Res 2013;92:956-62*

2.8 References

[1] Thomson JA, Itskovitz-Eldor J, Shapiro SS et al. Embryonic stem cell lines derived from human blastocysts. Science 1998;282:1145-7.

[2] Takahashi K, Tanabe K, Ohnuki M et al. Induction of pluripotent stem cells from adult human fibroblasts by defined factors. Cell 2007;131:861-72.

[3] Yu J, Vodyanik MA, Smuga-Otto K et al. Induced pluripotent stem cell lines derived from human somatic cells. Science 2007;318:1917-20.

[4] Nichols J, Smith A. Naive and primed pluripotent states. Cell Stem Cell 2009;4:487-92.

[5] Mahy B, Dykewicz C, Fisher-Hoch S et al. Virus zoonoses and their potential for contamination of cell cultures. Dev Bio Stand 1991;75:183-9.

[6] Martin MJ, Muotri A, Gage F et al. Human embryonic stem cells express an immunogenic nonhuman sialic acid. Nat Med 2005;11:228-32.

[7] Villa-Diaz LG, Pacut C, Slawny NA et al. Analysis of the Factors That Limit the Ability of Feeder-Cells to Maintain the Undifferentiated State of Human Embryonic Stem Cells. Stem Cells Dev 2008;18:641-51.

[8] Richards M, Tan S, Fong CY et al. Comparative evaluation of various human feeders for prolonged undifferentiated growth of human embryonic stem cells. Stem Cells 2003;21:546-56.

[9] Unger C, Gao S, Cohen M et al. Immortalized human skin fibroblast feeder cells support growth and maintenance of both human embryonic and induced pluripotent stem cells. Hum Reprod 2009;24:2567-81.

[10] Abraham S, Sheridan SD, Laurent LC et al. Propagation of human embryonic and induced pluripotent stem cells in an indirect co-culture system. Biochem Biophys Res Commun 2010;393:211-6.

[11] Xu C, Inokuma MS, Denham J et al. Feeder-free growth of undifferentiated human embryonic stem cells. Nat Biotechnol 2001;19:971-4.

[12] Braam SR, Zeinstra L, Litjens S et al. Recombinant vitronectin is a functionally defined substrate that supports human embryonic stem cell self-renewal via alphavbeta5 integrin. Stem Cells 2008;26:2257-65.

[13] Miyazaki T, Futaki S, Hasegawa K et al. Recombinant human laminin isoforms can support the undifferentiated growth of human embryonic stem cells. Biochem Biophys Res Commun 2008;375:27-32.

[14] Nagaoka M, Si-Tayeb K, Akaike T et al. Culture of human pluripotent stem cells using completely defined conditions on a recombinant E-cadherin substratum. BMC Dev Biol 2010;10:60.

[15] Villa-Diaz LG, Ross AM, Lahann J et al. Concise Review: The Evolution of human pluripotent stem cell culture: From feeder cells to synthetic coatings. Stem Cells 2013;31:1-7.

[16] Derda R, Li L, Orner BP et al. Defined substrates for human embryonic stem cell growth identified from surface arrays. ACS Chem Biol 2007;2:347-55.

[17] Klim JR, Li L, Wrighton PJ et al. A defined glycosaminoglycan-binding substratum for human pluripotent stem cells. Nat Methods 2010;7:989-94.

[18] Kolhar P, Kotamraju VR, Hikita ST et al. Synthetic surfaces for human embryonic stem cell culture. J Biotechnol 2010;146:143-6.

[19] Villa-Diaz LG, Nandivada H, Ding J et al. Synthetic polymer coatings for long-term growth of human embryonic stem cells. Nat Biotechnol 2010;28:581-3.

[20] Mei Y, Saha K, Bogatyrev SR et al. Combinatorial development of biomaterials for clonal growth of human pluripotent stem cells. Nat Mater 2010;9:768-78.

[21] Irwin EF, Gupta R, Dashti DC et al. Engineered polymer-media interfaces for the long-term self-renewal of human embryonic stem cells. Biomaterials 2011;32:6912-9.

[22] Li Y, Chuang E, Rodriguez R et al. Hydrogels as artificial matrices for human embryonic stem cell self-renewal. J Biomedical Mater Res A 2006;79:1-5.

[23] Brafman DA, Chang CW, Fernandez A et al. Long-term human pluripotent stem cell self-renewal on synthetic polymer surfaces. Biomaterials 2010;31:9135-44.

[24] Melkoumian Z, Weber JL, Weber DM et al. Synthetic peptide-acrylate surfaces for long-term self-renewal and cardiomyocyte differentiation of human embryonic stem cells. Nat Biotechnol 2010;28:606-10.

[25] Amit M, Carpenter MK, Inokuma MS et al. Clonally derived human embryonic stem cell lines maintain pluripotency and proliferative potential for prolonged periods of culture. Dev Biol 2000;227:271-8.

[26] Ludwig T, J AT. Defined, feeder-independent medium for human embryonic stem cell culture. Curr Protoc Stem Cell Biol 2007;Chapter 1:Unit 1C 2.

[27] Chen G, Gulbranson DR, Hou Z et al. Chemically defined conditions for human iPSC derivation and culture. Nat Methods 2011;8:424-9.

[28] Vallier L, Alexander M, Pedersen RA. Activin/Nodal and FGF pathways cooperate to maintain pluripotency of human embryonic stem cells. J Cell Sci 2005;118:4495-509.

[29] Bendall SC, Stewart MH, Menendez P et al. IGF and FGF cooperatively establish the regulatory stem cell niche of pluripotent human cells in vitro. Nature 2007;448:1015-21.

[30] Xu C, Rosler E, Jiang J et al. Basic fibroblast growth factor supports undifferentiated human embryonic stem cell growth without conditioned medium. Stem Cells 2005;23:315-23.

[31] Dvorak P, Dvorakova D, Koskova S et al. Expression and potential role of fibroblast growth factor 2 and its receptors in human embryonic stem cells. Stem Cells 2005;23:1200-11.

[32] James D, Levine AJ, Besser D et al. TGFbeta/activin/nodal signaling is necessary for the maintenance of pluripotency in human embryonic stem cells. Development 2005;132:1273-82.

[33] Sato N, Meijer L, Skaltsounis L et al. Maintenance of pluripotency in human and mouse embryonic stem cells through activation of Wnt signaling by a pharmacological GSK-3-specific inhibitor. Nat Med 2004;10:55-63.

[34] Xu RH, Peck RM, Li DS et al. Basic FGF and suppression of BMP signaling sustain undifferentiated proliferation of human ES cells. Nat Methods 2005;2:185-90.

[35] Brown SE, Tong W, Krebsbach PH. The derivation of mesenchymal stem cells from human embryonic stem cells. Cells Tissues Organs 2009;189:256-60.

[36] Xu RH, Chen X, Li DS et al. BMP4 initiates human embryonic stem cell differentiation to trophoblast. Nat Biotechnol 2002;20:1261-4.

[37] Chambers SM, Fasano CA, Papapetrou EP et al. Highly efficient neural conversion of human ES and iPS cells by dual inhibition of SMAD signaling. Nat Biotechnol 2009;27:275-80.

[38] Li XJ, Du ZW, Zarnowska ED et al. Specification of motoneurons from human embryonic stem cells. Nat Biotechnol 2005;23:215-21.

[39] D'Amour KA, Agulnick AD, Eliazer S et al. Efficient differentiation of human embryonic stem cells to definitive endoderm. Nat Biotechnol 2005;23:1534-41.

[40] Green MD, Chen A, Nostro MC et al. Generation of anterior foregut endoderm from human embryonic and induced pluripotent stem cells. Nat Biotechnol 2011;29:267-72.

[41] Cai J, Zhao Y, Liu Y et al. Directed differentiation of human embryonic stem cells into functional hepatic cells. Hepatology 2007;45:1229-39.

[42] Spence JR, Mayhew CN, Rankin SA et al. Directed differentiation of human pluripotent stem cells into intestinal tissue in vitro. Nature 2011;470:105-9.

[43] D'Amour KA, Bang AG, Eliazer S et al. Production of pancreatic hormone-expressing endocrine cells from human embryonic stem cells. Nat Biotechnol 2006;24:1392-401.

[44] Evseenko D, Zhu Y, Schenke-Layland K et al. Mapping the first stages of mesoderm commitment during differentiation of human embryonic stem cells. Proc Natl Acad Sci U S A 2010;107:13742-7.

[45] Yao S, Chen S, Clark J et al. Long-term self-renewal and directed differentiation of human embryonic stem cells in chemically defined conditions. Proc Natl Acad Sci U S A 2006;103:6907-12.

[46] Liu Y, Wang X, Kaufman DS et al. A synthetic substrate to support early mesodermal differentiation of human embryonic stem cells. Biomaterials 2011;32:8058-66.

[47] Oldershaw RA, Baxter MA, Lowe ET et al. Directed differentiation of human embryonic stem cells toward chondrocytes. Nat Biotechnol 2010;28:1187-94.

[48] Lian X, Hsiao C, Wilson G et al. Robust cardiomyocyte differentiation from human pluripotent stem cells via temporal modulation of canonical Wnt signaling. Proc Natl Acad Sci U S A 2012;109:E1848-57.

[49] Park IH, Zhao R, West JA et al. Reprogramming of human somatic cells to pluripotency with defined factors. Nature 2008;451:141-6.

[50] Selvaraj V, Plane JM, Williams AJ et al. Switching cell fate: the remarkable rise of induced pluripotent stem cells and lineage reprogramming technologies. Trends Biotechnol 2010;28:214-23.

[51] Zhou WB, Freed CR. Adenoviral Gene Delivery Can Reprogram Human Fibroblasts to Induced Pluripotent Stem Cells. Stem Cells 2009;27:2667-74.

[52] Fusaki N, Ban H, Nishiyama A et al. Efficient induction of transgene-free human pluripotent stem cells using a vector based on Sendai virus, an RNA virus that does not integrate into the host genome. Proc Jpn Acad Ser B Phys Biol Sci 2009;85:348-62.

[53] Seki T, Yuasa S, Oda M et al. Generation of induced pluripotent stem cells from human terminally differentiated circulating T cells. Cell Stem Cell 2010;7:11-4.

[54] Ban H, Nishishita N, Fusaki N et al. Efficient generation of transgene-free human induced pluripotent stem cells (iPSCs) by temperature-sensitive Sendai virus vectors. Proc Natl Acad Sci U S A 2011;108:14234-9.

[55] Warren L, Manos PD, Ahfeldt T et al. Highly efficient reprogramming to pluripotency and directed differentiation of human cells with synthetic modified mRNA. Cell Stem Cell 2010;7:618-30.

[56] Narsinh KH, Jia FJ, Robbins RC et al. Generation of adult human induced pluripotent stem cells using nonviral minicircle DNA vectors. Nature Protocols 2011;6:78-88.

[57] Hanna J, Saha K, Pando B et al. Direct cell reprogramming is a stochastic process amenable to acceleration. Nature 2009;462:595-601.

[58] Liao J, Wu Z, Wang Y et al. Enhanced efficiency of generating induced pluripotent stem (iPS) cells from human somatic cells by a combination of six transcription factors. Cell Res 2008;18:600-3.

[59] Mali P, Chou BK, Yen J et al. Butyrate greatly enhances derivation of human induced pluripotent stem cells by promoting epigenetic remodeling and the expression of pluripotency-associated genes. Stem Cells 2010;28:713-20.

[60] Huangfu D, Osafune K, Maehr R et al. Induction of pluripotent stem cells from primary human fibroblasts with only Oct4 and Sox2. Nat Biotechnol 2008;26:1269-75.

[61] Esteban MA, Wang T, Qin B et al. Vitamin C enhances the generation of mouse and human induced pluripotent stem cells. Cell Stem Cell 2010;6:71-9.

[62] Valamehr B, Abujarour R, Robinson M et al. A novel platform to enable the high-throughput derivation and characterization of feeder-free human iPSCs. Sci Rep 2012;2:213.

[63] Lin T, Ambasudhan R, Yuan X et al. A chemical platform for improved induction of human iPSCs. Nat Methods 2009;6:805-8.

[64] Zhu S, Li W, Zhou H et al. Reprogramming of human primary somatic cells by OCT4 and chemical compounds. Cell Stem Cell 2010;7:651-5.

[65] Yoshida Y, Takahashi K, Okita K et al. Hypoxia enhances the generation of induced pluripotent stem cells. Cell Stem Cell 2009;5:237-41.

[66] Liu X, Sun H, Qi J et al. Sequential introduction of reprogramming factors reveals a time-sensitive requirement for individual factors and a sequential EMT-MET mechanism for optimal reprogramming. Nat Cell Biol 2013;15:829-38.

[67] Weintraub H, Tapscott SJ, Davis RL et al. Activation of muscle-specific genes in pigment, nerve, fat, liver, and fibroblast cell lines by forced expression of MyoD. Proc Natl Acad Sci U S A 1989;86:5434-8.

[68] Ieda M, Fu JD, Delgado-Olguin P et al. Direct reprogramming of fibroblasts into functional cardiomyocytes by defined factors. Cell 2010;142:375-86.

[69] Lujan E, Chanda S, Ahlenius H et al. Direct conversion of mouse fibroblasts to self-renewing, tripotent neural precursor cells. Proc Natl Acad Sci U S A 2012;109:2527-32.

[70] Han DW, Tapia N, Hermann A et al. Direct reprogramming of fibroblasts into neural stem cells by defined factors. Cell Stem Cell 2012;10:465-72.

[71] Ring KL, Tong LM, Balestra ME et al. Direct reprogramming of mouse and human fibroblasts into multipotent neural stem cells with a single factor. Cell Stem Cell 2012;11:100-9.

[72] Ambasudhan R, Talantova M, Coleman R et al. Direct reprogramming of adult human fibroblasts to functional neurons under defined conditions. Cell Stem Cell 2011;9:113-8.

[73] Caiazzo M, Dell'Anno MT, Dvoretskova E et al. Direct generation of functional dopaminergic neurons from mouse and human fibroblasts. Nature 2011;476:224-7.

[74] Son EY, Ichida JK, Wainger BJ et al. Conversion of mouse and human fibroblasts into functional spinal motor neurons. Cell Stem Cell 2011;9:205-18.

[75] Zabierowski SE, Baubet V, Himes B et al. Direct reprogramming of melanocytes to neural crest stem-like cells by one defined factor. Stem Cells 2011;29:1752-62.

[76] Marro S, Pang ZP, Yang N et al. Direct lineage conversion of terminally differentiated hepatocytes to functional neurons. Cell Stem Cell 2011;9:374-82.

[77] Szabo E, Rampalli S, Risueno RM et al. Direct conversion of human fibroblasts to multilineage blood progenitors. Nature 2010;468:521-6.

[78] Kim J, Efe JA, Zhu S et al. Direct reprogramming of mouse fibroblasts to neural progenitors. Proc Natl Acad Sci U S A 2011;108:7838-43.

[79] Efe JA, Hilcove S, Kim J et al. Conversion of mouse fibroblasts into cardiomyocytes using a direct reprogramming strategy. Nat Cell Biol 2011;13:215-22.

[80] Hay DC, Sutherland L, Clark J et al. Oct-4 knockdown induces similar patterns of endoderm and trophoblast differentiation markers in human and mouse embryonic stem cells. Stem Cells 2004;22:225-35.

[81] Hart AH, Hartley L, Ibrahim M et al. Identification, cloning and expression analysis of the pluripotency promoting Nanog genes in mouse and human. Dev Dyn 2004;230:187-98.

[82] Hyslop L, Stojkovic M, Armstrong L et al. Downregulation of NANOG induces differentiation of human embryonic stem cells to extraembryonic lineages. Stem Cells 2005;23:1035-43.

[83] Fong H, Hohenstein KA, Donovan PJ. Regulation of self-renewal and pluripotency by Sox2 in human embryonic stem cells. Stem Cells 2008;26:1931-8.

[84] Wang Z, Oron E, Nelson B et al. Distinct lineage specification roles for NANOG, OCT4, and SOX2 in human embryonic stem cells. Cell Stem Cell 2012;10:440-54.

[85] Boyer LA, Lee TI, Cole MF et al. Core transcriptional regulatory circuitry in human embryonic stem cells. Cell 2005;122:947-56.

[86] Armstrong L, Hughes O, Yung S et al. The role of PI3K/AKT, MAPK/ERK and NFkappabeta signalling in the maintenance of human embryonic stem cell pluripotency and viability highlighted by transcriptional profiling and functional analysis. Hum Mol Genet 2006;15:1894-913.

[87] Li J, Wang GW, Wang CY et al. MEK/ERK signaling contributes to the maintenance of human embryonic stem cell self-renewal. Differentiation 2007;75:299-307.

[88] Vallier L, Reynolds D, Pedersen RA. Nodal inhibits differentiation of human embryonic stem cells along the neuroectodermal default pathway. Dev Biol 2004;275:403-21.

[89] Beattie GM, Lopez AD, Bucay N et al. Activin A maintains pluripotency of human embryonic stem cells in the absence of feeder layers. Stem Cells 2005;23:489-95.

[90] James D, Levine AJ, Besser D et al. TGF beta/activin/nodal signaling is necessary for the maintenance of pluripotency in human embryonic stem. Development 2005;132:1273-82.

[91] Chia NY, Chan YS, Feng B et al. A genome-wide RNAi screen reveals determinants of human embryonic stem cell identity. Nature 2010;468:316-20.

[92] Yamaji M, Seki Y, Kurimoto K et al. Critical function of Prdm14 for the establishment of the germ cell lineage in mice. Nat Genet 2008;40:1016-22.

[93] Ma Z, Swigut T, Valouev A et al. Sequence-specific regulator Prdm14 safeguards mouse ESCs from entering extraembryonic endoderm fates. Nat Struct Mol Biol 2011;18:120-7.

CHAPTER 3

ENHANCEMENT OF THE PROPAGATION OF HUMAN EMBRYONIC STEM CELLS BY MODIFICATIONS IN THE GEL ARCHITECTURE OF PMEDSAH POLYMER COATINGS

3.1 Abstract

Well-defined culture conditions are essential for realizing the full potential of human embryonic stem cells (hESCs) in regenerative medicine where large numbers of cells are required. Synthetic polymers, such as poly[2-(methacryloyloxy) ethyl dimethyl-(3-sulfopropyl) ammonium hydroxide] (PMEDSAH), offer multiple advantages over mouse embryonic fibroblasts (MEFs) and Matrigel^{TM} for hESC culture and expansion. However, there is limited understanding of the mechanisms by which hESCs are propagated on synthetic polymers coatings. Here, the effects of PMEDSAH gel architecture on hESC self-renewal were determined. By increasing the atom transfer radical polymerization (ATRP) reaction time, the thickness of PMEDSAH was increased and its internal hydrogel architecture was modified, while maintaining its overall chemical structure. A 105 nm thick ATRP PMEDSAH coating showed a significant increase in the expansion rate of hESCs. Theoretical calculations suggested that 20,000 hESCs cultured on this substrate could be expanded up to $4.7x10^9$ undifferentiated cells in five weeks. In addition, hESCs grown on ATRP PMEDSAH coatings retained pluripotency and displayed a normal

karyotype after long-term culture. These data demonstrate the importance of polymer physical properties in hESC expansion. This and similar modifications of PMEDSAH coatings may be used to obtain large populations of hESCs required for many applications in regenerative medicine.

3.2 Introduction

Because of the capacity to self-renew indefinitely and to differentiate into specialized cell types of all three germ layers and trophoectoderm, human embryonic stem cells (hESCs) have become a potential source of cells for regenerative medicine, tissue engineering, disease modeling and drug screening. However, the successful therapeutic application of hESCs and their derivatives is based on the ability to develop clinically compliant strategies for large-scale bioprocessing of therapeutically relevant cells [1-3].

Currently, the large-scale expansion methods for hESCs and induced pluripotent stem cells (iPSCs) are limited by xenogeneic components and poorly defined culture conditions that utilize feeder cells and other animal-based products to support hESC self-renewal [4-6]. To overcome these limitations, the use of human recombinant proteins like laminin isoforms -111, -332, 511, vitronectin, or E-cadherin have been tested for long-term maintenance of hESCs [7-9]. These findings suggest a trend in the evolution of hESC culture from feeder-cell dependence and ill-defined conditions, to feeder-free and defined microenvironments [10]. However, purification of human recombinant proteins is costly and significantly limits their potential for large-scale propagation of hESCs. Likewise, the inclusion of protein-based substrates adds a level of complexity to the study of the mechanisms by which a surface coating supports the pluripotency of hECSs.

Recently, synthetic substrates [11-19] have demonstrated high potential for large-scale expansion of hESCs because they exhibit the following effective features: completely defined chemical composition, stability during storage, reproducibly synthesized, cost-effectiveness, and compatibility with standard sterilization techniques [20]. Among these synthetic substrates is poly[2-(methacryloyloxy) ethyl dimethyl-(3-sulfopropyl) ammonium hydroxide] (PMEDSAH), a fully defined synthetic polymer coating, developed through a surface initiated graft polymerization technique, which has demonstrated effective capacity to support hESC self-renewal and expansion in long-term culture [14, 21].

Recent evidence suggests that physico-chemical properties, such as hydrophilicity [14], surface roughness [22] and stiffness [23, 24] can impact the capability of synthetic substrates to support hESC growth [10]. However, the mechanisms by which PMEDSAH and other synthetic substrates maintain self-renewal of hESCs are not yet clearly understood. Therefore, we hypothesized that the physical properties of PMEDSAH coatings, as determined by the interfacial architecture of the zwitterionic surface layer, can influence the self-renewal of hESCs. In this study, PMEDSAH films with different thicknesses were prepared on tissue culture polystyrene using a combination of chemical vapor deposition polymerization [24] and atom transfer radical polymerization (ATRP) [25]. The impact of gel architecture on hESC self-renewal was then tested on PMEDSAH polymer coatings over a range of thicknesses.

3.3 Materials and Methods

3.3.1 Synthetic Surface Preparation and Characterization

UVO-initiated Free Radical Polymerization

UVO-initiated free radical polymerization was carried out in a fume hood with connections for argon and vacuum. A 500 mL reaction vessel was degassed by vacuum for 60 minutes. While the reaction vessel was being evacuated, a monomer solution consisting of 0.25 M MEDSAH (Sigma Aldrich) was dissolved in a mixture of deionized water and ethanol (4:1, v/v). The solution was degassed for 40 minutes using an argon purge. Once the reaction vessel and solvent were degassed, the monomer solution was transferred to a reaction vessel and heated to 68-70°C. While the reaction vessel was being heated, TCPS dishes (BD Biosciences) were activated by UV ozone treatment (Jetlight Inc.) for 40 minutes to create initiation sites on the surface. Samples without functionalization that consisted of poly-p-xylylene coated silicon wafers and gold wafers were also added to the cell culture dishes to enable thickness and contact angle measurement. After activation, the dishes were transferred to a reaction vessel and the temperature was raised to 76-80°C. Surface-initiated polymerization occurred over a 2.5 hr time period under argon atmosphere at 76-80°C. Once the process was complete, TCPS plates and control samples were removed from the reaction vessel and were rinsed in a 1% saline (w/v) solution at 50 °C.

CVD and Ellipsometry

The initiator used for ATRP was synthesized through chemical vapor deposition (CVD) polymerization of 40 mg of [2.2]paracyclophane-4-methyl-2-bromoisobutyrate precursor, which was loaded into the sublimation zone. Sublimation occurred at 120°C, followed by pyrolysis at 540-550°C, after which a thin film of poly[(p-xylylene-4-methyl-2-bromoisobutyrate)-co-(p-xylylene)] was coated on the target substrates. The tissue culture polystyrene (TCPS) plates as well as surrogates (gold and silicon wafers) were placed on a rotating stage in the deposition chamber and were maintained at 15°C during CVD polymerization. Ellipsometry was performed

on the silicon wafers to measure thickness of the initiator coating before and after the ATRP. Film thickness was assessed with a multi-wavelength imaging null-ellipsometer (EP3 Nanofilm, Germany). Fixed values of the real (n=1.58) and imaginary (k=0) refractive index of the polymer coatings and the ellipsometric delta and psi were used to determine film thickness. After the reaction was completed, the thickness of PMEDSAH coating was calculated by subtracting the initial thickness from the post-reaction thickness.

Atom Transfer Radical Polymerization

Poly[2-(methacryloyloxy)ethyl dimethyl-(3-sulfopropyl)ammonium hydroxide] (PMEDSAH) (Monomer Polymer Dajac Labs, Trevose, PA) was polymerized using a ATRP procedure. Initiator coated substrates were prepared according to the CVD process described above. Initiator-coated samples and TCPS were placed in a glove bag and degassed using 3 cycles of vacuum-argon purge and left at room temperature under argon. A 4:1(v/v) mixture of methanol and water was degassed by three cycles of freeze-pump-thaw. Approximately 20% of the degassed solvent was transferred to a degassed flask. The monomer was then dissolved in the main flask and the copper/ligand mixture was dissolved in the second flask. After 10 minutes the catalyst mixture was added to the monomer solution and mixed thoroughly at room temperature. The polymerization solution was finally transferred to the glove bag and distributed among the TCPS and the surrogates, so that each substrate was submerged completely. The ATRP reaction was allowed to proceed for 1, 12, and 24 hours under argon atmosphere. After ATRP, surrogates and TCPS plates were rinsed with 1% sodium chloride solution and deionized water and dried. Residual copper was removed from the ATRP-modified surfaces by washing alternately with 5 mM ethylenedimaine tetracetic acid sodium salt (EDTA) and 5 mM calcium chloride solutions and finally with deionized water.

Contact Angle

Static contact angles of deionized water were measured using a contact angle goniometer (Ramé-Hart 200-F1 goniometer). Measurements were taken at three different locations and averaged.

Streaming Potential Measurement

Polymer coatings were prepared directly on polystyrene slides to measure surface charge. An electrokinetic analyser SurPASS (Anton Paar GmBH) was used in clamping cell mode to acquire zeta potential values of the samples across a 3-10 pH range. Two titrations were performed for each sample, one proceeding from the neutral to the acidic range and another from the neutral to the basic range. 0.1 M hydrochloric acid and 0.1M sodium hydroxide were used as titrants. 0.001 M potassium chloride was used as the electrolyte. pH changes were performed using an automated titration unit with pH being altered in steps of 0.3 with continuous stirring of the electrolyte solution. Streaming current was measured using Ag/AgCl electrodes and the helmohltz smoluchwski equation was used to compute the zeta potentials. Flow rates of 50-70 ml/minute were used at a pressure of 400 mbar and a gap of 100 microns between the sample and the polypropylene reference standard. Samples were rinsed for 3 minutes in between measurements at different pH points.

Atomic Force Microscopy (AFM)

The surface roughness of the PMEDSAH coatings was quantified via atomic force microscopy (AFM) using a Dimension Icon (Bruker, Madison, WI). Measurements were taken in tapping mode at room temperature in air using NSC15 cantilevers (MikroMasch, San Jose, CA) with resonant frequency and spring constants of 20-75 N/m and 265-400 kHz, respectively as probe tips. Measurements were taken at 1 Hz scan rate over a 2x2 micron area. Roughness values in the

form of root mean square roughness (R_a) were acquired through a statistical analysis performed by the AFM software (NanoScope Analysis) by averaging over the scanned region. Three values were acquired for each sample and averaged.

3.3.2 Preparation of Matrigel-coated Substrates

Matrigel (BD BioSciences) was diluted to a concentration of 0.1 mg/ml in cold Dulbecco's modified Eagle's medium/F12 (DMEM/F12; GIBCO) and then applied to tissue culture polystyrene (TCPS) dishes (35 mm; BD Falcon). The coating was allowed to polymerize during 2 h incubation at room temperature. Before plating cells, excess matrigel-DMEM/F12 solution was aspirated and the dishes were washed with sterilized Dulbecco's phosphate buffered saline (D-PBS).

3.3.3 hESC Culture

hESCs (H9 and H1, WiCell Research Institute, Madison, WI; CHB10, Children's Hospital Corporation, Boston, MA) were cultured on PMEDSAH with human-cell-conditioned medium (HCCM, Global Stem) supplemented with 5 ng/mL of human recombinant basic fibroblast growth factor (bFGF; Invitrogen™). Differentiated cells were mechanically removed using a sterile pulled-glass pipet under a stereomicroscope (LeicaMZ9.5, Leica Microsystems Inc., Buffalo Grove, IL). Undifferentiated colonies were cut and collected as small cell clusters into a 1.5 mL centrifuge tube. After centrifugation and brief washing with PBS, cells were treated with 0.5 mL 0.25% Trypsin-EDTA (GIBCO) at 37 °C. The trypsinization was terminated by the addition of 1ml HCCM and brief centrifugation. The cell pellet was dispersed in HCCM supplemented with 5 ng/mL bFGF and 10 μM of ROCK inhibitor (Sigma) [26] and passed through a 40 μm nylon mesh cell strainer (BD Biosciences, Bedford, MA) to remove large cell

aggregates. Single hESCs were counted and 20,000 cells (2000 cells/ cm^2) were plated on matrigel, PMEDSAH and three types of ATRP PMEDSAH (25nm, 105nm and 176nm thick) coated-dishes and cultured for 7 days. The culture medium was replaced every other day. Single hESCs were passaged once a week for 5 consecutive weeks using the same method without removing differentiated colonies before passage.

3.3.4 Alkaline Phosphatase Assay

An Alkaline Phosphatase Detection Kit (Millipore) was used for phenotypic assessment of hESC. Briefly, on day 7, cells were fixed with 4% paraformaldehyde in PBS for 1-2 minutes, then rinsed and incubated in staining solution in the dark at room temperature for 15 minutes. Cells were rinsed and covered with 1x PBS to prevent drying prior to quantitative analysis. Undifferentiated colonies were identified by specific alkaline phosphatase staining.

3.3.5 Quantitative Analysis of Undifferentiated Colony Formation and the Total Cell Number

ImageJ software (http://rsb.nih.gov/ij) was used to count the number and area of undifferentiated colonies stained by alkaline phosphatase. The total number of cells grown on each dish was counted with a hemocytometer at the time of passage during the 5 consecutive weekly passages. A theoretical yield of total cell number of hESCs obtained on different substrates was calculated assuming that all cells would be passaged each week instead of the only 20,000 single cells that were done. The theoretical yield of cells was determined with the formula $CN_{(n+1)} = CN_n \times TN_{(n+1)}/20000$, in which CN is the calculated total cell number, TN is the total cell number and n is the passage number.

3.3.6 Flow Cytometry Analysis

hESCs cultured on different substrates from week 1 to 5 were washed with PBS and harvest by incubation in 0.25% trypsin-EDTA (GIBCO). The trypsinization was terminated by adding1ml HCCM and the cells were incubated first with human IgG to block un-specific binding and then with human/mouse SSEA-4 PE-conjugated antibody (R&D systems) and analyzed by flow cytometry. Analysis was carried out with MoFlo® Astrios™ (Beckman Coulter) using standard procedures. Background fluorescence and autofluorescence were determined using cells incubated with Mouse IgG1 phycoerythrin isotype Control (R&D systems).

3.3.7 Immunofluorescence Staining

Cells grown on different substrates were fixed in 4% paraformaldehyde for 30 min at room temperature and then permeabilized with 0.1% Triton X-100 for 10 min. Primary antibodies raised against SSEA-4 (Santa Cruz Biotechnology), OCT3/4 (Santa Cruz Biotechnology), SOX2 (Millipore), TRA-1-60 (Santa Cruz Biotechnology), TRA-1-81 (Millipore), and NANOG (Abcam) were diluted in 1% normal serum and incubated overnight at 4°C and detected with respective secondary antibodies. Sample images were captured using a Nikon TE2000-S inverted microscope with a Nikon DS-Ri1 camera.

3.3.8 RNA Isolation and Quantitative RT-PCR

Cells grown on different substrates were manually scraped from dishes and pelleted by centrifugation. RNA was isolated and purified using the RNA easy Mini-Kit (Qiagen) following the manufacturer's protocol. RNA quality and concentration was checked with a Synergy NEO HTS Multi-Mode Microplate Reader (BioTek Instruments, Winooski, VT).

Reverse transcription from 1 mg of total RNA into cDNA was done using SuperScript™ III First-Strand Synthesis SuperMix (Invitrogen™). Quantitative PCR was performed using TaqMan probes (Applied Biosystems) and TaqMan Universal PCR Master Mix (Applied Biosystems) on 7900 HT Fast Real Time PCR system (Applied Biosystems). Gene expression data was normalized to the expression levels of GAPDH, and calculated using the delta-delta *cT* expression level.

3.3.9 Analysis of hESC Pluripotency

At passage 5, pluripotency of hESCs was tested by embryoid body (EB) formation and directed cell-lineage differentiation. EB formation was achieved by hESC clusters cultured in suspension in DMEM (Life Technologies) supplemented with 10% FBS for 10 days to promote differentiation. Directed cell-lineage differentiation was performed on matrigel using the following protocols [27]. hESCs were induced to differentiate in chemically defined medium (CDM) base consisting of DMEM/F12 (Invitrogen) supplemented with 1X N2 (Invitrogen), 1X B27 (Invitrogen), 0.11 mM 2-mercaptoethanol, 1 mM nonessential amino acids, 2 mM L-glutamine, and 0.5 mg/ml BSA (fraction V; Sigma Aldrich). To induce definitive endoderm (pancreatic differentiation) 100 ng/ml human recombinant activin A (STEMGENT) was added to CDM and cells were cultured in this condition for 6 days, followed by culture in CDM without activin A for an additional 9 days. For mesoderm (cardiomyocyte differentiation) cells were cultured in CDM supplemented with 50 ng/ml human recombinant BMP4 (STEMGENT) and 50 ng/ml human recombinant activin A (STEMGENT) for 4 days, then further cultured in CDM with no activin A and BMP4 for another 10 days. For ectoderm (neuronal differentiation), 100 ng/ml human recombinant Noggin (STEMGENT) was added to the CDM and cells were cultured in this condition for 8 days.

3.3.10 Cytogenetic Evaluation

After 5 weeks of cell culture, standard G-band analysis on at least 20 cells was performed on cells cultured on 105nm ATRP PMEDSAH by Cell Line Genetics (Madison, WI) using standard protocols.

3.3.11 Data Analysis

Three independent replicates for each experiment were performed. Two data sets were compared using unpaired student t-test function in Excel (Microsoft, Seattle, WA) to calculate p values. Multiple data sets were compared using one way ANOVA analysis followed by the Tukey's post hoc test to calculate p values. Levels of statistical significance were set at $p < 0.05$.

3.4 Results

3.4.1 Differences in Properties of PMEDSAH Coatings

PMEDSAH polymer coatings were fabricated using two different surface-initiated polymerization procedures: UVO-initiated free radical polymerization (UVO-grafting) [21] and atom transfer radical polymerization (ATRP) conducted at three different reaction times. Physicochemical comparison between these four coatings was based on film thickness, wettability, surface roughness and zeta potential measurements (Figure 3-1). The thickness of films prepared through UVO-grafting was of 25 ± 6.5 nm. In contrast, ATRP-prepared coatings displayed a gradual augmentation in film thickness with increasing reaction time: 25 ± 3 nm in a 1 hour-reaction; 105 ± 8 nm in a 12 hour-reaction; and up to 176 ± 18.2 nm in a 24 hour reaction (Figure 3-1A). The contact angle of UVO-grafted PMEDSAH was 16.6 ± 1.6°, while ATRP film thicknesses that ranged between 25 nm and 176 nm demonstrated an increase in the contact

angle from 21.9 ± 9.4° to 75.3 ± 4° (Figure 3-1B). In several studies, engineering roughness into soft cell culture substrates in the form of nano-grooves and pillars has been shown to play a role in mediating cell adhesion [28]. Thus, the roughness of the four coatings was quantified with a topographical examination using atomic force microscopy. Differences in roughness, as measured by root-mean-square roughness values, were not statistically significant among the four coatings (Figure 3-1A). The zeta potential of grafted PMEDSAH was less negative than ATRP coatings. In addition, the 25 nm and 176 nm thick PMEDSAH coatings exhibited more negative charge than the 105nm thick coating in the neutral range of pH values. The isoelectric point of the 105 nm thick ATRP coating shifted slightly to the right from that of the other two coatings, indicating that it was less negative in terms of charge (Figure 3-1C).

3.4.2 Propagation of Undifferentiated hESCs Colonies

Alkaline phosphatase activity was used to identify undifferentiated hESC colonies. When CBH10 hESCs were initially cultured as single cells on ATRP PMEDSAH with a surface thickness of 105 nm, the number of undifferentiated colonies was similar to that of the matrigel control group (Figure 3-2A, B). However, compared to the other experimental groups, a significantly higher number of colonies were detected on the 105 nm thickness group. No significant differences in colony surface area were observed among experimental groups (Figure 3-2A, B). Similar results were obtained with the H9 hESC line, which limits the possibility of a hESC line-specific effect (Figure 3-3). Taken together, these results indicated that the gel architecture of PMEDSAH coatings influenced hESC colony formation.

3.4.3 Expansion of hESCs

To quantify the impact of gel architecture on long-term expansion of hESCs, a consistent number (20,000) of hESCs cultured initially as single cells on matrigel, PMEDSAH and ATRP PMEDSAH (25 nm, 105 nm, 176 nm) were passaged weekly for five consecutive weeks. Prior to each passage to newly coated dishes, the total cell number was quantified and flow cytometry was performed on a subset of cells to evaluate the expression of SSEA-4, a hESC marker (Figure 3-4). The percentage of SSEA-4 positive cells ranged from 96.65% to 99.95% and was not statistically ($p>0.05$) different among the different substrates and passages. However, the total number of cells that adhered to matrigel decreased after each passage and cells on matrigel did not survive after four consecutive passages. In contrast, single hESCs cultured on ATRP PMEDSAH and grafted PMEDSAH continued to thrive with each passage. Growth of hESCs was particularly robust on the ATRP PMEDSAH with a 105 nm surface thickness that supported a significantly ($p <0.05$) higher total cell number than all other experimental groups (Figure 3-2C).

The hypothetical yield of total hESCs achieved after five passages on each substrate was calculated assuming that all cells obtained at each passage were sub-cultured, instead of the 20,000 cells that were actually propagated. The theoretical yield of cells was determined using the formula $CN_{(n+1)} = CN_n \times TN_{(n+1)}/20000$. In this formula, *CN* was the calculated total cell number, *TN* was the total cell number in the determined week and *n* represented the culture week. Using this formula, it was estimated that on the 105nm thick-ATRP PMEDSAH, the expansion of 20,000 cells over a period of five weeks would yield up to 4.7×10^9 undifferentiated stem cells. This level of hESC expansion on the 105 nm thick-ATRP PMEDSAH was 33.6-, 1.6- and 12.7-fold greater than the theoretical yield calculated when cultured on grafted PMEDSAH, 25 nm and 176 nm thickness-ATRP PMEDSAH, respectively (Table 3-1). These calculated total cell

numbers strongly demonstrated that modifying the gel architecture significantly facilitated the expansion of hESCs.

3.4.4 hESC Pluripotency and Genomic Stability

Quantitative RT-PCR analysis of cells after five passages demonstrated that RNA expression levels of hESC markers *OCT4, SOX2, KLF4* and *NANOG* were similar among hESCs cultured on grafted PMEDSAH and ATRP PMEDSAH (25nm, 105nm, 176nm; Figure 3-5A). Immunofluorescent staining of OCT4 and SSEA-4 in hESCs was also strong when cultured on both grafted PMEDSAH and ATRP PMEDSAH (25 nm, 105 nm and 176 nm) coatings (Figure 3-5B). Because 105 nm ATRP PMEDSAH demonstrated a stronger capacity to support hESC self-renewal and expansion, an additional hESC line was also cultured on 105 nm ATRP PMEDSAH during the same period of time. In addition to OCT4 and SSEA-4, primary antibodies to SOX2, NANOG, TRA-1-60 and TRA-1-81 were used for immunofluorescence staining of H1 hESCs and all stem cell markers were strongly expressed (Figure 3-5C).

The pluripotency of hESCs cultured on the 105 nm thick-ATRP PMEDSAH was determined by embryoid body (EB) formation and directed cell-lineage differentiation after five passages. Clusters of hESCs cultured on 105 nm thick-ATRP PMEDSAH formed EBs when cultured in suspension and expressed genes representing endoderm, mesoderm and ectoderm (Table 3-2). Furthermore, specific cell-lineage differentiation was successfully directed *in vitro* with chemically defined conditions, as demonstrated by a significant increase in expression of representative genes for each germ layer: *AFP FOXA2, PDX1* and *SOX17 for endoderm*; *HESX1, NKX2-5* and *TNN13* for mesoderm; and *NES, NEUROD1, PAX6* and *SOX1* for ectoderm (Figure

3-6). These results demonstrated that ATRP PMEDSAH with a 105 nm surface thickness supported the pluripotency of hESCs.

Because chromosomal changes may occur during long-term culture of hESCs [29], the genetic stability of cells cultured on 105 nm thick-ATRP PMEDSAH was evaluated by standard G-band analysis after five passages. The results demonstrated a normal human male karyotype for the H1 cell line (Figure3-5D).

3.5 Discussion

The evolution of hESC culture from feeder-cell dependence and non-defined conditions to feeder-free and defined microenvironments has been enabled by the development of new culture materials. Because of its strong capacity to support hESC and induced pluripotent stem cell (iPSC) growth with chemically-defined and xenogeneic-free medium, the PMEDSAH-coating has the potential to serve as a substrate to generate high numbers of clinical grade pluripotent stem cells [10]. Thus, the elucidation of mechanisms by which PMEDSAH is able to support hESC self-renewal, pluripotency and long-term propagation will not only advance our knowledge of pluripotent stem cell biology, but also increase the effectiveness of hESC and iPSC expansion on defined conditions for potential human applications.

Because matrigel is the most commonly used feeder-free substrate for hESC culture, it was used as a control in our experiments. We found that the number of hESCs grown on matrigel decreased after each passage, which may be due to the poor survival of hESCs on matrigel after cell dissociation [26, 30]. In contrast, both grafted and ATRP PMEDSAH supported hESC expansion during the five-week expansion period. In particular, the ATRP PMEDSAH with a 105 nm surface thickness led to significantly higher total cell numbers compared to all other

experimental groups (Table 3-1). In addition, hESCs retained their pluripotency and a normal karyotype after multiple passages during culture, which indicates that hESCs maintained their unique characteristics and genetic stability. These findings are well aligned with the long-term goal of large-scale production of clinical grade hESCs.

The different surface preparations tested in this study affected the gel architecture of the substrates. The UVO-grafted PMEDSAH surface had thin, poly-dispersed and unassociated polymer brushes. Whereas the ATRP process was capable of producing thick and mono-dispersed polymer brushes [31, 32]. Moreover, the gel architectures were also different among the three ATRP surfaces due to differences in the ATRP reaction time. These data suggest that the gel architecture of the 105 nm thick ATRP coating best supported hESC growth, supporting the hypothesis that gel architecture of the zwitterionic surface layer is capable of influencing the culture and expansion of hESCs.

The thickness of PMEDSAH produced using a 1-hour ATRP reaction time was nearly equal to that of the UVO-grafted surface (Figure 3-1). However, the former was capable of expanding the stem cell population at a higher rate than the latter. Interestingly, the 176 nm thick coating exhibited a lower capacity for hESC expansion than both the thinnest coating (25 nm) and the best-performing PMEDSAH surface for hESC expansion (105 nm). The molecular weight of the UVO-grafted films could not be precisely controlled due to the kinetics of conventional free radical polymerization, where the radical lifetime is short and the termination step is rapid [33]. However, the molecular weight of ATRP films was controlled and augmented as the film thickness increased by longer ATRP reactions. Therefore, the observation that 105 nm thick ATRP films supported hESC self-renewal better than the other ATRP groups with reduced or increased thickness, suggests that an optimal range of molecular weight for synthetic polymer

coatings exists for the support hESC self-renewal. This finding is consistent with a recent study in which polymer molecular weight influenced hESC growth in a non-monotonic manner [18]. Another study comparing substrates with different chemical structures demonstrated that hydrophobic materials are less permissive for hESC adhesion [14]. Here, however, we investigated the effects of hydrophilicity on hESC behavior using PMEDSAH surfaces with identical chemical compositions with different degrees of wettability. The UVO- grafted and the 25 nm ATRP-PMEDSAH, which have a contact angle of 16.6° and 21.9°, respectively, were the most hydrophilic surfaces tested. The 176 nm thick ATRP coating, with a contact angle of 75.3°, was the least hydrophilic of all PMEDSAH surfaces tested. However, all three surface coatings demonstrated lower hESC expansion rates compared to the 105 nm thick ATRP-PMEDSAH coating, which had a contact angle of 43.7°. Thus, modifying the PMEDSAH surface to a moderate hydrophilicity led to better support of hESC growth than surfaces at the extremes of contact angle.

The hydrophilicity of UVO-grafted PMEDSAH is attributed to water affinity of the anionic sulphonate and cationic quaternary ammonium present in their side chains. The tendency of these functional groups to be hydrated leads to water penetration, swelling of the polymer brush and a lower contact angle. For film thicknesses between 25 nm and 176 nm, the contact angle increased from 21.9° to 75.3° (Figure 3-1B). This transition from hydrophilic to hydrophobic behavior of PMEDSAH was first explained in terms of whether inter-chain associations dominate the hydration behavior of the polymer brush [34]. Differences in wettability between UVO-grafted and ATRP polymer coatings can be attributed to the effect of grafting density and polymer chain length on the balance of inter- and intra-polymer chain associations [35].

Because neither grafting density nor molecular weight distribution can be precisely controlled [36] in UVO-grafted films, the resulting polymer brush is likely to be thin, poly-dispersed and unassociated. In the unassociated state, ionic attractions between the sulphonate and the ammonium groups in the side chains are not dominant, allowing the polymer to be fully hydrated, resulting in a low contact angle [37]. In contrast, ATRP coatings have a controllable and high grafting density that results in greater proximity of polymer chains and increased opportunities for short-range ionic interactions. The 25 nm films would exhibit only a slight degree of association behavior, as they do not have a sufficient number of ion-pairs and are therefore hydrophilic. The 105 nm and 176 nm coatings, being of higher molecular weight, have a greater number of ion pairs and are able to form stronger intermolecular associations that lead to dehydration and collapse of the brush. This ion-ion pairing prevents complete hydration of the ionic groups and is effective in sealing out water from the polymer coating. As the PMEDSAH polymer grows in length, more ion pairs are created, increasing the strength of the association, extent of water exclusion and contact angle [34] .

In the absence of systematic intermolecular associations, the UVO-grafted PMEDSAH brush remains fully hydrated [37]. It was initially believed that water molecules in the polymer brush could reduce the zeta potential through charge screening. Thus, the higher isoelectric point of UVO-grafted PMEDSAH within the ATRP films was attributed to the lack of ion-pairing effects between polymer side chains. In the ATRP coated PMEDSAH films, the 25 nm and 176 nm thick ATRP-PMEDSAH coatings exhibited more cumulative negative charge than the 105 nm thick coating in the neutral range of pH values. The isoelectric point of the 105 nm thick ATRP coating was shifted to the right of the other two coatings, indicating that it was less negative in charge (Figure 3-1C). Since even the hydrophilic 25 nm coating had a highly negative surface

charge, differences in surface charge among the ATRP coatings could not be attributed to the level of hydration. The coatings with the highest and lowest degrees of ion-pairing (176 and 25 nm, respectively) were similar in their surface charge with their zeta potential plots overlapping in the neutral region. For reasons not yet fully understood, the 105 nm PMEDSAH coating had the least negative surface charge among the three ATRP coatings and this may render this surface as more favorable for cell adhesion.

It has been shown that surfaces with a roughness of Rq = 1 nm, which are categorized as smooth, support hESCs growth better than nano-rough surfaces with a Rq of 75-150 nm [22]. Our analyses of substrate roughness on all four surfaces showed a Ra lower than 2 nm and had no statistical differences among them, which suggested that all these surfaces could be considered as smooth surfaces. It has also been shown that an optimum range of surface charge is associated with maximal cell adhesion to metallic biomaterial surfaces [38]. In our study, it was also observed that an optimum range of surface charge of PMEDSAH supports hESC expansion. The 105 thick-ATRP PMEDSAH films were more favorable for hESC expansion compared to the UVO-grafted films with a lower negative charge and to the 25 nm and 176 nm thick ATRP PMEDSAH films that exhibited a more negative charge. The more negatively charged 25 nm and 176 nm ATRP films may generate stronger repelling forces to cells, as cell membrane potential is typically negative, which may result in an adverse effect on hESC adhesion. However, this would not explain the lower cell expansion observed on UVO-grafted surfaces with the less negative charge. Thus, it is possible that hESCs prefer an optimum range of repelling forces. Alternatively, the UVO-grafted surfaces had unique gel architecture with polydispersed and unassociated polymer brushes compared to the well-uniformed ATRP surfaces.

If this were true, then the surface charge may not be the key factor leading to the differences of hESC expansion between UVO-grafted and ATRP PMEDSAH.

Taken together, the observed trend in hESC expansion (105 nm thick PMEDSAH > 25 nm thick PMEDSAH > 176 nm thick PMEDSAH > UVO-grafted PMEDSAH) could not be attributed alone to a single physical property of the substrates studied here. Comparing thickness and contact angle helped establish that differences in gel architecture between coatings existed. Balance between ion-pairing driven inter-molecular association and hydration behaviors of PMEDSAH brushes may dictate the gel architecture adopted in each substrate. Thus, the data suggest that the 105 nm thick ATRP PMEDSAH coating possesses the optimal gel architecture for hESC expansion with its intermediate thickness, hydrophilicity, surface charge, and a moderate degree of inter-chain association. In addition to significantly higher efficiency in hESC expansion during long-term culture, the 105 nm ATRP-PMEDSAH has the following advantages compared to matrigel: defined molecular composition, more stably on long-term storage minimal lot-to-lot variability, ease of preparation and compatible with standard sterilization techniques. All of these feature make the 105 nm thick ATRP PMEDSAH a very promising substrate to obtain scalable populations of clinical grade hESCs. This could be accomplished by reducing the cell expansion time, production cost, as well as possible contamination and population drift under current culture conditions.

Our results revealed differences in gel architecture between UVO-grafted PMEDSAH and in among ATRP-PMEDSAH substrates that point towards alterations in the balance of inter-molecule associations between polymer chains. This in turn influences the interfacial properties of the substrate and exercises a profound effect on the culture and expansion of hESCs. While all four coatings were able to maintain their pluripotency over long-term culture, significant

differences in cell expansion were observed. The 105 nm thick ATRP-based coating was found to perform significantly better than the other three substrates. In conclusion, the physical properties influenced the ability of PMEDSAH to support hESC expansion. The newly developed 105 nm thick ATRP-PMEDSAH described here may be effective in the scalable production of hESCs for application in regenerative medicine.

3.6 Figures

A

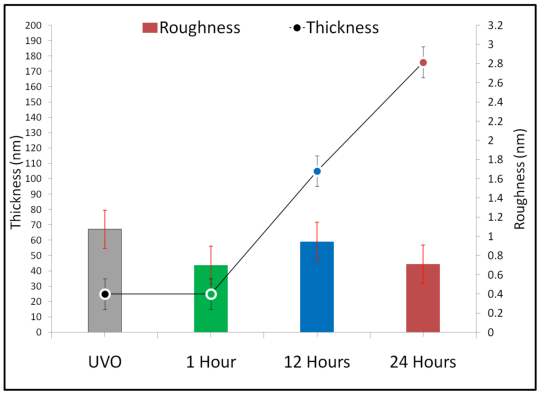

B

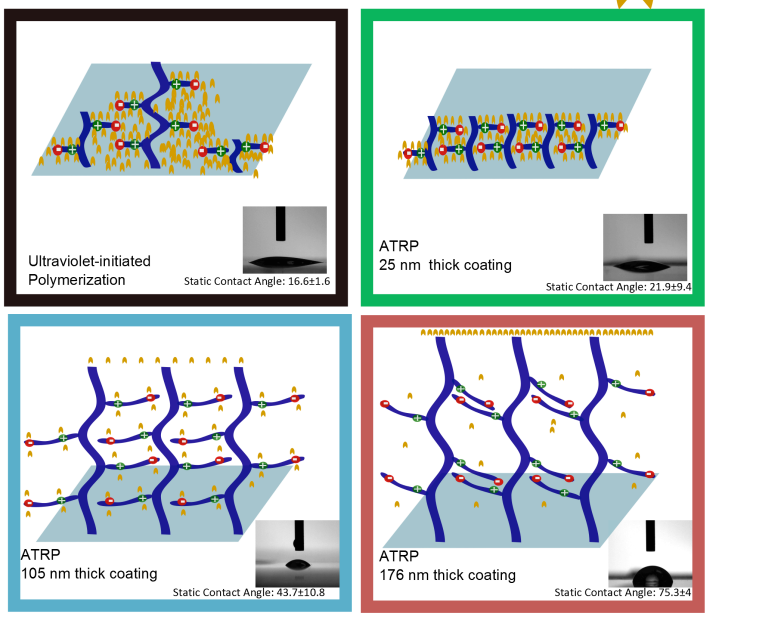

C

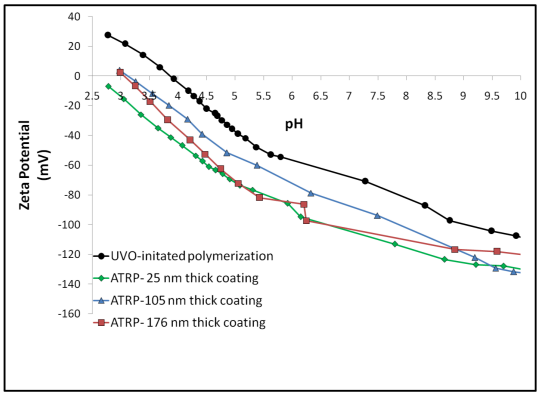

Figure 3-1. Differences in properties of PMEDSAH coatings (A) Thickness (circles) and roughness (columns) of PMEDSAH coatings polymerized through UVO-grafting and ATRP. Thickness of ATRP coatings increased with ATRP reaction time. (1 hour-25 nm, 12 hours-105 nm, 24 hours-176 nm) (B) Cartoons depict polymer conformations adopted by the four PMEDSAH coatings studied. Water molecules have been represented in yellow. Differences in hydration and ion-pairing behaviour have been illustrated. Inset- Photographs of static contact angle measurements performed with deionized water on PMEDSAH coatings. Contact angle values are displayed below the respective images. (C) Comparison of zeta potential values of PMEDSAH coatings polymerized through UVO-grafting and ATRP. *Credit: Xu Qian, et al. Biomaterials 2014;35:9581-90*

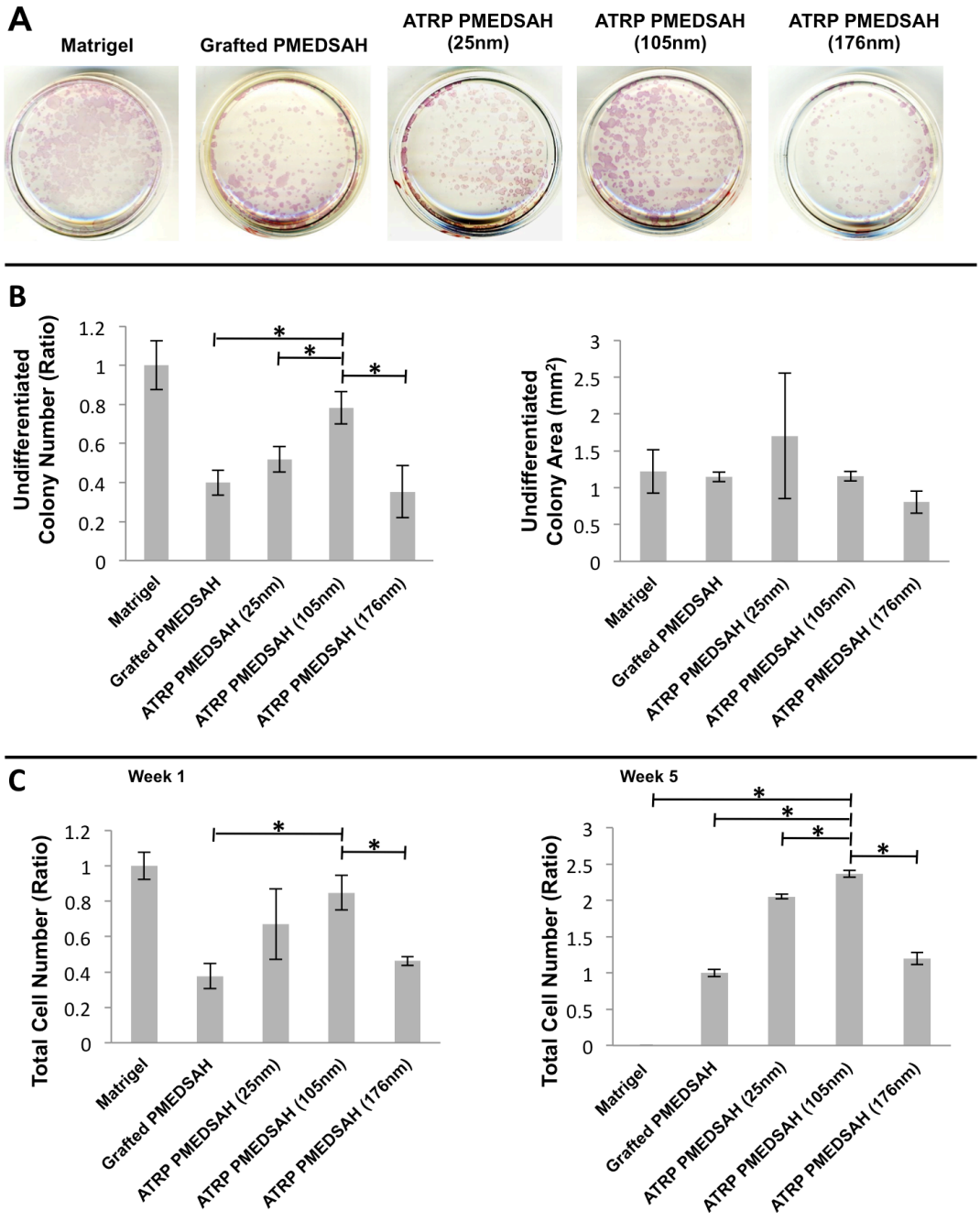
A
Matrigel
Grafted PMEDSAH
ATRP PMEDSAH (25nm)
ATRP PMEDSAH (105nm)
ATRP PMEDSAH (176nm)
B
Undifferentiated Colony Number (Ratio)
1.2
1
0.8
0.6
0.4
0.2
0
*
*
*
Matrigel
Grafted PMEDSAH
ATRP PMEDSAH (25nm)
ATRP PMEDSAH (105nm)
ATRP PMEDSAH (176nm)
Undifferentiated Colony Area (mm²)
3
2.5
2
1.5
1
0.5
0
Matrigel
Grafted PMEDSAH
ATRP PMEDSAH (25nm)
ATRP PMEDSAH (105nm)
ATRP PMEDSAH (176nm)
C
Week 1
Total Cell Number (Ratio)
1.2
1
0.8
0.6
0.4
0.2
0
*
*
Matrigel
Grafted PMEDSAH
ATRP PMEDSAH (25nm)
ATRP PMEDSAH (105nm)
ATRP PMEDSAH (176nm)
Week 5
Total Cell Number (Ratio)
3
2.5
2
1.5
1
0.5
0
*
*
*
*
Matrigel
Grafted PMEDSAH
ATRP PMEDSAH (25nm)
ATRP PMEDSAH (105nm)
ATRP PMEDSAH (176nm)

Figure 3-2. Gel architecture influences the undifferentiated colony formation and expansion of hESCs (CHB 10 cells). (A) Undifferentiated colonies were identified by alkaline phosphatase assay after 7 days of culture on different substrates. (B) Plot of undifferentiated colony number ratio compared to Matrigel indicated ATRP PMEDSAH with a 105nm hydrogel thickness lead to a higher number of undifferentiated colonies compared to other experimental groups. Plot of undifferentiated colony area indicated that the areas of undifferentiated colonies cultured on different substrates had no significant differences. (C) Plot of total cell number ratio compared to Matrigel after 1 week and compared to grafted PMEDSAH after 5 weeks indicated ATRP PMEDSAH with a 105nm hydrogel thickness lead to a higher total cell number compared to other experimental groups. Data in (B) & (C) presented as mean ± standard deviation (SD) from three independent experiments (* $p<0.05$). *Credit: Xu Qian, et al. Biomaterials 2014;35:9581-90*

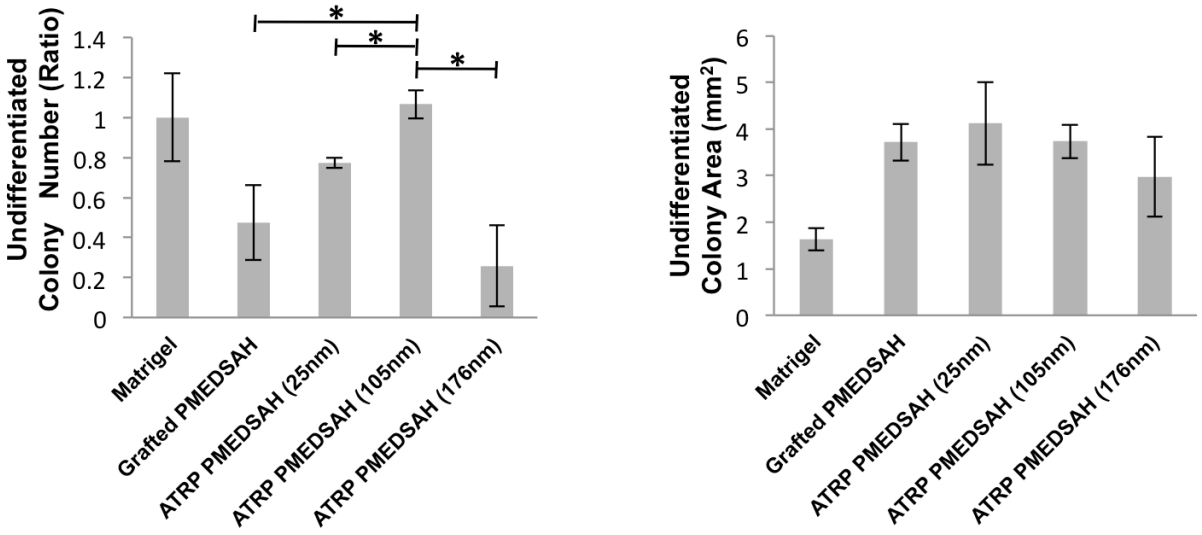

Figure 3-3. Gel architecture influences the undifferentiated colony formation of hESCs (H9 cells). Plot of undifferentiated colony number ratio compared to matrigel indicated ATRP PMEDSAH with a 105nm hydrogel thickness led to a higher number of undifferentiated colonies compared to other experimental groups. Plot of undifferentiated colony area indicated no significant differences among cells cultured on different polymer substrates. Data presented as mean ± SD from three independent experiments (* $p<0.05$). *Credit: Xu Qian, et al. Biomaterials 2014;35:9581-90*

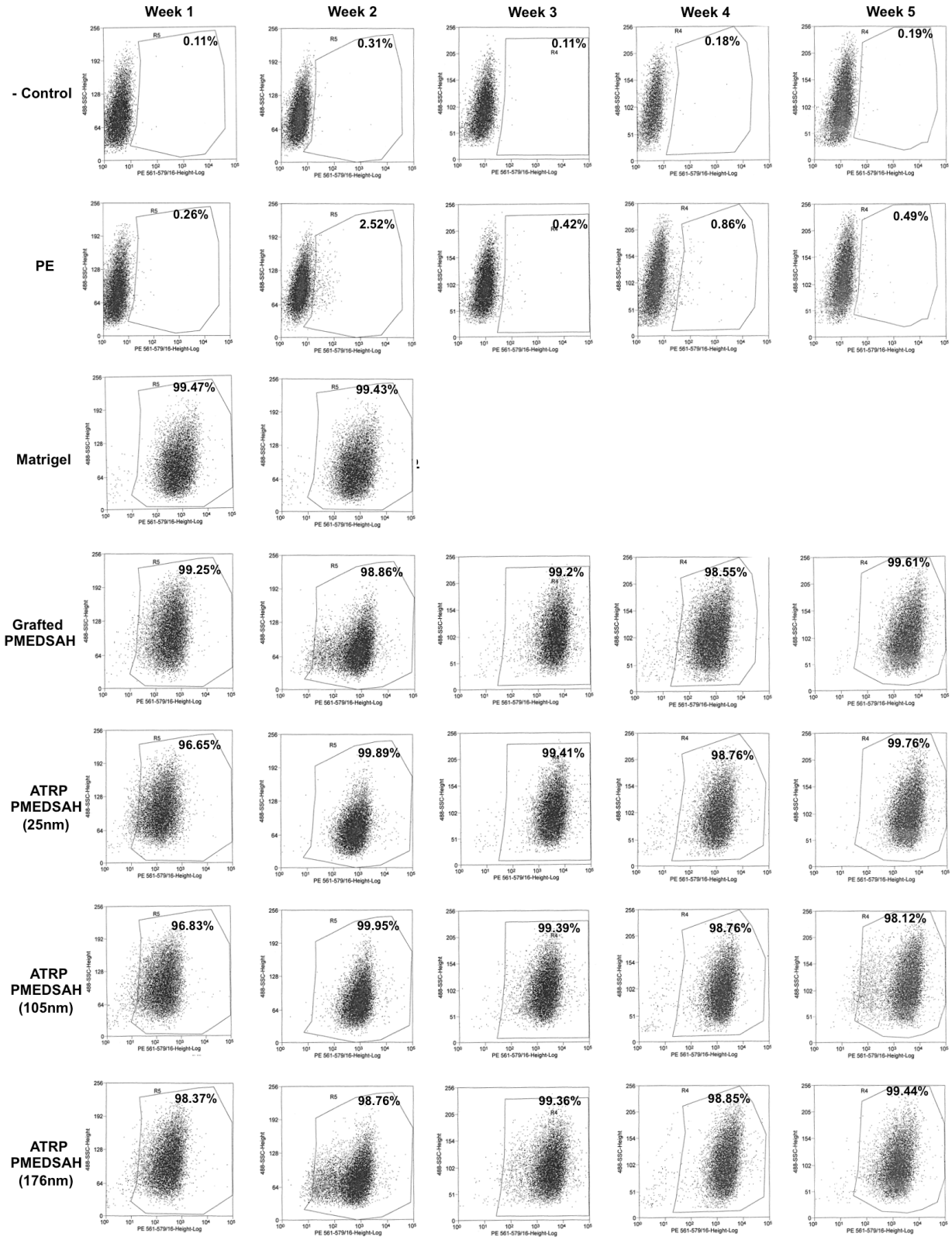
Week 1
Week 2
Week 3
Week 4
Week 5
- Control
0.11%
0.31%
0.11%
0.18%
0.19%
PE
0.26%
2.52%
0.42%
0.86%
0.49%
Matrigel
99.47%
99.43%
Grafted PMEDSAH
99.25%
98.86%
99.2%
98.55%
99.61%
ATRP PMEDSAH (25nm)
96.65%
99.89%
99.41%
98.76%
99.76%
ATRP PMEDSAH (105nm)
96.83%
99.95%
99.39%
98.76%
98.12%
ATRP PMEDSAH (176nm)
98.37%
98.76%
99.36%
98.85%
99.44%
488-SSC-Height
PE 561-579/16-Height-Log

Figure 3-4. **Expression of SSEA-4 in hESCs cultured on different substrates after multiple passages.** hESCs cultured on different substrates from week 1 to week 5 were analyzed by flow cytometry to determine the percentage of SSEA-4 expressing cells. Background fluorescence and autofluorescence were determined using cells without treatment (-Control) and treated with Mouse IgG1 Phycoerythrin Isotype Control (PE). Because cells grown on matrigel decreased after each passage, the amount of cells was not enough for flow cytometry from week 3. *Credit: Xu Qian, et al. Biomaterials 2014;35:9581-90*

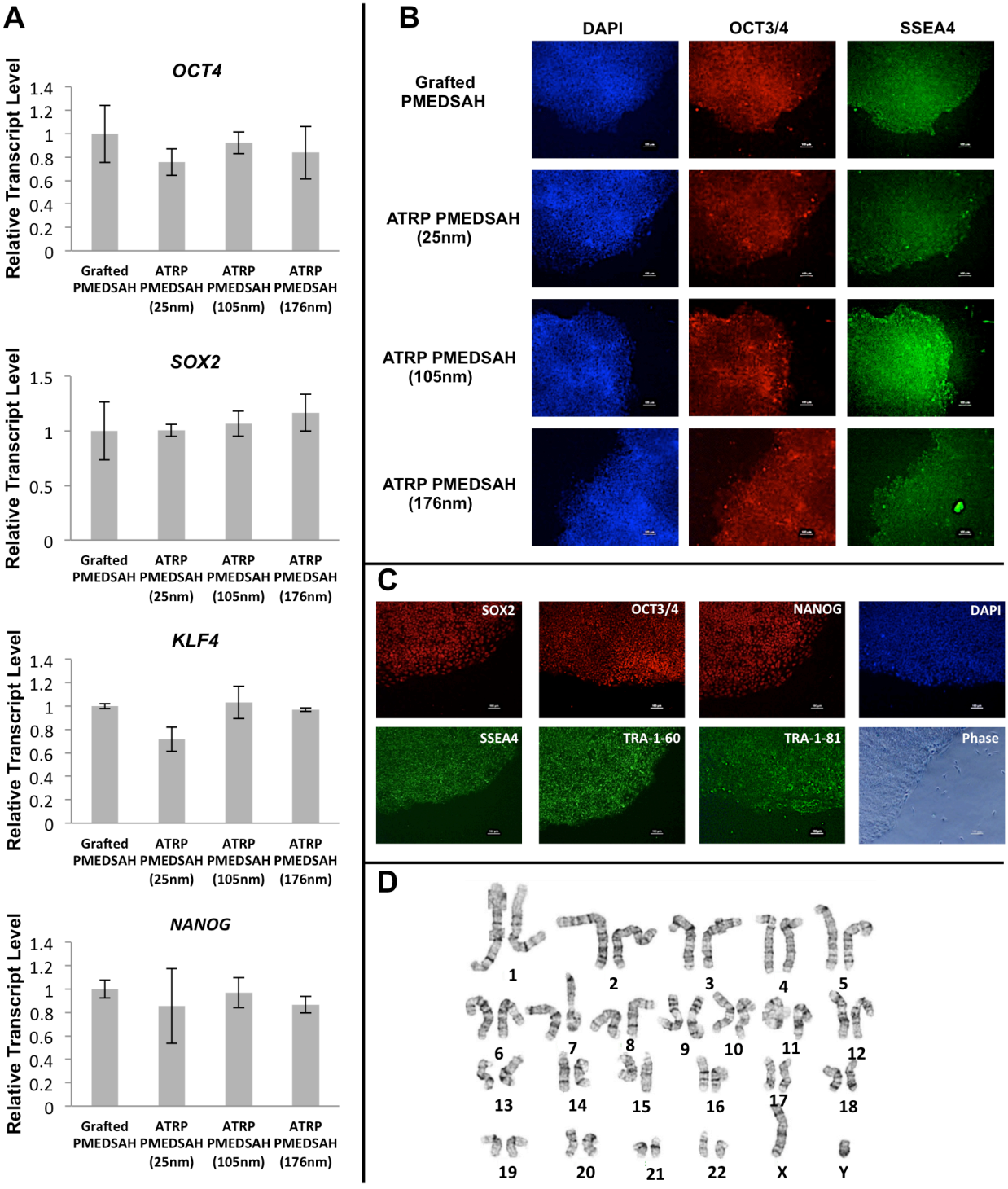
A
OCT4
SOX2
KLF4
NANOG
Relative Transcript Level
Grafted PMEDSAH
ATRP PMEDSAH (25nm)
ATRP PMEDSAH (105nm)
ATRP PMEDSAH (176nm)
B
DAPI
OCT3/4
SSEA4
Grafted PMEDSAH
ATRP PMEDSAH (25nm)
ATRP PMEDSAH (105nm)
ATRP PMEDSAH (176nm)
C
SOX2
OCT3/4
NANOG
DAPI
SSEA4
TRA-1-60
TRA-1-81
Phase
D

Figure 3-5. Modified PMEDSAH supports hESC stemness and keeps the genomic stability. (A) Relative transcript levels of OCT4, SOX2, KLF4 and NANOG from hESCs cultured on grafted PMEDSAH and ATRP PMEDSAH after 5 passages had no significant differences. Data presented as mean ± SD from three independent experiments. (B) Fluorescence micrographs of colonies of hESCs cultured on grafted PMEDSAH and ATRP PMEDSAH showing expression of pluripotent markers after 5 passages. Primary antibodies OCT4 and SSEA-4 were used to detect the expression of these markers from hESCs cultured on grafted PMEDSAH and ATRP PMEDSAH (25nm, 105nm and 176nm). hESC cultured on 105nm ATRP PMEDSAH after 5 passages (C) showed expression of pluripotent markers in fluorescence micrographs and (D) kept a normal karyotype. *Credit: Xu Qian, et al. Biomaterials 2014;35:9581-90*

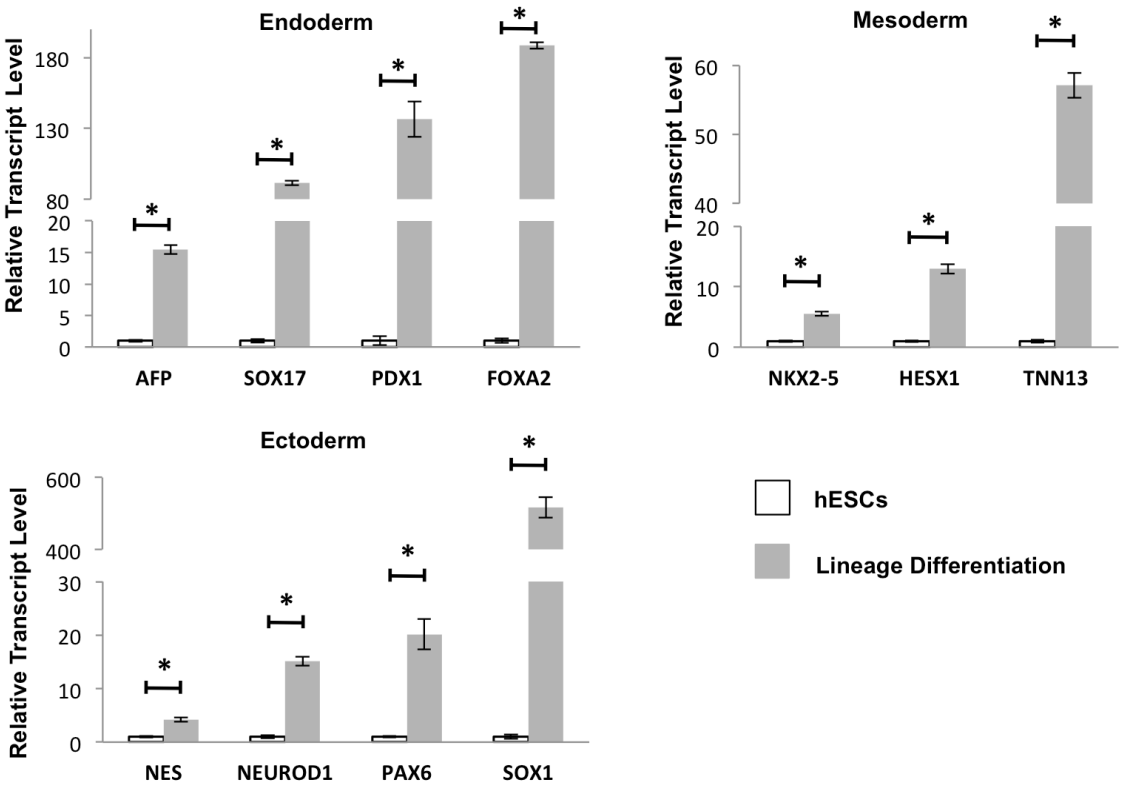

Figure 3-6. Modified PMEDSAH supports hESC pluripotency. hESCs cultured on 105nm ATRP PMEDSAH after 5 passages retained pluripotency as demonstrated by induced specific lineage differentiation with expression of genes representing different germ layers. Data presented in as mean ± SD from three independent experiments. *Credit: Xu Qian, et al. Biomaterials 2014;35:9581-90*

3.7 Tables

Table 3-1. Calculated total cell number of hESCs cultured on different substrates

Substrates	Calculated total cell numbers from Week 0 to Week 5					
	W0	W1	W2	W3	W4	W5
Matrigel	$2x10^4$	$3.7x10^5$	$2.4x10^6$	$3.5x10^6$	$1.2x10^6$	/
Grafted PMEDSAH	$2x10^4$	$1.4x10^5$	$8.2x10^5$	$5.0x10^6$	$2.7x10^7$	$1.4x10^8$
ATRP PMEDSAH (25nm)	$2x10^4$	$2.5x10^5$	$2.4x10^6$	$3.4x10^7$	$2.9x10^8$	$2.9x10^9$
ATRP PMEDSAH (105nm)	$2x10^4$	$3.2x10^5$	$4.0x10^6$	$4.9x10^7$	$4.0x10^8$	$4.7x10^9$
ATRP PMEDSAH (176nm)	$2x10^4$	$1.7x10^5$	$1.4x10^6$	$1.0x10^7$	$6.2x10^7$	$3.7x10^8$

Formula: $CN_{(n+1)=} CN_n \times TN_{(n+1)}/20000$
CN: Calculated total cell number, *TN*: total cell number, *n*: culture week number

Credit: Xu Qian, et al. Biomaterials 2014;35:9581-90

Table 3-2 Embryoid body (EB) formation with expression of genes representing different germ layers. EBs were formed from hESCs cultured on 105nm ATRP PMEDSAH after 5 passages. Quantitative RT-PCR showed increasing transcript levels of genes representing different germ layers from EBs compared to the undifferentiated hESCs grown on 105 nm ATRP PMEDSAH after 5 passages.

	Gene	Relative Transcript Levels ± SD
Endoderm	*PDX1*	35.58 ± 2.58
	AFP	53.14 ± 4.76
	SOX17	159.47 ± 12.51
	FOXA2	249.12 ± 25.67
Mesoderm	*HESX1*	10.21 ± 0.84
	TNN13	94.32 ± 6.99
	NKX2-5	117.31 ± 4.04
Ectoderm	*NES*	3.58 ± 0.15
	SOX1	37.26 ± 1.35
	PAX6	107.36 ± 7.27
	NEUROD1	860.77 ± 97.08

Credit: Xu Qian, et al. Biomaterials 2014;35:9581-90

3.8 References

[1] McCall MD, Toso C, Baetge EE et al. Are stem cells a cure for diabetes? Clin Sci 2010;118:87-97.

[2] Dominguez-Bendala J, Inverardi L, Ricordi C. Stem cell-derived islet cells for transplantation. Curr Opin Organ Tran 2011;16:76-82.

[3] Laflamme MA, Chen KY, Naumova AV et al. Cardiomyocytes derived from human embryonic stem cells in pro-survival factors enhance function of infarcted rat hearts. Nat Biotechnol 2007;25:1015-24.

[4] Thomson JA, Itskovitz-Eldor J, Shapiro SS et al. Embryonic stem cell lines derived from human blastocysts. Science 1998;282:1145-7.

[5] Richards M, Tan S, Fong CY et al. Comparative evaluation of various human feeders for prolonged undifferentiated growth of human embryonic stem cells. Stem Cells 2003;21:546-56.

[6] Xu C, Inokuma MS, Denham J et al. Feeder-free growth of undifferentiated human embryonic stem cells. Nat Biotechnol 2001;19:971-4.

[7] Braam SR, Zeinstra L, Litjens S et al. Recombinant vitronectin is a functionally defined substrate that supports human embryonic stem cell self-renewal via alphavbeta5 integrin. Stem Cells 2008;26:2257-65.

[8] Miyazaki T, Futaki S, Hasegawa K et al. Recombinant human laminin isoforms can support the undifferentiated growth of human embryonic stem cells. Biochem Biophys Res Commun 2008;375:27-32.

[9] Nagaoka M, Si-Tayeb K, Akaike T et al. Culture of human pluripotent stem cells using completely defined conditions on a recombinant E-cadherin substratum. BMC Dev Biol 2010;10:60.

[10] Villa-Diaz LG, Ross AM, Lahann J et al. Concise Review: The Evolution of human pluripotent stem cell culture: From feeder cells to synthetic coatings. Stem Cells 2013;31:1-7.

[11] Derda R, Li L, Orner BP et al. Defined substrates for human embryonic stem cell growth identified from surface arrays. ACS Chem Biol 2007;2:347-55.

[12] Klim JR, Li L, Wrighton PJ et al. A defined glycosaminoglycan-binding substratum for human pluripotent stem cells. Nat Methods 2010;7:989-94.

[13] Kolhar P, Kotamraju VR, Hikita ST et al. Synthetic surfaces for human embryonic stem cell culture. J Biotechnol 2010;146:143-6.

[14] Villa-Diaz LG, Nandivada H, Ding J et al. Synthetic polymer coatings for long-term growth of human embryonic stem cells. Nat Biotechnol 2010;28:581-3.

[15] Mei Y, Saha K, Bogatyrev SR et al. Combinatorial development of biomaterials for clonal growth of human pluripotent stem cells. Nat Mater 2010;9:768-78.

[16] Irwin EF, Gupta R, Dashti DC et al. Engineered polymer-media interfaces for the long-term self-renewal of human embryonic stem cells. Biomaterials 2011;32:6912-9.

[17] Li Y, Chuang E, Rodriguez R et al. Hydrogels as artificial matrices for human embryonic stem cell self-renewal. J Biomedical Mater Res A 2006;79:1-5.

[18] Brafman DA, Chang CW, Fernandez A et al. Long-term human pluripotent stem cell self-renewal on synthetic polymer surfaces. Biomaterials 2010;31:9135-44.

[19] Melkoumian Z, Weber JL, Weber DM et al. Synthetic peptide-acrylate surfaces for long-term self-renewal and cardiomyocyte differentiation of human embryonic stem cells. Nat Biotechnol 2010;28:606-10.

[20] Qian X, Villa-Diaz LG, Krebsbach PH. Advances in culture and manipulation of human pluripotent stem cells. J Dent Res 2013;92:956-62.

[21] Nandivada H, Villa-Diaz LG, O'Shea KS et al. Fabrication of synthetic polymer coatings and their use in feeder-free culture of human embryonic stem cells. Nature Protocols 2011;6:1037-43.

[22] Chen W, Villa-Diaz LG, Sun Y et al. Nanotopography influences adhesion, spreading, and self-renewal of human embryonic stem cells. ACS Nano 2012;6:4094-103.

[23] Sun Y, Villa-Diaz LG, Lam RH et al. Mechanics regulates fate decisions of human embryonic stem cells. PLoS One 2012;7:e37178.

[24] Jiang XW, Chen HY, Galvan G et al. Vapor-based initiator coatings for atom transfer radical polymerization. Adv Funct Mater 2008;18:27-35.

[25] Wang J, Matyjaszewski K. Controlled/"living" radical polymerization. halogen atom ransfer radical polymerization promoted by a Cu(I)/Cu(11) redox process. Macromolecules 1995;28:7901-10.

[26] Watanabe K, Ueno M, Kamiya D et al. A ROCK inhibitor permits survival of dissociated human embryonic stem cells. Nat Biotechnol 2007;25:681-6.

[27] Yao S, Chen S, Clark J et al. Long-term self-renewal and directed differentiation of human embryonic stem cells in chemically defined conditions. Proc Natl Acad Sci U S A 2006;103:6907-12.

[28] Ross AM, Jiang ZX, Bastmeyer M et al. Physical Aspects of Cell Culture Substrates: Topography, Roughness, and Elasticity. Small 2012;8:336-55.

[29] Baker DE, Harrison NJ, Maltby E et al. Adaptation to culture of human embryonic stem cells and oncogenesis in vivo. Nat Biotechnol 2007;25:207-15.

[30] Pyle AD, Lock LF, Donovan PJ. Neurotrophins mediate human embryonic stem cell survival. Nat Biotechnol 2006;24:344-50.

[31] Ejaz M, Yamamoto S, Ohno K et al. Controlled graft polymerization of methyl methacrylate on silicon substrate by the combined use of the Langmuir-Blodgett and atom transfer radical polymerization techniques. Macromolecules 1998;31:5934-6.

[32] Huang X, Wirth MJ. Surface initiation of living radical polymerization for growth of tethered chains of low polydispersity. Macromolecules 1999;32:1694-6.

[33] Tang W, Matyjaszewski K. Kinetic Modeling of Normal ATRP, Normal ATRP with [Cu-II](o), Reverse ATRP and SR&NI ATRP. Macromol Theor Simul 2008;17:359-75.

[34] Cheng N, Brown AA, Azzaroni O et al. Thickness-Dependent Properties of Polyzwitterionic Brushes (vol 41, pg 6317, 2008). Macromolecules 2008;41:8288-.

[35] Rubinstein M, Dobrynin AV. Associations leading to formation of reversible networks and gels. Curr Opin Colloid In 1999;4:83-7.

[36] Huang WX, Skanth G, Baker GL et al. Surface-initiated thermal radical polymerization on gold. Langmuir 2001;17:1731-6.

[37] Azzaroni O, Brown AA, Huck WTS. UCST wetting transitions of polyzwitterionic brushes driven by self-association. Angew Chem Int Edit 2006;45:1770-4.

[38] Hallab NJ, Bundy KJ, OConnor K et al. Cell adhesion to biomaterials: Correlations between surface charge, surface roughness, adsorbed protein, and cell morphology. J Long-Term Eff Med 1995;5:209-31.

CHAPTER 4

DPPA5 PROMOTES PLURIPOTENCY AND REPROGRAMMING BY REGULATING NANOG TURNOVER

4.1 Abstract

Although a specific group of transcription factors, such as OCT4, SOX2 and NANOG are known to play essential roles in pluripotent stem cell (PSC) self-renewal, pluripotency and reprogramming, other factors and the key signaling pathways regulating these important properties are not completely understood. Here, we demonstrate that the PSC marker Developmental Pluripotency Associated 5 (DPPA5) plays an important role in human PSC (hPSC) self-renewal and cell reprogramming in feeder-free conditions. Compared to PSCs grown on mouse embryonic fibroblasts (MEFs), cells cultured on feeder-free substrates, such as matrigel, laminin-511, vitronectin, or the synthetic polymer poly[2-(methacryloyloxy) ethyl dimethyl-(3-sulfopropyl) ammonium hydroxide] (PMEDSAH), had significantly higher DPPA5 gene expression and protein levels. Overexpression of DPPA5 in hPSCs increased NANOG protein levels via a post-transcriptional mechanism. Co-immunoprecipitation, protein stability assays and quantitative RT-PCR, demonstrated that DPPA5 directly interacted, stabilized and enhanced the function of NANOG in hPSCs. Additionally, DPPA5 increased the reprogramming efficiency of human somatic cells to induced pluripotent stem cells (hiPSCs). Our study provides

new insight into the function of DPPA5 in hPSCs, and may further improve current protocols to enhance reprogramming efficiency into hiPSCs.

4.2 Introduction

Human pluripotent stem cells (hPSCs), which include embryonic stem cells (hESCs) derived from the inner cell mass of blastocyst-stage embryos, and induced pluripotent stem cells (hiPSCs) generated by reprogramming somatic cells through overexpression of key transcription factors [1-3], are a promising resource for regenerative medicine. An improved understanding of these pluripotent cells may also provide insight into early human embryonic development because they are able to indefinitely self-renew and differentiate into specialized cell types of all three germ layers and trophoectoderm. A key to unlocking this potential is a more advanced understanding of the molecular mechanisms governing hPSC self-renewal and the network of factors that enable pluripotency. Although it is known that an assembly of transcription factors, including OCT4, SOX2 and NANOG, play important roles in hESC self-renewal and pluripotency [4-7], the crucial signaling pathways and factors regulating hPSC biology are not completely understood.

The *Developmental Pluripotency Associated 5 (DPPA5)* gene, also designated *ESG1*, belongs to the *KHDC1/DPPA5/ECAT1/OOEP* gene family. These genes encode structurally related proteins characterized by an atypical RNA-binding K Homology (KH) domain and are specifically expressed in mammalian oocytes and ESCs [8]. Because of its high expression in pluripotent stem cells, DPPA5 has been used as an informative marker for cell pluripotency and stemness [9-14]. However, there is limited information regarding the function of DPPA5 in mouse or human ESCs [15].

The homeobox transcription factor NANOG has been proposed as a gatekeeper of pluripotency in hPSCs. Studies indicate that down-regulation of NANOG in hESCs induces differentiation [6], while overexpression of *NANOG* prevents neuroectoderm differentiation and blocks progression along endodermal and mesodermal lineages [16-18]. In methods to reprogram somatic cells into iPSCs, the addition of *NANOG* to the *OCT4*, *SOX2*, *KLF4*, and *C-MYC* (OSKM) reprograming cocktail enhances reprogramming kinetics [19]. Likewise, hiPSCs have been generated by the overexpression of *NANOG* in cooperation with the expression of *OCT4*, *SOX2*, and *LIN28* [3].

In Chapter 3, we describe the studies to investigate the effects of hydrogel physical properties on the ability of synthetic polymer coatings to support hPSC self-renewal. Here in Chapter 4, our work is focusing on determining which molecules and signaling pathways play critical roles in supporting hPSC self-renewal on synthetic polymers. We used DPPA5 as a PSC marker to investigate the mechanism by which synthetic polymer coatings such as poly[2-(methacryloyloxy) ethyl dimethyl-(3-sulfopropyl) ammonium hydroxide] (PMEDSAH) support hPSC self-renewal [20, 21]. Our data initially revealed higher expression of DPPA5 in hPSCs cultured on PMEDSAH compared to irradiated mouse embryonic fibroblasts (MEFs), the most widely used culture condition [22]. This finding led us to raise the hypothesis that DPPA5 has a unique role in hPSCs self-renewal when cultured on synthetic substrates.

In this study, we first compared the gene expression and protein levels of DPPA5 in hPSCs cultured on MEFs and several feeder-free conditions. In response to *DPPA5* overexpression, we found that NANOG protein levels were stabilized by DPPA5. Because of the central role of NANOG in hPSC pluripotency, we investigated the mechanism by which DPPA5 regulates NANOG and the effects of DPPA5 on NANOG target genes in hESCs. We also studied the

function of DPPA5 in the derivation of hiPSCs and found *DPPA5* enhanced the reprogramming efficiency when combined with *OCT4*, *SOX2*, *KLF4*, and *C-MYC*.

4.3 Materials and Methods

4.3.1 Cell Culture Substrates Preparation

All cell culture was performed in designated incubators at 5% CO2 and high humidity. Irradiated MEFs (GlobalStem) were plated at a density of 2 X 10^4 cells/cm^2 on gelatin-coated tissue culture dishes. The fibroblast culture medium was composed of high-glucose DMEM (GIBCO), 10% fetal bovine serum (FBS; GIBCO), 1% nonessential amino acids (GIBCO), 1% GlutaMax (GIBCO) and 1% penicillin streptomycin (GIBCO).

The synthetic surface PMEDSAH was prepared as described previously [23]. Briefly, through ultraviolet ozone (UVO)-initiated free radical polymerization in a fume hood with connections for argon, a 500 mL reaction vessel was degassed by vacuum for 1 hour. When the reaction vessel was being evacuated, a monomer solution consisting of 0.25 M MEDSAH (Sigma-Aldrich) was dissolved in a mixture of deionized water and ethanol (4:1, v/v). The solution was degassed for 40 minutes with an argon purge. After the reaction vessel and solvent were degassed, the monomer solution was transferred to a reaction vessel and heated to 68-70°C. While the reaction vessel was being heated, tissue culture polystyrene (TCPS) dishes (BD BioSciences) were activated by UVO treatment (Jetlight Inc.) for 40 minutes to create initiation sites on the surface. After activation, the dishes were transferred to a reaction vessel and the temperature was increased to 76-80°C. Surface-initiated polymerization occurred over a 2.5 hour time period under argon atmosphere at 76-80°C. Once the process was complete, TCPS dishes and control samples were removed from the reaction vessel, and rinsed in a 1% saline (w/v) solution at 50°C.

Matrigel (BD BioSciences) was diluted to a concentration of 100 μg/ml in cold Dulbecco's modified Eagle's medium/F12 (DMEM/F12; GIBCO) and then applied to TCPS dishes or flasks (BD BioSciences). The coating was allowed to polymerize during 2 hours incubation at room temperature. Before plating cells, excess matrigel-DMEM/F12 solution was aspirated and the dishes were washed with sterilized Dulbecco's phosphate buffered saline (D-PBS; GIBCO). Human laminin-511 (Biolamina) was diluted to a concentration of 10 μg/ml in PBS (GIBCO). Vitronectin (R&D Systems) was diluted to 5 μg/ml in PBS (GIBCO). Coating of Laminin and vitronectin was respectively applied to TCPS dishes following the manufacturer's protocols.

4.3.2 Cell Culture of hPSCs

Unless otherwise specified, hESCs (H1 (NIH registration # 0043) and H9 (NIH registration number # 0062), WiCell Research Institute, Madison, WI; CHB10 (NIH registration number 0009), Children's Hospital Corporation, Boston, MA) and hiPSCs derived in our lab [24] from human gingival fibroblasts and foreskin fibroblasts, hGF2-iPSCs, hGF4-iPSCs and hFF-iPSCs were cultured on PMEDSAH, matrigel, human laminin-511, vitronectin and MEFs with hPSC culture medium (human-cell-conditioned medium (HCCM, Global Stem) supplemented with 5 ng/mL of human recombinant basic fibroblast growth factor (bFGF; Invitrogen™) and 1% Antibiotic-Antimycotic (GIBCO)). The hPSC culture medium was replaced every other day. Differentiated cells were mechanically removed with a sterile pulled-glass pipet under a stereomicroscope (LeicaMZ9.5, Leica Microsystems Inc). Undifferentiated colonies were cut and passed as small cell clusters for three passages for each culture condition before analysis.

4.3.3 MEF-conditioned Medium Preparation and Extracellular Matrix (ECM) Deposition

Twenty-four hours after plating irradiated MEFs at a density of 2 X 10^4 cells/cm^2 on gelatin-coated tissue culture dishes, fibroblast culture medium was replaced with hPSC culture medium, and collected the following day, and was labeled as MEF1-CM. Then, hPSC culture medium was replaced every other day and conditioned medium was collected again after 6 days (MEF7-CM). These MEF-conditioned media were stored at −20°C before being used in hPSC culture. MEF-ECM deposits were prepared as described previously [22]. Briefly, irradiated MEFs were culture as described above and during the same period of time. At the time of isolating the ECM deposits, MEFs were washed twice with phosphate buffered saline (PBS), and then lysed in buffer containing 0.5% (v/v) of Triton X-100/PBS and 35 μL of ammonium hydroxide solution (NH4OH) per 100 mL for 5 minutes at room temperature. Plates with ECM deposited were washed three times with PBS before being used in cell culture.

4.3.4 Microarray Analysis

Total RNA (10 μg) from hESCs grown on PMEDSAH or MEFs was hybridized to Affymetrix Human Genome U133 Plus 2.0 microarray (Affymetrix; Santa Clara, CA) following the manufacturer's instructions. Data analysis was performed with a Robust Multi-array average algorithm that converted the plot of perfect match probe intensities into an expression value for each gene. Genes with different expression levels were detected by fitting a linear model to each probe-set and selecting those with a multiplicity-adjusted $p < 0.05$.

4.3.5 RNA Isolation and Quantitative RT-PCR

RNA was isolated and purified with the RNA easy Mini-Kit (Qiagen) following the manufacturer’s protocol. RNA quality and concentration was measured with a Synergy NEO HTS Multi-Mode Microplate Reader (BioTek Instruments, Winooski, VT). Reverse transcription

from 1 μg of total RNA into cDNA was done using SuperScript™ III First-Strand Synthesis SuperMix (Invitrogen™). Quantitative PCR was performed by TaqMan probes (Applied Biosystems) and TaqMan Universal PCR Master Mix (Applied Biosystems) on 7900 HT Fast Real Time PCR system (Applied Biosystems). Gene expression data was normalized to the expression levels of GAPDH, and calculated by the delta-delta *cT* expression level.

4.3.6 Western Blot Analysis

The following antibodies were used: OCT4 antibody (1:2,000; Santa Cruz Biotechnology Inc.), SOX2 antibody (1:1,000; Cell Signaling Technology), KLF4 antibody (1:1,000; Cell Signaling Technology), C-MYC antibody (1:1,000; Cell Signaling Technology), NANOG antibody (1:1,000; Cell Signaling Technology), DPPA5 antibody (2 μg/mL; R&D systems), α-tubulin antibody (1:3,000; Santa Cruz Biotechnology Inc.) and β-actin antibody (1:1,000; Cell Signaling Technology). Whole cell lysates were prepared from cells, separated on 10% SDS-polyacrylamide gel, and transferred to polyvinylidene difluoride membranes. The membranes were incubated with 5% milk in TBST (w/v) for 0.5 hour and then incubated with primary anti-bodies overnight at 4°C. Blots were incubated with horseradish peroxidase- coupled secondary antibodies (Promega; R&D systems) for 1 hour, and protein expression was detected with SuperSignal West Pico Chemiluminescent Substrate or SuperSignal West Femto Chemiluminescent Substrate (Thermo Scientific). ImageJ software (http://rsb.nih.gov/ij) was used for quantification of Western blots.

4.3.7 Directed Cell-lineage Differentiation and Embryoid Body (EB) Formation

EB formation was achieved by culturing clusters of hESCs in suspension with DMEM (GIBCO) supplemented with 10% FBS for 10 days. Directed cell-lineage differentiation was performed on

matrigel coated dishes using the following protocols [25]. hESCs were induced to differentiate in chemically defined medium (CDM) base consisting of DMEM/F12 (GIBCO) supplemented with 1X N2 (Invitrogen), 1X B27 (Invitrogen), 0.11 mM 2-mercaptoethanol, 1 mM nonessential amino acids, 2 mM L-glutamine, and 0.5 mg/ml BSA (fraction V; Sigma Aldrich). To induce definitive endoderm (pancreatic differentiation), 100 ng/ml human recombinant activin A (STEMGENT) was added to CDM and cells were then cultured in this condition for 6 days, followed by culture in CDM without activin A for another 9 days. For mesoderm (cardiomyocyte differentiation), cells were cultured in CDM supplemented with 50 ng/ml human recombinant BMP4 (STEMGENT) and 50 ng/ml human recombinant activin A (STEMGENT) for 4 days, then further cultured in CDM without activin A and BMP4 for an additional 10 days. For ectoderm (neuronal differentiation), 100 ng/ml human recombinant Noggin (STEMGENT) was added to the CDM and cells were cultured for 8 days.

4.3.8 Retrovirus Production and Transduction into Cells

Retrovirus (10X) was produced with the plasmids (*pMXs-hOCT3/4*, *pMXs-hSOX2*, *pMXs-hKLF4*, *pMXs-hC-MYC*, *pMXs-DPPA5* and *pMXs-GW* (as control), respectively; Addgene plasmid #: 17217, 17218, 17219, 17220, 13352 and 18656) by University of Michigan Vector Core using standard protocols. Unless otherwise specified, after trypsinization, 2 X 10^4 single hPSCs were plated on a matrigel-coated 60 mm TCPS dish in hPSC culture medium supplemented with 10 μM of Rho-associated coiled coil forming protein serine/threonine kinase (ROCK) inhibitor (Sigma-Aldrich). Besides, 1.5 X 10^5 fibroblasts were plated on a 35 mm TCPS dish in fibroblast culture medium. Cells were infected by 1X viruses plus polybrene (10 μg/mL; Sigma-Aldrich) when the confluency reached about 60%.

4.3.9 *DPPA5* Overexpression

Fibroblasts and hPSCs were infected by *DPPA5* retroviruses using the method described above. In addition, fibroblasts were also transfected in a 35 mm TCPS dish with 2 μg pCMV6-Entry plasmid containing *DPPA5* human cDNA ORF Clone (OriGene) using FuGENE6 (Promega). The construct pCMV6-Entry (OriGene) was used as control.

4.3.10 Co-immunoprecipitation

Immunoprecipitation (IP) was performed using the ImmunoCruz™ IP/WB Optima C System (Santa Cruz Biotechnology) following the manufacturer's protocol. Briefly, hESCs protein extracts were prepared in CHAPS lysis and IP buffer (FIVEphoton Biochemicals) with protease inhibitor (FIVEphoton Biochemicals) and phosphatase inhibitor (FIVEphoton Biochemicals). hESC lysate (700 μg of total protein) was precleared with Preclearing Matrix C-mouse (Santa Cruz Biotechnology) for 1.5 hours at 4°C on a rotator. Meanwhile, 2.6 μg NANOG-specific antibody (Abcam) or normal mouse IgG (Santa Cruz Biotechnology) were mixed and incubated to form IP antibody-IP matrix complex and the control-IP matrix complex, respectively. After 1 hour of incubation at 4°C on a rotator, IP antibody-IP matrix complex was washed with PBS (GIBCO). The supernatant was discarded after centrifugation. The precleared hPSCs lysate supernatant was transferred after centrifugation to the pelleted IP antibody-IP matrix complex and incubated at 4°C on a rotator overnight. After incubation and centrifugation, pelleted matrix was washed with PBS and Western blot analysis was performed to detect the interaction between NANOG and DPPA5 proteins. Whole hPSCs lysate was used as input.

4.3.11 Protein Stability Assay

hPSCs were infected with DPPA5 or control (pMXs-GW) retroviruses. After 72 hours, cycloheximide (CHX; Sigma-Aldrich) was added to the culture media at a concentration of 45 μg/ml. CHX treatment lasted until cells were subsequently harvested at different time points (0.5 hours, 1 hours, 1.5 hours after CHX addition). Equal amounts of protein were loaded from each treated sample and analyzed by Western blot assays.

4.3.12 Immunofluorescence Staining

Cells were fixed in 4% paraformaldehyde for 30 minutes at room temperature and then permeabilized with 0.1% Triton X-100 for 10 minutes. Primary antibodies against DPPA5 (R&D systems) and NANOG (Abcam) were diluted in 1% normal serum (v/v) and incubated overnight at 4°C and detected with respective secondary antibodies. Sample images were captured using a Nikon TE2000-S inverted microscope with a Nikon DS-Ri1 camera, or using Nikon confocal microscope system $A1^{+}$.

4.3.13 Derivation of hiPSCs

For the control group, human gingival fibroblasts (hGF2) were infected on day 0 by retroviruses (*OCT4*, *SOX2*, *KLF4* and *C-MYC*) using the method described above. On day three, cells were trypsinized and passed to matrigel coated flasks (75 cm^2). At that time, the fibroblast culture medium was replaced by hPSC culture medium supplemented with 10 μM of ROCK inhibitor (Sigma-Aldrich). The hPSC culture medium with ROCK inhibitor was refreshed every day until day 23, when cells were fixed and stained for alkaline phosphatase. The following experimental groups were analyzed: fibroblasts infected by retroviruses (*OCT4*, *SOX2*, *KLF4* and *C-MYC*) on day 0. In addition, fibroblasts were infected with retroviruses carrying *DPPA5* on day 0, day 6, day 9 and day 12, respectively.

4.3.14 Alkaline Phosphatase Assay

An Alkaline Phosphatase Staining Kit (STEMGENT) was used for phenotypic assessment of hiPSCs. Briefly, on day 23 after fibroblasts were infected with *OCT4*, *SOX2*, *KLF4* and *C-MYC* viruses, cells were fixed with Fix Solution for 2-5 minutes, then rinsed and incubated in AP Substrate Solution in the dark at room temperature for 15 minutes. Cells were rinsed and covered with 1 X PBS to prevent drying before quantitative analysis. hiPSC colonies were identified by positive alkaline phosphatase staining and morphological characteristics of colonies such as: well defined borders and high nuclei/cytoplasmic ratio.

4.3.15 Data Analysis

Three independent replicates of each experiment were performed. Two data sets were compared using unpaired student t-test function in Excel (Microsoft, Seattle, WA) to calculate p-values. Multiple data sets were compared using one-way ANOVA analysis followed by the Tukey's post-hoc test to calculate p-values. Level of statistical significance was set at $p < 0.05$.

4.4 Results

4.4.1 DPPA5 Expression is Higher When hPSCs are Cultured on Feeder-free Substrates Than on MEFs

To investigate the mechanism by which synthetic substrates such as PMEDSAH support hPSC self-renewal, we compared the gene expression of hESCs cultured on PMEDSAH versus on irradiated MEFs, after 3 consecutive passages. Microarray and Quantitative RT-PCR analysis demonstrated that *DPPA5* gene expression levels were significantly higher in hESCs cultured on PMEDSAH compared to on MEFs, while the expression of other pluripotency-related factors

such as *OCT4*, *SOX2*, *KLF4*, *C-MYC* and *NANOG* showed no significant differences (Figure 4-1, Figure 4-2A). Similar results were obtained with the CHB10 hESC line and three independent hiPSC lines (Figure 4-2B). Western blot analysis demonstrated that protein levels of DPPA5 and NANOG were higher in hPSCs cultured on PMEDSAH compared to MEFs, while other pluripotency-related factors showed no significant differences (Figure 4-2C). The gene expression of *DPPA5* of hPSCs was then compared to cells cultured on MEFs and other feeder-free conditions (matrigel, laminin-511 and vitronectin). Quantitative RT-PCR analysis demonstrated higher gene expression of *DPPA5* in hPSCs grown on feeder-free substrates compared to cells cultured on MEFs, while no significant RNA expression differences were observed among hESCs cultured in these feeder-free conditions (Figure 4-2D).

Previously, we demonstrated that both the extracellular matrix (ECM) and soluble factors secreted by MEFs significantly impact the self-renewal of hESCs [22]. Therefore, we hypothesized that the ECM and soluble factors secreted by MEFs may inhibit *DPPA5* expression in hPSCs, compared to feeder-free conditions. MEF-conditioned medium and ECM deposits were prepared on TCPS dishes as described in the Materials and Methods section, and used to cultured hESCs for three passages in a combinatorial experiment. The combination of PMEDSAH and HCCM was set as the control culture condition. In addition, cells were cultured on PMEDSAH plus day 1 or day 7 MEF-conditioned medium, and day 1 or day 7 MEF-ECM plus HCCM. The RNA expression of *OCT4* was used as an indicator of the undifferentiated state of hESCs. Quantitative RT-PCR analysis demonstrated that, compared to the control condition, hPSCs expressed lower levels of *DPPA5* in PMEDSAH with day 7 MEF-conditioned medium (Figure 4-3A), indicating that soluble factors secreted by MEFs inhibit *DPPA5* expression. Similarly, compared to the control condition, the expression of *DPPA5* was lower in hPSCs

cultured on MEF-ECM plus HCCM (Figure 4-3B), indicating that the ECM deposited by MEFs also inhibits *DPPA5* expression in hPSCs. Taken together, these data suggested that soluble factors and ECM deposited by irradiated MEF inhibits the gene expression and protein levels of DPPA5 in hPSCs.

We analyzed *DPPA5* gene expression levels in hPSCs and their differentiated derivative cells. Quantitative RT-PCR demonstrated that *DPPA5* expression levels were significantly up-regulated in hiPSCs compared to their corresponding parental fibroblasts (Figure 4-4A). When compared to undifferentiated hESCs, *DPPA5* expression levels significantly decreased after embryoid body (EB) formation (Figure 4-4B) and in cells induced to endodermal, mesodermal and ectodermal lineages (Figure 4-4C). Cell lineage differentiation and EB formation was confirmed by the increasing expression of factors representative of each germ layer (Figure 4-5, Table 4-1). Our finding that *DPPA5* expression was higher in undifferentiated hPSCs compared to differentiated cells is consistent with other studies that used DPPA5 as a PSC marker [9, 12-14, 26-29]. This specific expression pattern suggested that DPPA5 may play an important role in hPSC self-renewal and pluripotency.

4.4.2 DPPA5 Regulates NANOG Protein Levels

The higher expression of DPPA5 in hPSCs cultured under feeder-free conditions compared to MEFs provoked our interest in elucidating the function of DPPA5. Overexpression of *DPPA5* in fibroblasts did not significantly affect gene expression of *OCT4, SOX2, KLF4, C-MYC* and *NANOG* (Figure 4-6A). However, in addition to detecting a significant increase in DPPA5 protein levels, we also demonstrated an increase in NANOG protein levels via Western blot analysis (Figure 4-6B). No changes in protein levels were observed for other pluripotency-

related factors. The same pattern was observed when *DPPA5* was overexpressed in hESCs. NANOG protein levels dramatically increased without significant changes in gene expression (Figure 4-6C, D). These data indicated that DPPA5 functions as a positive regulator of NANOG protein at the post-transcriptional level.

4.4.3 DPPA5 Protein Interacts with and Stabilizes NANOG Protein

We next investigated the extent to which DPPA5 may affect NANOG protein levels in hPSCs. Immunofluorescence staining and confocal microscopy analysis illustrated that DPPA5 was localized in both the cytoplasm and nucleus of hESCs. In addition, DPPA5 co-localized with NANOG in the nucleus (Figure 4-7A), indicating a possible interaction between these two proteins. Co-immunoprecipitation was performed to investigate this possible interaction between DPPA5 and NANOG in hESCs. Western blot analysis demonstrated that NANOG was successfully pulled down by a NANOG IP antibody-IP matrix complex. Concurrent with this finding, DPPA5 was strongly co-precipitated by NANOG, indicating the interaction between DPPA5 and NANOG protein. No protein was co-precipitated by the normal mouse IgG-IP matrix complex, suggesting that nonspecific binding did not play a role in these experiments (Figure 4-7B). Protein stability assays were then performed to identify the extent to which DPPA5 inhibits NANOG protein degradation in hESCs. Western blot analysis showed that the degradation of NANOG was significantly delayed by *DPPA5* overexpression in the presence of cycloheximide (Figure 4-7C). Taken together, these data indicated that DPPA5 interacts with and stabilizes NANOG in hPSCs.

4.4.4 DPPA5 Enhances the Function of NANOG on Its Target Genes

Recent studies reported that NANOG increases the transcription of *SALL4*, and represses the transcription of *GATA6* and *SOCS3* through binding to their proximal gene promoters [30-34]. To study the extent to which DPPA5 enhances the function of NANOG in hPSCs, we examined the expression of NANOG target genes (*SALL4*, *GATA6* and *SOCS3)* in response to *DPPA5* overexpression (Figure 4-6C, D). We found that gene expression of *SALL4* was increased, while *GATA6* and *SOCS3* was repressed after *DPPA5* overexpression (Figure 4-8). This evidence suggested that DPPA5 not only increased NANOG protein levels through post-translational stabilization, but also facilitated the function of NANOG on its target genes.

4.4.5 DPPA5 Increases hiPSC-reprogramming Efficiency

Because of the stabilizing action of DPPA5 on NANOG in hESCs, and the critical role of NANOG on hPSCs self-renewal and in the generation of hiPSCs [3, 19], we investigated whether DPPA5 would have a positive effect during reprograming of fibroblasts into hiPSCs. *DPPA5* was added to the *OCT4*, *SOX2*, *KLF4*, and *C-MYC* cocktail (Figure 4-9) to determine its effect on reprogramming. Retroviruses (*OCT4, SOX2, KLF4*, and *C-MYC*) were used to infect fibroblasts in both control and experimental groups on day 0. Experimental group cells were additionally infected with retroviruses encoding *DPPA5* on day 0, day 6, day 9 and day 12 (experimental group-d0+D, d6+D, d9+D and d12+D, respectively). On day 23, iPSC colonies were identified by positive alkaline phosphatase staining and morphological characteristics (Figure 4-9C). Surprisingly, we found that the transduction of *DPPA5* retroviruses on day 6, day 9, day 12, but not day 0, significantly enhanced the generation of hiPSC colonies compared to controls, indicating that DPPA5 increases iPSC-reprogramming efficiency of *OCT4, SOX2, KLF4*, and *C-MYC.* Clusters of hiPSCs formed EBs when cultured in suspension and expressed

genes representing endoderm, mesoderm and ectoderm (Table 4-2, 4-3), indicating the pluripotency of these cells.

4.5 Discussion

In this study, we performed a comprehensive analysis of the role of DPPA5 in hPSCs and identified new functions of DPPA5 in hPSC biology, NANOG regulation and iPSC-reprogramming.

The potential for successful therapeutic application of hPSCs and their derivatives is based on the ability to develop clinically compliant strategies for large-scale production of therapeutically relevant cells [35-37]. Currently, the large-scale expansion of hPSCs is limited by xenogeneic components and poorly defined culture conditions that utilize feeder cells and other animal-based products to support hESC self-renewal [1, 38, 39]. To overcome these limitations, the use of human recombinant proteins like Laminin and Vitronectin have been tested for long-term maintenance of hESCs [39, 40]. Moreover, synthetic substrates such as PMEDSAH [20, 21] have demonstrated great potential for large-scale propagation of hESCs [42]. Our data suggest that MEF conditions, including the synthesis of soluble factors and the deposition of an ECM, inhibit DPPA5 expression in hPSCs compared to feeder-free culture conditions. These findings are consistent with a recent study that showed the capacity of γ-irradiated MEFs to support hESC self-renewal is compromised over time due to changes in the secretion of soluble factors and ECM of MEFs [22]. These data support the trend in the evolution of hPSC culture from feeder-cell dependence and ill-defined conditions, to feeder-free and defined microenvironments [43].

Pluripotency and self-renewal are maintained in PSCs by a network of interacting transcription factors, influenced by specific signaling pathways [44], and may be different depending on the *in*

vitro culture conditions. Our data clearly identifies DPPA5 as a new component in this regulatory network of pluripotency that is differentially expressed depending on the culture conditions. DPPA5 is highly expressed in feeder-free conditions (PMEDSAH, matrigel, laminin-511 and vitronectin) compared to feeder-dependent conditions (irradiated MEFs), suggesting that DPPA5 may play a more important role in hPSC maintenance under feeder-free conditions. Our finding that the molecular mechanisms supporting hPSC pluripotency are different depending on the culture conditions, as well as the species differences between human and mouse ESCs, may be, in part, responsible for a previous study that found no significant impact on mouse ESC self-renewal when cultured on MEFs and when *DPPA5* was knocked out in these cells [11].

The identification of a functionally significant role for DPPA5 in hPSC self-renewal is essential for our understanding of the mechanism by which feeder-free conditions are able to support hPSC self-renewal. This is especially true since the use of hPSCs in regenerative medicine will likely be dependent on expanding these cells in xenogenic, feeder-free conditions. Our data indicate that in hPSCs, DPPA5 regulates NANOG protein stability and enhances the function of NANOG on its target genes. This new finding that up-regulation of NANOG by DPPA5 is important because of the central role of NANOG in the pluripotency regulatory network in PSCs. NANOG is a homeodomain protein that binds to DNA and regulates the transcriptional levels of other genes, such as *SALL4*, *GATA6* and *SOCS3* [30-34, 45]. Previous findings demonstrating that down-regulation of NANOG in hESCs induces differentiation [6], while its overexpression prevents differentiation [16-18], suggest that sufficient levels of NANOG are critical for hPSC self-renewal. Here, we demonstrate that DPPA5 may be a significant contributor in maintaining NANOG protein levels in hPSCs. Moreover, our finding that NANOG target gene expression is impacted by DPPA5 overexpression in hPSCs further suggests that the increased NANOG

protein stability by DPPA5 does actively function in hPSCs. Together, our study suggests that DPPA5 plays an important role in supporting hPSC self-renewal by facilitating the protein levels of NANOG, a master transcriptional regulator for hPSC pluripotency. DPPA5 inhibits hPSC differentiation by stabilizing NANOG protein levels and enhancing the up-regulatory effects of NANOG on *SALL4*, a transcription factor required for ESC pluripotency, and down-regulatory effects of NANOG on *GATA6 and SOCS3*, well-known NANOG target genes that function in early stages of differentiation [34, 46, 47].

Another novel and potentially important finding is the mechanism by which DPPA5 facilitates NANOG protein levels. Previous studies have reported transcriptional regulation of *NANOG* by other pluripotency-related factors such as OCT4, SOX2 and KLF4 [48, 49]. Meanwhile, DPPA5 has been reported to be an RNA binding protein because it contains a KH domain [8]. Interestingly, we found that NANOG protein levels increased after *DPPA5* overexpression without significant changes at *NANOG* mRNA levels. We also found that both mRNA and protein levels of other key pluripotent-related transcription factors (OCT4, SOX2 and KLF4) remained unchanged after *DPPA5* overexpression. These findings led us to raise the hypothesis that DPPA5 directly interacts with and stabilizes NANOG proteins, which is supported by the co-immunoprecipitation and protein stability results. In support of these findings, a previous study showed that DPPA5 does not bind to, and regulate NANOG RNA after an immunoprecipitation-microarray screening [15]. In addition, our findings of the post-translational regulation of NANOG are consistent with other studies showing that, like other pluripotency-related transcription factors such as OCT4, KLF4 and C-MYC, NANOG is also an unstable protein with a relatively short half-life in hPSCs. These transcription factors are degraded through ubiquitin-dependent proteolysis [50-54], while proteasome inhibitors are able

to block NANOG protein degradation in hPSCs and extend its half-life [55]. Our findings that DPPA5 interacts with and stabilizes NANOG provide an additional model of regulation of NANOG in hPSCs, suggesting that in addition to the broadly investigated transcriptional regulation of pluripotency-related transcription factors, post-translational regulation also plays a role in the hPSC pluripotency regulatory network. Thus, this regulatory model not only supports the hypothesis that DPPA5 is able to regulate NANOG, but also furthers our understanding of the molecular mechanisms that define hPSC pluripotency. We also observed that DPPA5 protein, like NANOG and other pluripotency-related factors, is degraded in a rapid manner in hPSCs

Human iPSCs reprogrammed from adult somatic cells by the process of induced pluripotency, holds great potential for disease modeling, drug screening and cell replacement therapy [56]. Currently, hiPSC-reprogramming is significantly limited by the low iPSC generation efficiency. We found that the addition of *DPPA5* to the reprogramming cocktail *(OCT4, SOX2, KLF4* and *C-MYC: OSKM*) increased the generation of iPSCs greater than 3-fold when compared to controls. This identification of the function of DPPA5 in iPSC generation suggests that DPPA5 has potential for improving our current reprogramming techniques by decreasing the reprogramming time, production cost, as well as reducing the risk of contamination by shortening the length of the reprogramming process. Our data demonstrate that, compared to the OSKM control group, DPPA5 enhances iPSC-reprogramming efficiency when transduced into cells at 6, 9 or 12 days after initial *OSKM* cocktail treatment, whereas the reprogramming efficiency remains the same compared to the *OSKM* control group, if *DPPA5* is over-expressed together with *OSKM* on day 0. This observation suggests that *DPPA5* may have an optimal time window for being overexpressed in the cells to efficiently promote iPSC-reprogramming and may be related to the timing of NANOG expression in the reprogramming process. The central

role of NANOG in reprogramming of somatic cells into iPSCs [3, 19, 57, 58], combined with our finding that DPPA5 regulates NANOG protein levels, suggest that DPPA5 may promote hiPSC-generation efficiency by enhancing NANOG and its function during this optimal time. This new finding is consistent with a recent study showing the benefit of sequential introduction of reprogramming factors [59] in which a sequential EMT-MET (epithelial-to-mesenchymal transition followed by mesenchymal-to-epithelial transition) mechanism optimizes reprogramming. Taken together, our data suggest the important function of DPPA5 in iPSC generation and extends our knowledge of iPSC-reprogamming, and may further advance our current reprogramming protocols.

In this study, we provide new molecular insight into the function of the pluripotent stem cell marker DPPA5 in hPSCs. *In vitro* culture conditions influence the expression of DPPA5 in hPSCs. The ECM deposited by irradiated MEFs, as well as secreted soluble factors, inhibit the expression of DPPA5 in hPSCs, while its expression and function is permissive under feeder-free conditions. DPPA5 stabilizes protein levels and enhances the function of NANOG, a key transcription factor for hPSC pluripotency. Finally, *DPPA5* increases the reprogramming efficiency of somatic cells into human iPSCs when transduced with *OCT4, SOX2, KLF4* and *C-MYC*. In conclusion, DPPA5 plays an important role in supporting hPSC self-renewal and reprogramming. Our findings advance our knowledge of hPSC biology and offer improvements to current protocols in hPSC maintenance and reprogramming, which may contribute to the future application of these cells in regenerative medicine.

4.6 Figures

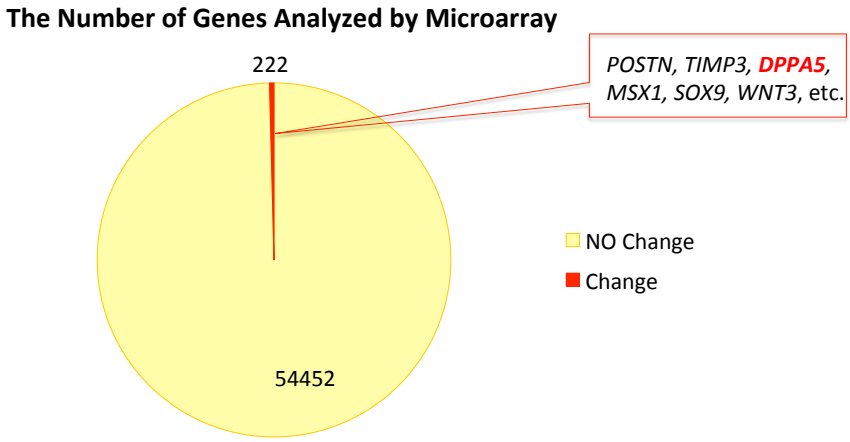

Figure 4-1. Gene expression differences between hESCs cultured on PMEDSAH versus on MEFs Out of 54674 analyzed by microarray, 222 genes were found expressing at significantly different levels between hESCs cultured on PMEDSAH and MEFs. The gene expression of *DPPA5* was significantly higher in hESCs cultured on PMEDSAH compared to on MEFs, while the expression of other pluripotency-related factors such as *OCT4*, *SOX2*, *KLF4*, *C-MYC* and *NANOG* showed no significant differences.

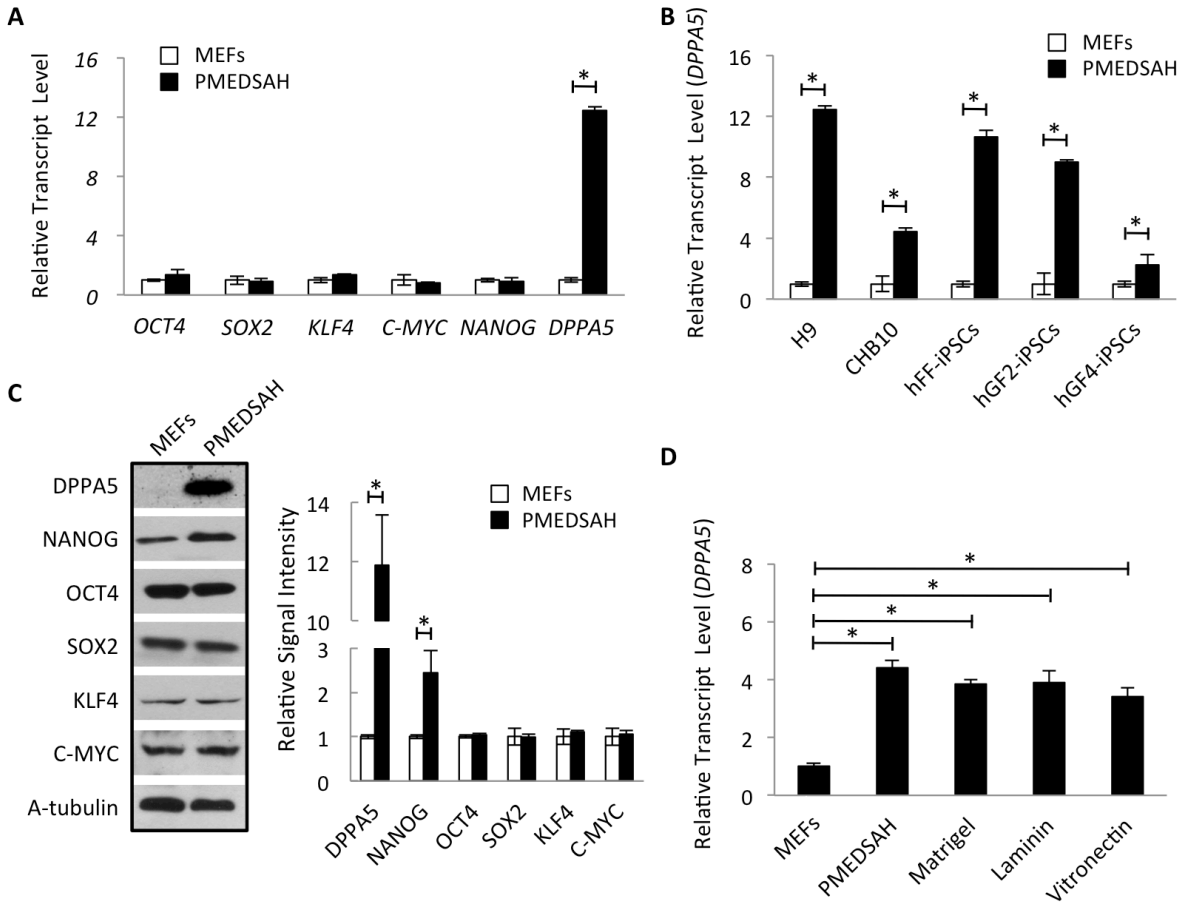

Figure 4-2. Differences in *DPPA5* gene expression and protein levels in hPSCs cultured on irradiated MEFs and feeder-free substrates. (A) Relative transcript levels of *DPPA5* were higher in hESCs (H9) cultured on PMEDSAH compared to on MEFs, while relative transcript levels of *OCT4, SOX2, KLF4, C-MYC* and *NANOG* showed no significant differences in expression. (B) Relative transcript levels of *DPPA5* were higher in multiple types of hPSCs (H9, CHB10, hFF-iPSCs, hGF2-iPSCs, and hGF4-iPSCs) cultured on PMEDSAH compared to MEFs. (C) Western blot analysis and relative signal intensity of DPPA5, NANOG, OCT4, SOX2, KLF4 and C-MYC proteins in hESCs cultured on MEFs and PMEDSAH. α-tubulin was used as a loading control. (D) Compared to when cultured on MEFs, the relative transcript levels of *DPPA5* were higher in hESCs (CHB10) cultured on feeder-free substrates such as PMEDSAH, matrigel, laminin and vitronectin. Plot data presented as mean ± standard deviation (SD) from three independent experiments (* $p<0.05$). *Credit: Xu Qian, et al. Stem Cells. manuscript under revision*

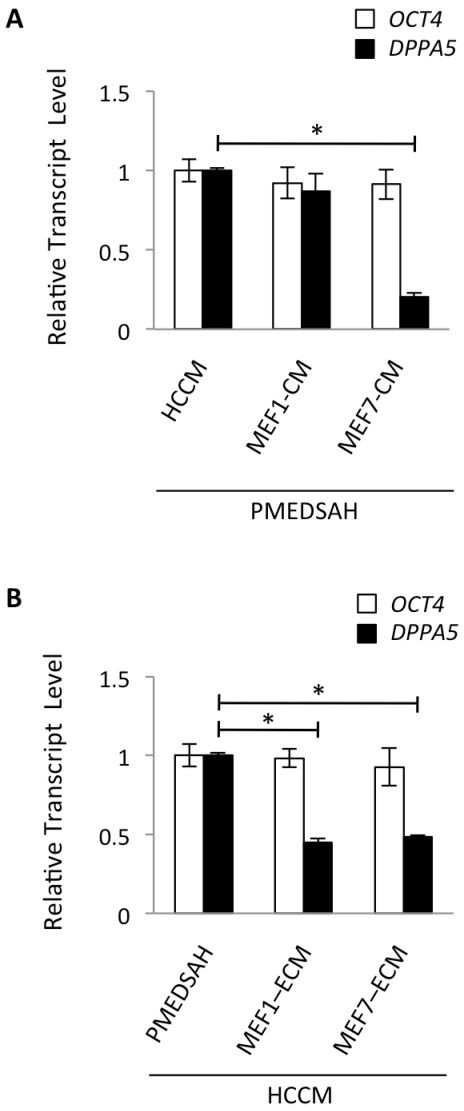

Figure 4-3. Soluble factors and ECM secreted by irradiated MEFs inhibited *DPPA5* expression in hPSCs compared to feeder-free conditions. The control culture condition was PMEDSAH (substrate) plus HCCM (medium). (A) Relative transcript levels of *DPPA5* in hESCs cultured in control culture condition, PMEDSAH plus day 1 MEF-conditioned medium, and PMEDSAH plus day 7 MEF-conditioned medium. (B) Relative transcript levels of *DPPA5* in hESCs cultured in control culture condition, day 1 MEF-ECM plus HCCM, and day 7 MEF-ECM plus HCCM. *OCT4* gene expression was used as a marker indicating the undifferentiated state of the collected hESCs. Data presented as mean ± standard deviation (SD) from three independent experiments (* $p<0.05$). *Credit: Xu Qian, et al. Stem Cells. manuscript under revision*

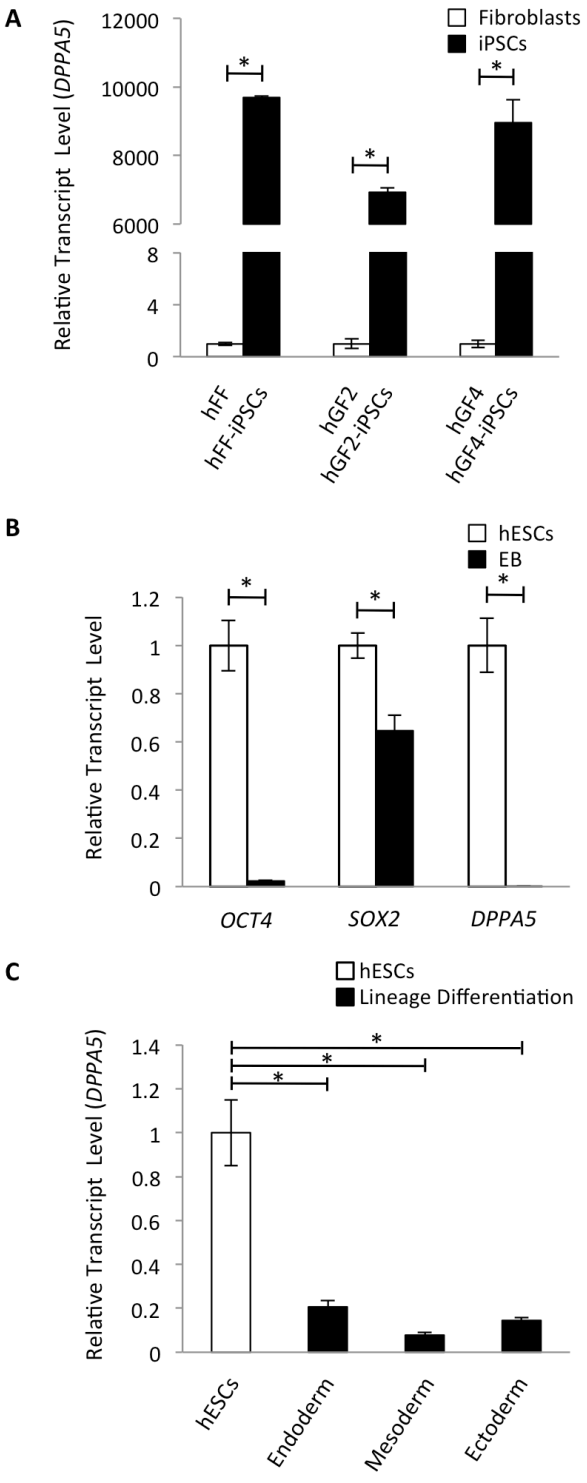
A
Relative Transcript Level (DPPA5)
12000
10000
8000
6000
8
4
0
Fibroblasts
iPSCs
*
*
*
hFF
hFF-iPSCs
hGF2
hGF2-iPSCs
hGF4
hGF4-iPSCs
B
hESCs
EB
Relative Transcript Level
1.2
1
0.8
0.6
0.4
0.2
0
*
*
*
OCT4
SOX2
DPPA5
C
hESCs
Lineage Differentiation
Relative Transcript Level (DPPA5)
1.4
1.2
1
0.8
0.6
0.4
0.2
0
*
*
*
hESCs
Endoderm
Mesoderm
Ectoderm

Figure 4-4. Differences in *DPPA5* expression between hPSCs and differentiated cells (A) Relative transcript levels of *DPPA5* increased in iPSCs (hFF-iPSCs, hGF2-iPSCs and hGF4-iPSCs) compared to corresponding parental fibroblasts. (B) Relative transcript levels of *OCT4*, *SOX2* and *DPPA5* decreased after embryoid body formation from hESCs. (C) Relative transcript levels of *DPPA5* decreased after directed cell lineage differentiation from hESCs into endodermal, mesodermal and ectodermal derivatives. Data presented as mean ± standard deviation (SD) from three independent experiments (* $p<0.05$). *Credit: Xu Qian, et al. Stem Cells. manuscript under revision*

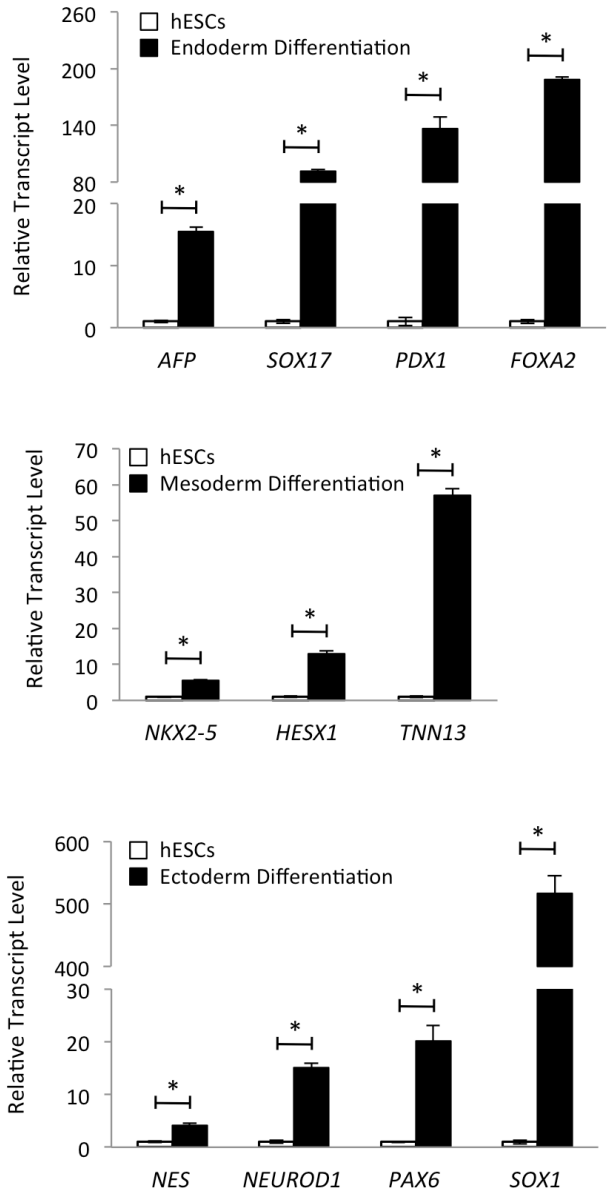

Figure 4-5. Induced specific lineage differentiation from hESCs with expression of genes representing different germ layers. Quantitative RT-PCR data presented as mean ± SD from three independent experiments (* $p<0.05$). *Credit: Xu Qian, et al. Stem Cells. manuscript under revision*

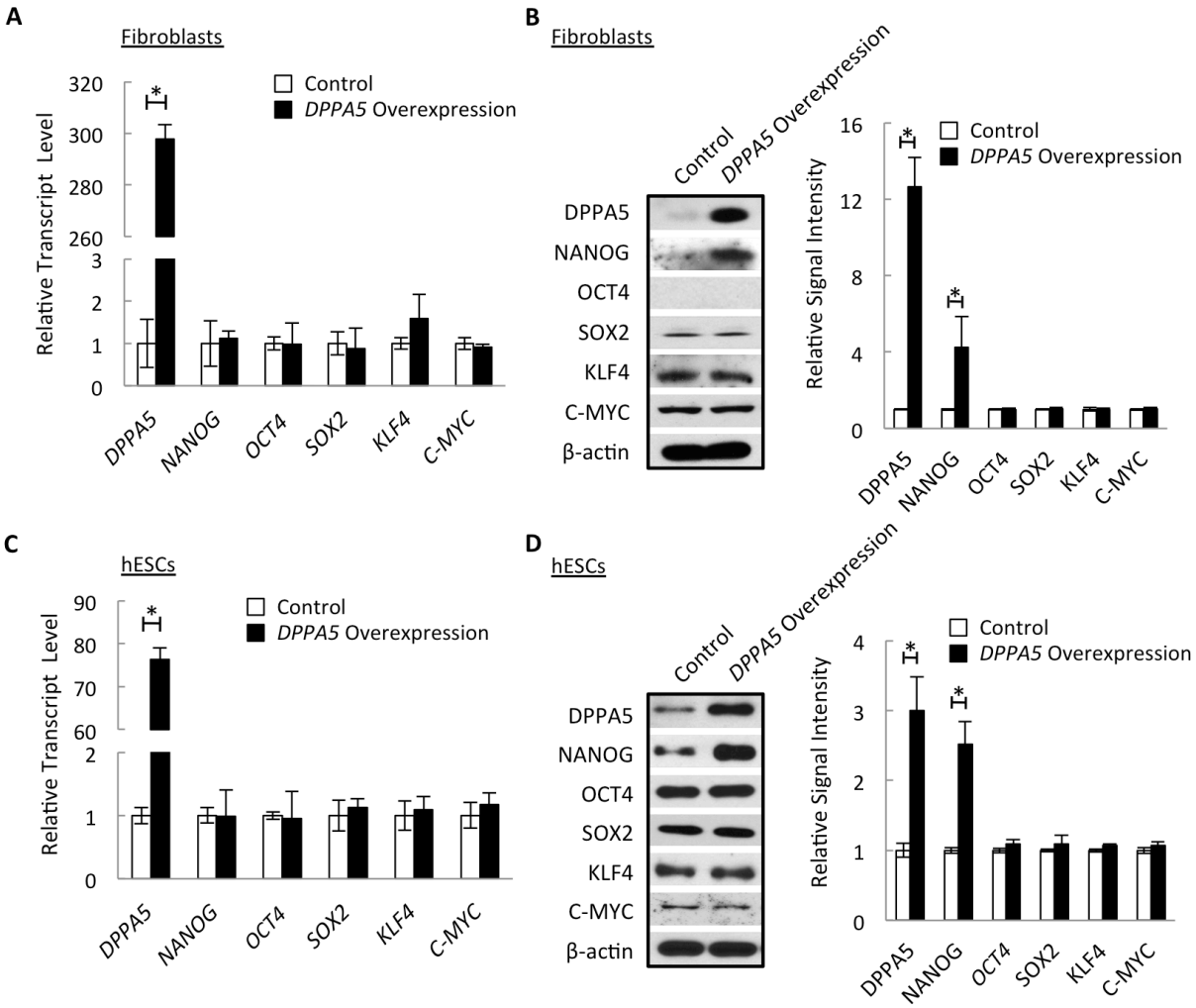

Figure 4-6. The regulation of NANOG protein levels by DPPA5 in hPSCs (A) Relative transcript levels of *DPPA5, NANOG, OCT4, SOX2, KLF4 and C-MYC* between control fibroblasts and with *DPPA5* overexpression. (B) Western blot analysis and relative signal intensity of DPPA5, NANOG, OCT4, SOX2, KLF4 and C-MYC proteins between control fibroblasts and with *DPPA5* overexpression. β-actin was used as a loading control. (C) Relative transcript levels of *DPPA5, NANOG, OCT4, SOX2, KLF4 and C-MYC* between control hESCs and with *DPPA5* overexpression. (D) Western blot analysis and relative signal intensity of DPPA5, NANOG, OCT4, SOX2, KLF4 and C-MYC proteins between control hESCs as control and with *DPPA5* overexpression. β-actin was used as a loading control. Plot data presented as mean ± standard deviation (SD) from three independent experiments (* $p<0.05$). *Credit: Xu Qian, et al. Stem Cells. manuscript under revision*

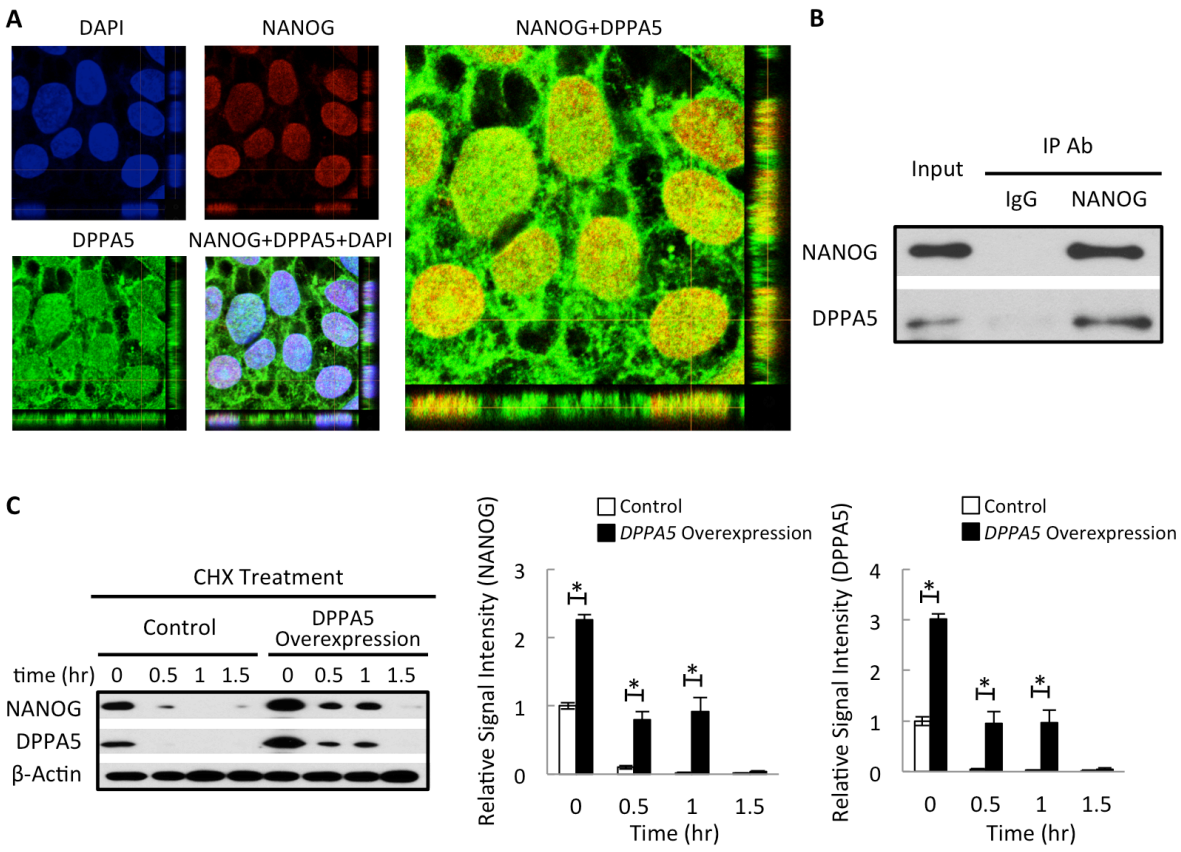

Figure 4-7. Protein interaction and stabilization between DPPA5 and NANOG in hPSCs

(A) Confocal microscopy images of immunofluorescence staining of hESCs with NANOG and DPPA5 primary antibodies. 4', 6-diamidino-2-phenylindole (DAPI) shows nuclear staining. The merged images indicate the co-localization of DPPA5 and NANOG in hESC nucleus. (B) Co-immunoprecipitation of endogenous NANOG and DPPA5 in hESCs. hESCs extracts prepared in CHAPS lysis and IP buffer were immunoprecipitated with anti-NANOG or control IgG antibody. The immune complexes and the input (whole hESC lysate) were analyzed by Western blot with antibody specific to NANOG or DPPA5. (C) The protein levels of NANOG and DPPA5 at the indicated time points after CHX (45 μg/ml) treatment were analyzed in control hESCs or with *DPPA5* overexpression. Western blot analysis and relative signal intensity indicated that DPPA5 supports NANOG protein stability in hESCs. β-actin was used as a loading control. Plot data presented as mean ± standard deviation (SD) from three independent experiments (* $p<0.05$).

Credit: Xu Qian, et al. Stem Cells. manuscript under revision

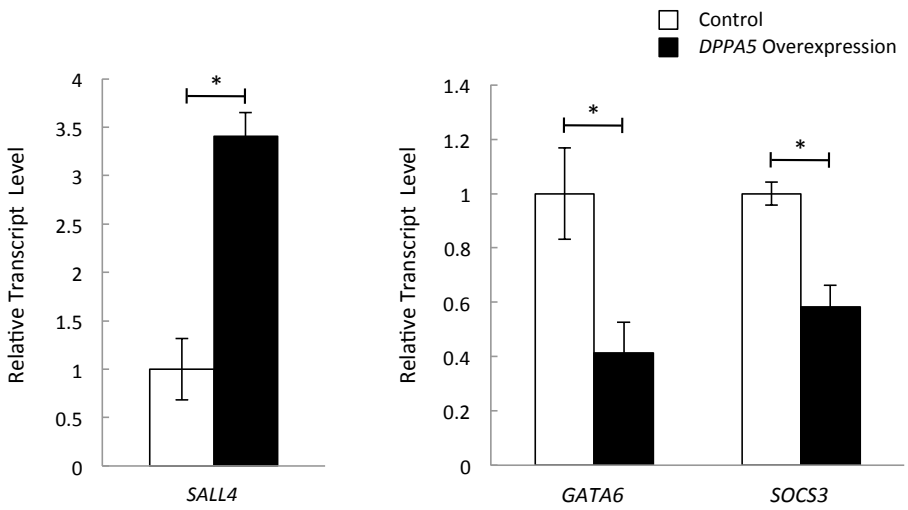

Figure 4-8. Regulation of the expression of NANOG target genes by DPPA5 in hPSCs
SALL4 is positively regulated by NANOG. *GATA6* and *SOCS3* are negatively regulated by NANOG. Relative transcript level of *SALL4* was higher, while *GATA6* and *SOCS3* were lower in hESCs with *DPPA5* overexpression compared to control hESCs. Data presented as mean ± standard deviation (SD) from three independent experiments (* $p<0.05$). *Credit: Xu Qian, et al. Stem Cells. manuscript under revision*

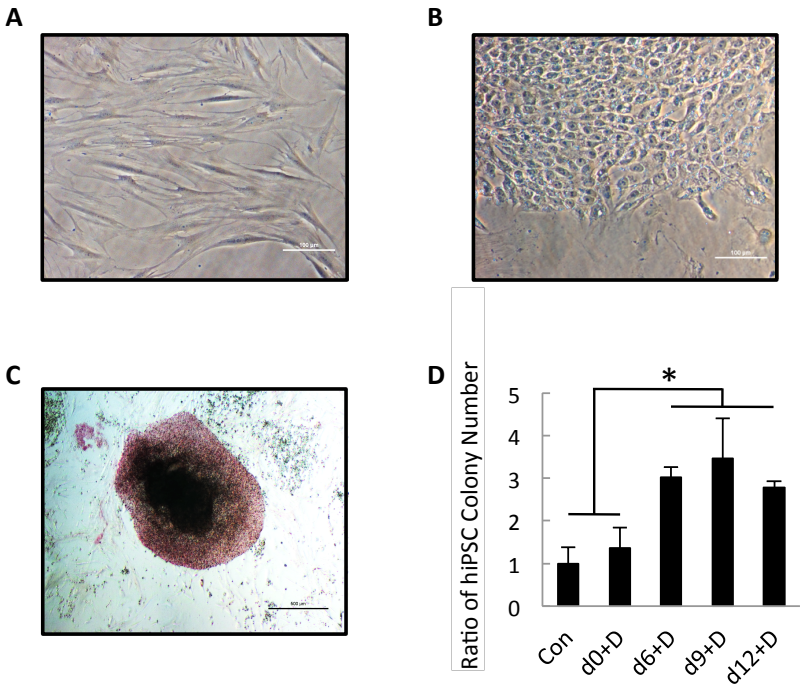

Figure 4-9. DPPA5 increased hiPSC-reprogramming efficiency Bright-field images of (A) fibroblasts (hGF2) and (B) iPSCs (hGF2-iPSCs) reprogramed from fibroblasts. Scale bars, 100 μm. (C) Bright-field image of an alkaline phosphatase positive iPSC (hGF2-iPSCs) colony after reprogramming. Scale bars, 500 μm. (D) Ratio of iPSC colony number demonstrated that day 6, day 9 and day 12-DPPA5 added groups (d6+D, d9+D, d12+D) had higher iPSC colony number compared to control group and day 0-DPPA5 added group (d0+D). In the control group, fibroblasts (hGF2) were transduced on day 0 by retroviruses (*OCT4, SOX2, KLF4* and *C-MYC*). For experimental groups, retroviruses (DPPA5) were transduced into cells respectively on day 0, day 6, day 9 and day 12, in addition to *OCT4, SOX2, KLF4* and *C-MYC* cocktail transduction on day 0. iPSC colonies were identified by positive alkaline phosphatase (ALP) staining and morphological characteristics of colonies as in (C). The number of the iPSC colonies was counted. Plot data presented as mean ± standard deviation (SD) from three independent experiments (* $p<0.05$). *Credit: Xu Qian, et al. Stem Cells. manuscript under revision*

4.7 Tables

Table 4-1. Embryoid body (EB) formation from hESCs with expression of genes representing different germ layers

	Gene	Relative Transcript Level ± SD
Endoderm	*PDX1*	28.24 ± 3.70
	AFP	42.18 ± 4.39
	SOX17	126.57 ± 6.58
	FOXA2	237.87 ± 20.9
Mesoderm	*HESX1*	11.2 ± 1.88
	TNN13	110.88 ± 2.28
	NKX2-5	122.86 ± 17.48
Ectoderm	*NES*	3.84 ± 0.67
	SOX1	34.76 ± 1.98
	PAX6	89.24 ± 3.03
	NEUROD1	683.19 ± 89.38

Credit: Xu Qian, et al. Stem Cells. manuscript under revision

Table 4-2. Embryoid body (EB) formation from Con-hiPSCs with expression of genes representing different germ layers

	Gene	Relative Transcript Level ± SD
Endoderm	*SOX17*	4.97 ± 0.23
	FOXA2	10.50 ± 1.11
	AFP	625.62 ± 20.32
Mesoderm	*T*	1.67 ± 0.35
	HESX1	3.42 ± 0.13
	NKX2-5	33.26 ± 1.14
Ectoderm	*NEUROD1*	3.12 ± 0.13
	SOX1	4.57 ± 0.17
	PAX6	9.93 ± 0.47

Credit: Xu Qian, et al. Stem Cells. manuscript under revision

Table 4-3. Embryoid body (EB) formation from d6+D-hiPSCs with expression of genes representing different germ layers

	Gene	Relative Transcript Level ± SD
Endoderm	*SOX17*	5.07 ± 0.30
	FOXA2	4.80 ± 0.29
	AFP	878.20 ± 54.71
Mesoderm	*T*	1.45 ± 0.27
	HESX1	4.45 ± 0.14
	NKX2-5	29.31 ± 7.51
Ectoderm	*NEUROD1*	7.77 ± 0.08
	SOX1	7.99 ± 0.31
	PAX6	18.84 ± 2.43

Credit: Xu Qian, et al. Stem Cells. manuscript under revision

4.8 References

[1] Thomson JA, Itskovitz-Eldor J, Shapiro SS et al. Embryonic stem cell lines derived from human blastocysts. Science 1998;282:1145-7.

[2] Takahashi K, Tanabe K, Ohnuki M et al. Induction of pluripotent stem cells from adult human fibroblasts by defined factors. Cell 2007;131:861-72.

[3] Yu J, Vodyanik MA, Smuga-Otto K et al. Induced pluripotent stem cell lines derived from human somatic cells. Science 2007;318:1917-20.

[4] Hay DC, Sutherland L, Clark J et al. Oct-4 knockdown induces similar patterns of endoderm and trophoblast differentiation markers in human and mouse embryonic stem cells. Stem Cells 2004;22:225-35.

[5] Boyer LA, Lee TI, Cole MF et al. Core transcriptional regulatory circuitry in human embryonic stem cells. Cell 2005;122:947-56.

[6] Hyslop L, Stojkovic M, Armstrong L et al. Downregulation of NANOG induces differentiation of human embryonic stem cells to extraembryonic lineages. Stem Cells 2005;23:1035-43.

[7] Fong H, Hohenstein KA, Donovan PJ. Regulation of self-renewal and pluripotency by Sox2 in human embryonic stem cells. Stem Cells 2008;26:1931-8.

[8] Pierre A, Gautier M, Callebaut I et al. Atypical structure and phylogenomic evolution of the new eutherian oocyte- and embryo-expressed KHDC1/DPPA5/ECAT1/OOEP gene family. Genomics 2007;90:583-94.

[9] Kim SK, Suh MR, Yoon HS et al. Identification of developmental pluripotency associated 5 expression in human pluripotent stem cells. Stem Cells 2005;23:458-62.

[10] Western P, Maldonado-Saldivia J, van den Bergen J et al. Analysis of Esg1 expression in pluripotent cells and the germline reveals similarities with Oct4 and Sox2 and differences between human pluripotent cell lines. Stem Cells 2005;23:1436-42.

[11] Amano H, Itakura K, Maruyama M et al. Identification and targeted disruption of the mouse gene encoding ESG1 (PH34/ECAT2/DPPA5). BMC Dev Biol 2006;6:11.

[12] Aoki T, Ohnishi H, Oda Y et al. Generation of induced pluripotent stem cells from human adipose-derived stem cells without c-MYC. Tissue Eng Part A 2010;16:2197-206.

[13] Mamidi MK, Pal R, Mori NA et al. Co-culture of mesenchymal-like stromal cells derived from human foreskin permits long term propagation and differentiation of human embryonic stem cells. J Cell Biochem 2011;112:1353-63.

[14] Zhang Y, Wei C, Zhang P et al. Efficient reprogramming of naive-like induced pluripotent stem cells from porcine adipose-derived stem cells with a feeder-independent and serum-free system. PLoS One 2014;9:e85089.

[15] Tanaka TS, Lopez de Silanes I, Sharova LV et al. Esg1, expressed exclusively in preimplantation embryos, germline, and embryonic stem cells, is a putative RNA-binding protein with broad RNA targets. Dev Growth Differ 2006;48:381-90.

[16] Wang Z, Oron E, Nelson B et al. Distinct lineage specification roles for NANOG, OCT4, and SOX2 in human embryonic stem cells. Cell Stem Cell 2012;10:440-54.

[17] Vallier L, Mendjan S, Brown S et al. Activin/Nodal signalling maintains pluripotency by controlling Nanog expression. Development 2009;136:1339-49.

[18] Suzuki A, Raya A, Kawakami Y et al. Nanog binds to Smad1 and blocks bone morphogenetic protein-induced differentiation of embryonic stem cells. Proc Natl Acad Sci U S A 2006;103:10294-9.

[19] Hanna J, Saha K, Pando B et al. Direct cell reprogramming is a stochastic process amenable to acceleration. Nature 2009;462:595-601.

[20] Villa-Diaz LG, Nandivada H, Ding J et al. Synthetic polymer coatings for long-term growth of human embryonic stem cells. Nature Biotechnology 2010;28:581-3.

[21] Nandivada H, Villa-Diaz LG, O'Shea KS et al. Fabrication of synthetic polymer coatings and their use in feeder-free culture of human embryonic stem cells. Nat Protoc 2011;6:1037-43.

[22] Villa-Diaz LG, Pacut C, Slawny NA et al. Analysis of the Factors that Limit the Ability of Feeder Cells to Maintain the Undifferentiated State of Human Embryonic Stem Cells. Stem Cells Dev 2009;18:641-51.

[23] Qian X, Villa-Diaz LG, Kumar R et al. Enhancement of the propagation of human embryonic stem cells by modifications in the gel architecture of PMEDSAH polymer coatings. Biomaterials 2014;35:9581-90.

[24] Villa-Diaz LG, Kim JK, Lahann J et al. Derivation and long-term culture of transgene-free human induced pluripotent stem cells on synthetic substrates. Stem Cells Transl Med 2014;3:1410-7.

[25] Yao S, Chen S, Clark J et al. Long-term self-renewal and directed differentiation of human embryonic stem cells in chemically defined conditions. Proc Natl Acad Sci U S A 2006;103:6907-12.

[26] Adjaye J, Huntriss J, Herwig R et al. Primary differentiation in the human blastocyst: comparative molecular portraits of inner cell mass and trophectoderm cells. Stem Cells 2005;23:1514-25.

[27] Xue F, Ma Y, Chen YE et al. Recombinant rabbit leukemia inhibitory factor and rabbit embryonic fibroblasts support the derivation and maintenance of rabbit embryonic stem cells. Cell Reprogram 2012;14:364-76.

[28] Kues WA, Herrmann D, Barg-Kues B et al. Derivation and characterization of sleeping beauty transposon-mediated porcine induced pluripotent stem cells. Stem Cells Dev 2013;22:124-35.

[29] Koh S, Thomas R, Tsai S et al. Growth requirements and chromosomal instability of induced pluripotent stem cells generated from adult canine fibroblasts. Stem Cells Dev 2013;22:951-63.

[30] Frankenberg S, Gerbe F, Bessonnard S et al. Primitive endoderm differentiates via a three-step mechanism involving Nanog and RTK signaling. Dev Cell 2011;21:1005-13.

[31] Singh AM, Hamazaki T, Hankowski KE et al. A heterogeneous expression pattern for Nanog in embryonic stem cells. Stem Cells 2007;25:2534-42.

[32] Marson A, Levine SS, Cole MF et al. Connecting microRNA genes to the core transcriptional regulatory circuitry of embryonic stem cells. Cell 2008;134:521-33.

[33] Stuart HT, van Oosten AL, Radzisheuskaya A et al. NANOG amplifies STAT3 activation and they synergistically induce the naive pluripotent program. Curr Biol 2014;24:340-6.

[34] Lim CY, Tam W, Zhang et al. Sall4 regulates distinct transcription circuitries in different blastocyst-derived stem cell Lineages. Cell Stem Cell 2008; 3:543-54.

[35] McCall MD, Toso C, Baetge EE et al. Are stem cells a cure for diabetes? Clin Sci 2010;118:87-97.

[36] Dominguez-Bendala J, Inverardi L, Ricordi C. Stem cell-derived islet cells for transplantation. Curr Opin Organ Tran 2011;16:76-82.

[37] Laflamme MA, Chen KY, Naumova AV et al. Cardiomyocytes derived from human embryonic stem cells in pro-survival factors enhance function of infarcted rat hearts. Nature Biotechnology 2007;25:1015-24.

[38] Richards M, Tan S, Fong CY et al. Comparative evaluation of various human feeders for prolonged undifferentiated growth of human embryonic stem cells. Stem Cells 2003;21:546-56.

[39] Xu C, Inokuma MS, Denham J et al. Feeder-free growth of undifferentiated human embryonic stem cells. Nat Biotechnol 2001;19:971-4.

[40] Braam SR, Zeinstra L, Litjens S et al. Recombinant vitronectin is a functionally defined substrate that supports human embryonic stem cell self-renewal via alphavbeta5 integrin. Stem Cells 2008;26:2257-65.

[41] Miyazaki T, Futaki S, Hasegawa K et al. Recombinant human laminin isoforms can support the undifferentiated growth of human embryonic stem cells. Biochem Biophys Res Commun 2008;375:27-32.

[42] Qian X, Villa-Diaz LG, Krebsbach PH. Advances in culture and manipulation of human pluripotent stem cells. J Dent Res 2013;92:956-62.

[43] Villa-Diaz LG, Ross AM, Lahann J et al. Concise Review: The Evolution of human pluripotent stem cell culture: From feeder cells to synthetic coatings. Stem Cells 2013;31:1-7.

[44] Ng HH, Surani MA. The transcriptional and signalling networks of pluripotency. Nat Cell Biol 2011;13:490-6.

[45] Jauch R, Ng CK, Saikatendu KS et al. Crystal structure and DNA binding of the homeodomain of the stem cell transcription factor Nanog. J Mol Biol 2008;376:758-70.

[46] Nagy A, Vintersten K. Murine embryonic stem cells. Methods Enzymol 2006;418:3-21.

[47] Chambers I, Smith A. Self-renewal of teratocarcinoma and embryonic stem cells. Oncogene 2004;23:7150-60.

[48] Rodda DJ, Chew JL, Lim LH et al. Transcriptional regulation of nanog by OCT4 and SOX2. J Biol Chem 2005;280:24731-7.

[49] Chan KK, Zhang J, Chia NY et al. KLF4 and PBX1 directly regulate NANOG expression in human embryonic stem cells. Stem Cells 2009;27:2114-25.

[50] Chen ZY, Wang X, Zhou Y et al. Destabilization of Kruppel-like factor 4 protein in response to serum stimulation involves the ubiquitin-proteasome pathway. Cancer Res 2005;65:10394-400.

[51] Gregory MA, Hann SR. c-Myc proteolysis by the ubiquitin-proteasome pathway: stabilization of c-Myc in Burkitt's lymphoma cells. Mol Cell Biol 2000;20:2423-35.

[52] Moretto-Zita M, Jin H, Shen Z et al. Phosphorylation stabilizes Nanog by promoting its interaction with Pin1. Proc Natl Acad Sci U S A 2010;107:13312-7.

[53] Liao B, Jin Y. Wwp2 mediates Oct4 ubiquitination and its own auto-ubiquitination in a dosage-dependent manner. Cell Res 2010;20:332-44.

[54] Xu H, Wang W, Li C et al. WWP2 promotes degradation of transcription factor OCT4 in human embryonic stem cells. Cell Res 2009;19:561-73.

[55] Ramakrishna S, Suresh B, Lim KH et al. PEST motif sequence regulating human NANOG for proteasomal degradation. Stem Cells Dev 2011;20:1511-9.

[56] Ebben JD, Zorniak M, Clark PA et al. Introduction to induced pluripotent stem cells: advancing the potential for personalized medicine. World Neurosurgery 2011;76:270-5.

[57] Liao J, Wu Z, Wang Y et al. Enhanced efficiency of generating induced pluripotent stem (iPS) cells from human somatic cells by a combination of six transcription factors. Cell Res 2008;18:600-3.

[58] Silva J, Nichols J, Theunissen TW et al. Nanog Is the Gateway to the Pluripotent Ground State. Cell 2009;138:722-37.

[59] Liu X, Sun H, Qi J et al. Sequential introduction of reprogramming factors reveals a time-sensitive requirement for individual factors and a sequential EMT-MET mechanism for optimal reprogramming. Nat Cell Biol 2013;15:829-38.

CHAPTER 5

CONCLUSION AND PROSPECTUS

5.1 Summary

Because human pluripotent stem cells (hPSCs), including human embryonic stem cells (hESCs) and human induced pluripotent stem cells (hiPSCs), can be directed to differentiate towards cells from all three germ layers and trophoectoderm, these cells have more potential and versatility than any adult stem cells. Recent advances in the culture and manipulation of hPSCs have improved the prospects for making meaningful progress in regenerative medicine, disease modeling, and drug screening [1]. For example, the development of synthetic polymers for hPSC culture offers xenogeneic-free and defined microenvironments that are very promising for the large-scale production of clinical-grade hPSCs and thus may provide an alternative cell source for tissue regeneration strategies [2-10]. These goals can only be achieved by the complete understanding of the mechanisms by which synthetic polymers support hPSC self-renewal, which however has not yet been well defined.

In a previous study, we described the development of a completely synthetic polymer coating to culture and expand hESCs [4, 11]. We subsequently published the derivation of hiPSCs on the substrate, poly[2-(methacryloyloxy) ethyl dimethyl-(3-sulfopropyl) ammonium hydroxide] (PMEDSAH) [12]. Although other synthetic substrates have been developed for pluripotent stem

cell culture, PMEDSAH is currently the only fully synthetic substrate that contains no biologic components such as proteins, peptides or sugars. In this thesis, we studied the mechanism by which synthetic polymers PMEDSAH supports hPSC self-renewal from both the material and molecular biological approaches.

From the material perspective, we investigated the extent to which the physical properties of PMEDSAH impact its capacity to support hPSC self-renewal. By increasing the reaction time of atom transfer radical polymerization (ATRP), we modified the gel architecture of PMEDSAH without changing its chemical structure. Polymer characterization determined differences in gel architecture among UVO-grafted PMEDSAH and ATRP PMEDSAH substrates that point towards alterations in the balance of inter-molecule associations between polymer chains. These alterations further influenced the interfacial properties of the substrate and demonstrated a profound effect on the culture and expansion of hPSCs. While all four coatings were able to maintain hPSC self-renewal and pluripotency over long-term culture, the 105 nm thick ATRP PMEDSAH was found to perform significantly better than the other three substrates because of its optimal gel architecture for hPSC expansion with intermediate thickness, hydrophilicity, surface charge, and a moderate degree of inter-chain association. Our results demonstrated that the physical properties significantly influenced the ability of PMEDSAH to support hPSC expansion. The newly developed 105 nm thick ATRP PMEDSAH can be used as an effective substrate for scalable production of hPSCs for application in regenerative medicine.

From the molecular biological perspective, the pluripotency of hPSCs is maintained by a network of transcription factors and signaling pathways [13]. The culture conditions that are appropriate for hPSC maintenance are ones that are able to support pluripotency via this network. Although a specific group of transcription factors such as OCT4, SOX2 and NANOG are known

to compose this core circuitry [14-18], this regulatory network is not well characterized because many other pluripotency-related factors and their function are still unknown. It is also unclear whether this regulatory network is impacted by different *in vitro* culture conditions. In this thesis, we compared the gene expression of hPSCs cultured on PMEDSAH and other substrates. Interestingly, we found that the gene expression of *Developmental Pluripotency Associated 5 (DPPA5)*, a pluripotency marker with unknown function in PSCs, was consistently higher on PMEDSAH and other feeder-free substrates compared to the most widely used hPSC culture condition, mouse embryonic fibroblasts (MEFs). We further determined the protein levels of DPPA5 in hPSCs cultured on different substrates and investigated the function of DPPA5 in hPSC pluripotency and reprogramming.

Our results demonstrated that *in vitro* culture conditions influence the gene expression and protein levels of DPPA5 in hPSCs. The extracellular matrix (ECM) and soluble factors secreted by irradiated MEFs inhibit the expression of DPPA5 in hPSCs, while its expression and function is permissive under feeder-free conditions such as PMEDSAH. DPPA5 stabilizes protein levels and enhances the function of NANOG, a master transcription factor regulating hPSC pluripotency. Moreover, *DPPA5* increases the reprogramming efficiency of somatic cells into hiPSCs when transduced with *OCT4*, SOX2, *KLF4* and *C-MYC* reprogramming cocktail. Taken together, DPPA5 plays an important role in supporting hPSC self-renewal, pluripotency and reprogramming. Our findings provide novel molecular insight into the mechanism by which synthetic polymer PMEDSAH and other feeder-free substrates support hPSC self-renewal. The newly discovered function of the PSC marker DPPA5 in hPSCs not only advances our knowledge of stem cell biology, but also offers improvements to current protocols in hPSC maintenance and reprogramming. In addition, the protein and protein interaction and

stabilization of NANOG by DPPA5 suggest that in addition to the broadly investigated transcriptional regulation of pluripotency-related factors, post-translational regulation also plays a crucial role in the hPSC pluripotency regulatory network.

In summary, we investigated the mechanism by which synthetic polymers support hPSC self-renewal by determining the role of hydrogel physical properties and specific pluripotency-related factors in this process. We found that physical properties influence the ability of synthetic polymer coatings to support hPSC self-renewal. A specific range of hydrogel thickness may enhance the expansion of hPSCs on PMEDSAH. Modifying the gel architecture of PMEDSAH surface coating by increasing its thickness may advance our current techniques of hPSC expansion and maintenance. We also determined that DPPA5 functions in hPSCs to support hPSC self-renewal, pluripotency and reprogramming by regulating NANOG turnover. The expression and function of DPPA5 are permissive under feeder-free conditions including PMEDSAH, while MEF-extracellular matrix (ECM) and secreted soluble factors inhibit its expression in hPSCs, which suggests that the pluripotency regulatory network in hPSCs is influenced by *in vitro* culture conditions. The new insights of the function of DPPA5 in hPSCs extend our understanding of hPSCs biology and may further advance our current hPSC maintenance and reprogramming techniques. Our work builds a bridge from culture substrates, to molecular biology, to cell behavior, which truly merges the physical and life sciences.

5.2 Prospectus

5.2.1 Human Embryonic Stem Cells or Human Induced Pluripotent Stem Cells-Which Way to Go?

Because of the great potential in regenerative medicine, especially their specific advantages for research and clinical purposes, both hESCs and hiPSCs will continue to attract tremendous scientific interests.

As the field progresses, the study of hPSCs, such as hESCs, will remain an important area of research because no other human cell-type has as much capacity to reveal insights into early events in human development. hESCs also represent normal human cells that have not undergone genetic manipulation and since hESCs can be derived from embryos with naturally occurring genetic mutations, the study of disease-specific ESCs should lead to improved diagnosis and treatment for specific inherited diseases.

However, the study of hiPSCs, and the recent advances in direct cell reprogramming will likely surpass hESCs in the potential for regenerative medicine as methods are developed to safely and reproducibly generate personalized cells. Because of the epigenetic modifications of DNA that are inherent in genetic reprogramming may be influenced by the character of the parental cell type [19], iPSCs may turn out to be more easily directed to differentiate toward specific tissues that their parental cells are from. For example, hiPSCs generated from cells of dental origin may have a greater potential to regenerate many of the unique structures in the oral cavity.

5.2.2 Future Directions of Physico-chemical Property Modifications of Synthetic Polymer Coatings for Human Pluripotent Stem Cell Propagation

In this thesis, we successfully generated a novel experimental model to test the effect of hydrogel gel architecture on hPSC behavior, which suggests that physical properties of synthetic polymer coatings play an important role in hPSC expansion. In order to thoroughly understand the mechanism by which synthetic polymer coatings such as PMEDSAH support hPSC self-renewal,

we may also investigate the impact of other hydrogel physico-chemical properties on hPSC function. These investigations can be achieved by the following modifications of PMEDSAH structure: 1) replace the sulfonate group with a phosphonate group; 2) increase the distance between cationic and anionic groups; 3) change the linkage to the polymer backbone from ester to amide; 4) synthesize a head-end type variant (R^2) (Figure 5-1). Similar to our current experimental model, cell adhesion, proliferation and self-renewal will be determined by the number and area of undifferentiated colonies, total cell number, stem cell marker expression and pluripotency of the hPSCs cultured on different modified PMEDSAH. By screening which physico-chemical properties of PMEDSAH may be critical for hPSC maintenance, we may further advance our knowledge and improve our current techniques in hPSC self-renewal and expansion. Based on these potential findings, it is very promising to establish a database of substrate physico-chemical properties that impact hPSC behavior, and allow new synthetic substrates to be designed and optimized with high efficiency.

We found in this thesis that 105 nm thick ATRP PMEDSAH performs significantly better for hPSC expansion than the other substrates because of its optimal gel architecture for hPSC expansion. It would be interesting to determine whether this optimal gel architecture enhances the expression of molecules related to specific cell behaviors. Cell adhesion on different synthetic substrates is one example of this experimental question. Cell surface proteins such as E-cadherin, epithelial cell adhesion molecule (EpCAM), α-integrins 1-6 and v and β-integrin 1 and 2 are known to mediate cell-matrix interactions [20] By comparing the expression profiles of these cell adhesion molecules in hPSCs on different substrates as well as the subsequent functional assays, we may determine which molecules function as the “link” through which polymer gel architecture regulates hPSC adhesion. These potentially determined molecules and

their involved signaling pathways may extend our understanding of how physical properties of synthetic substrates impact hPSC behavior and further fill in the hole in the currently missing part of our knowledge connecting material physics and hPSC biology.

5.2.3 Further Consideration of the Role of DPPA5 in Pluripotency Regulatory Network and Reprogramming

Our findings that DPPA5 interacts with and stabilizes NANOG protein provide new insights into the regulation of NANOG in hPSCs, suggesting that in addition to the broadly investigated transcriptional regulation of pluripotency-related factors, post-translational regulation also plays a role in the pluripotency regulatory network. Recent studies indicate that NANOG could be regulated by post-translational modifications such as ubiquitination or phosphorylation in hPSCs [21-23]. It will be interesting to identify if DPPA5 stabilizes NANOG by blocking ubiquitin-dependent proteolysis or through phosphorylation. Through modifications of the potentially involved residues, we may further determine the binding sites of DPPA5 in NANOG proteins. These studies may provide a more profound understanding of the molecular mechanism that how DPPA5 regulates NANOG in hPSCs.

A major concern for reprogramming is the oncogenic potential of reprogramming factors. C-MYC and KLF4 are well known oncogenic proteins that are overexpressed in a broad range of human cancers and are often associated with poor prognoses [24, 25]. We found that the addition of *DPPA5* to the reprogramming cocktail (*OCT4, SOX2, KLF4* and *C-MYC*: *OSKM*) increased the generation of iPSCs greater than 3-fold when compared to the *OSKM* control group. The key role of NANOG in iPSC-reprogramming [26-29], combined with our finding that DPPA5 regulates NANOG protein levels, suggests that DPPA5 may promote hiPSC-reprogramming

efficiency by enhancing NANOG and its function during the reprogramming process. Therefore, it would be very important to determine if DPPA5 is able to replace C-MYC or/and KLF4 for hiPSC-reprogramming. If true, this approach may decrease the risk of tumorigenicity of hiPSCs and their derivatives by our current reprogramming protocols and live up to its full potential for regenerative medicine.

5.3 Figures

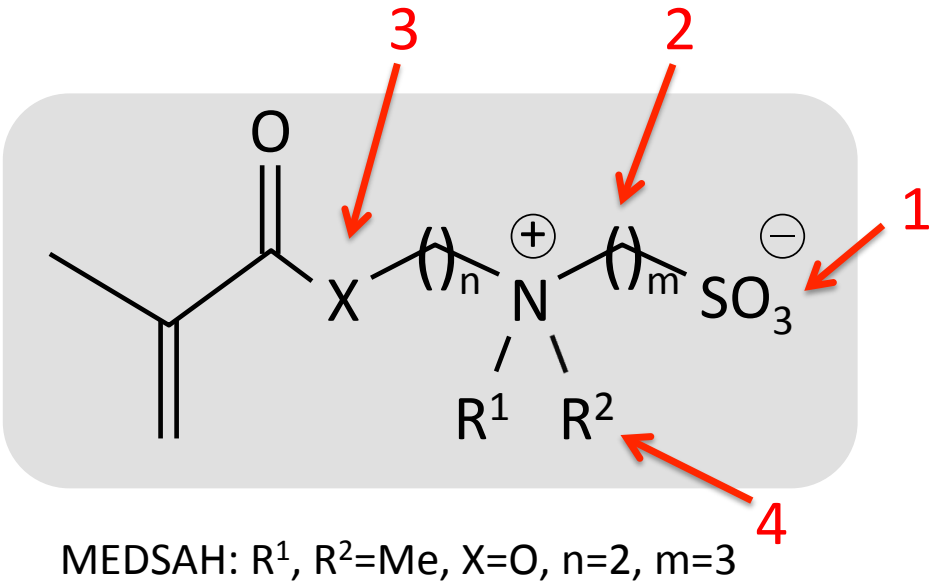

Figure 5-1. Future modifications of PMEDSAH structure The impact of hydrogel physico-chemical properties on hPSC behaviors will be investigated by cell culture on PMEDSAH with the following modifications: 1. replace the sulfonate group with a phosphonate group; 2. increase the distance between cationic and anionic groups; 3. change the linkage to the polymer backbone from ester to amide; 4. synthesize a head-end type variant (R^2).

5.4 References

[1] Villa-Diaz LG, Ross AM, Lahann J et al. Concise review: The evolution of human pluripotent stem cell culture: from feeder cells to synthetic coatings. Stem Cells 2013;31:1-7.

[2] Derda R, Li L, Orner BP et al. Defined substrates for human embryonic stem cell growth identified from surface arrays. ACS Chem Biol 2007;2:347-55.

[3] Kolhar P, Kotamraju VR, Hikita ST et al. Synthetic surfaces for human embryonic stem cell culture. J Biotechnol 2010;146:143-6.

[4] Villa-Diaz LG, Nandivada H, Ding J et al. Synthetic polymer coatings for long-term growth of human embryonic stem cells. Nat Biotechnol 2010;28:581-3.

[5] Klim JR, Li L, Wrighton PJ et al. A defined glycosaminoglycan-binding substratum for human pluripotent stem cells. Nat Methods 2010;7:989-94.

[6] Mei Y, Saha K, Bogatyrev SR et al. Combinatorial development of biomaterials for clonal growth of human pluripotent stem cells. Nat Mater 2010;9:768-78.

[7] Irwin EF, Gupta R, Dashti DC et al. Engineered polymer-media interfaces for the long-term self-renewal of human embryonic stem cells. Biomaterials 2011;32:6912-9.

[8] Li Y, Chuang E, Rodriguez R et al. Hydrogels as artificial matrices for human embryonic stem cell self-renewal. J Biomedical Mater Res A 2006;79:1-5.

[9] Brafman DA, Chang CW, Fernandez A et al. Long-term human pluripotent stem cell self-renewal on synthetic polymer surfaces. Biomaterials 2010;31:9135-44.

[10] Melkoumian Z, Weber JL, Weber DM et al. Synthetic peptide-acrylate surfaces for long-term self-renewal and cardiomyocyte differentiation of human embryonic stem cells. Nat Biotechnol 2010;28:606-10.

[11] Nandivada H, Villa-Diaz LG, O'Shea KS et al. Fabrication of synthetic polymer coatings and their use in feeder-free culture of human embryonic stem cells. Nat Protoc 2011;6:1037-43.

[12] Villa-Diaz LG, Kim JK, Lahann J et al. Derivation and long-term culture of transgene-free human induced pluripotent stem cells on synthetic substrates. Stem Cells Transl Med 2014;3:1410-7.

[13] Ng HH, Surani MA. The transcriptional and signalling networks of pluripotency. Nat Cell Biol 2011;13:490-6.

[14] Hay DC, Sutherland L, Clark J et al. Oct-4 knockdown induces similar patterns of endoderm and trophoblast differentiation markers in human and mouse embryonic stem cells. Stem Cells 2004;22:225-35.

[15] Hart AH, Hartley L, Ibrahim M et al. Identification, cloning and expression analysis of the pluripotency promoting Nanog genes in mouse and human. Dev Dyn 2004;230:187-98.

[16] Hyslop L, Stojkovic M, Armstrong L et al. Downregulation of NANOG induces differentiation of human embryonic stem cells to extraembryonic lineages. Stem Cells 2005;23:1035-43.

[17] Fong H, Hohenstein KA, Donovan PJ. Regulation of self-renewal and pluripotency by Sox2 in human embryonic stem cells. Stem Cells 2008;26:1931-8.

[18] Wang Z, Oron E, Nelson B et al. Distinct Lineage Specification Roles for NANOG, OCT4, and SOX2 in Human Embryonic Stem Cells. Cell Stem Cell 2012;10:440-54.

[19] Kim K, Doi A, Wen B et al. Epigenetic memory in induced pluripotent stem cells. Nature 2010;467:285-90.

[20] Zhang R, Mjoseng HK, Hoeve MA et al. A thermoresponsive and chemically defined hydrogel for long-term culture of human embryonic stem cells. Nat Commun 2013;4.

[21] Ramakrishna S, Suresh B, Lim KH et al. PEST motif sequence regulating human NANOG for proteasomal degradation. Stem Cells Dev 2011;20:1511-9.

[22] Ho B, Olson G, Figel S et al. Nanog increases focal adhesion kinase (FAK) promoter activity and expression and directly binds to FAK protein to be phosphorylated. J Biol Chem 2012;287:18656-73.

[23] Bourguignon LYW, Xia WL, Wong G. Hyaluronan-mediated CD44 Interaction with p300 and SIRT1 Regulates beta-Catenin Signaling and NF kappa B-specific Transcription Activity Leading to MDR1 and Bcl-x(L) Gene Expression and Chemoresistance in Breast Tumor Cells. Journal of Biological Chemistry 2009;284:2657-71.

[24] Pelengaris S, Khan M, Evan G. c-MYC: more than just a matter of life and death. Nat Rev Cancer 2002;2:764-76.

[25] Rowland BD, Peeper DS. KLF4, p21 and context-dependent opposing forces in cancer. Nat Rev Cancer 2006;6:11-23.

[26] Yu J, Vodyanik MA, Smuga-Otto K et al. Induced pluripotent stem cell lines derived from human somatic cells. Science 2007;318:1917-20.

[27] Hanna J, Saha K, Pando B et al. Direct cell reprogramming is a stochastic process amenable to acceleration. Nature 2009;462:595-601.

[28] Liao J, Wu Z, Wang Y et al. Enhanced efficiency of generating induced pluripotent stem (iPS) cells from human somatic cells by a combination of six transcription factors. Cell Res 2008;18:600-3.

[29] Silva J, Nichols J, Theunissen TW et al. Nanog Is the Gateway to the Pluripotent Ground State. Cell 2009;138:722-37.